COMPARISON OF SERVICE LIFE OF A RIVETED STEEL RAILWAY BRIDGE UNDER DIFFERENT OPERATING SCENARIOS

MD Shafiul Azam

Supervisors: Professor Dr. Raffaele Landolfo and
Assistant Professor Dr. Mario D'Aniello

European Commission
ERASMUS
MUNDUS

Thesis submitted in partial fulfilment of the requirements
For the Degree of Master of Science in Construction of Steel and Composite Structures
European Erasmus Mundus Masters Course
Sustainable Construction Under Natural Hazards and Catastrophic Events

University of Naples " Federico II"

Date: 20.01.2013

STATEMENT OF THESIS APPROVAL

This thesis prepared by **MD Shafiul Azam** entitled 'Comparison of service life of a riveted steel railway bridge under different operating Scenarios' is approved in partial fulfillment of the requirements for the degree of Master of Science by the following faculty members served as the supervisory committee chair and members

____, Chair ________________
Date Approved

____, Member ________________
Date Approved

____, Member ________________
Date Approved

Student's signature ____

Date of Submission ____

ACKNOWLEDGEMENT

First and foremost, I would like to thank the Almighty Allah who had answered my prayers to finish this thesis.

I also want to thank my supervisor Dr. Mario D'Aniello for giving me his time, patience, assistance, contribution and continuous support. I would also like to express my gratitude to professor Landolfo for his valuable advice and inspiration.

On this research, I was so glad to deal with Lin Chuan and Ingrid Krause who had given me their hands and I give them all my respect and appreciation. At the last, special thanks to my family, country, parents, friends for trusting and believing me. I want to acknowledge all their sacrifices and express my heartfelt gratitude.

ABSTRACT

In this thesis, a comprehensive framework has been developed to assess the service life of an old riveted bridge taking into account the effect of traffic load, earthquake load and corrosion leading to loss of effective cross sectional area. The riveted railway bridge on the river Gesso, Italy, which was put into service in the year 1966, has been taken as a case study for the purpose of this analysis. In this study different magnitude and frequency of train load (Italian code and RFI), three artificial earthquake events applied at three hypothetical instants of time , environmental corrosion and two maintenance strategies to counteract the effect of corrosion has been taken into account to develop 16 sets of operating scenarios. For all these operating scenarios, the cumulative damage ratio of a critical element of the bridge has been calculated at every ten year interval for a period of 150 years and the service life is taken as the time corresponding to unit cumulative damage ratio. From the results, it is observed that, the contribution of the three earthquakes in the total cumulative damage ratio is very insignificant for all the operating scenarios compared to the damage contribution by the train load. The minimum service life of the bridge has been found to be 39.6 years for an operating condition where train load is applied as per Italian code and where no maintenance intervention has been adopted to limit the effect of corrosion. This report also addresses the key issue for managing cost-effective decision regarding maintenance and rehabilitation. It is observed that, for all load cases, maintenance in every 10 years for the first thirty years is more effective in controlling fatigue damage than maintenance in every 30 years option.

TABLE OF CONTENTS

LIST OF TABLES

LIST OF FIGURES

CHAPTER 1
INTRODUCTION

1.1 INTRODUCTION:

Fatigue damage is one of the most important degradation mechanisms of railway bridges and as such the assessment of remaining fatigue and service life of a riveted railway bridge is a matter of paramount importance to all railway authorities. The increase and unpredictability of traffic load and the various aggressive environmental conditions leading to corrosion can significantly affect the serviceability of a railway bridge. Besides this, natural events like earthquake can cause load cycles of high stress amplitude leading to low-cycle fatigue. However it is evident that, timely adoption of maintenance strategies can limit the corrosive degradation of the bridge material and enhance the serviceability of the bridge, but this brings forward the issues of proper planning and economic factors. Considering all these, the development of a comprehensive fatigue assessment methodology that accounts for the effect of variability in traffic load coupled with the environmental phenomenon on the service life of riveted railway bridges is crucial.

In this report, the riveted railway bridge on the river Gesso, Italy, which was put into service in the year 1966, has been taken as case study for the assessment of fatigue life. Different train load scenarios (Italian code and RFI), three hypothetical earthquake load and the effect of corrosive environmental condition has been taken into account to develop a set of operating scenarios with a view to formulating a comprehensive framework for the service life assessment of the bridge. In addition, two assumed maintenance strategies have been analyzed to examine the effectiveness of those strategies on the service life of the bridge.

1.2 OBJECTIVES:

The objectives of this study are

- Assessment of the residual service life of a riveted railway bridge under different operating scenarios based on incident load, environmental action and maintenance strategies.
- Determination of the contribution of train load and earthquake load in the cumulative damage ratio of the riveted railway bridge
- Investigation of the effect of corrosion on the residual service life of the bridge
- Observation of the effectiveness of the assumed maintenance strategies to limit the detrimental effect of decay due to corrosion

1.3 METHODOLOGY:

A step by step procedure has been followed for the assessment of residual service life of the riveted railway bridge comprising of a code-based approach for fatigue verification and evaluation of corrosion degradation for a predetermined set of operating scenarios. A number of twelve operating conditions are developed on the basis of different combination of loading condition and maintenance program. The residual service life assessment for each operating condition is determined by the procedure described in the following:

- The bridge is modelled in SAP2000 and the model is verified with respect to the theoretical modes of vibration and experimental modes of vibration.
- Structural analysis is performed and the critical member has been identified for fatigue strength verification.
- The stress spectra acting on the member due to the passage of train is determined by multi-step static analysis in SAP2000 taking into account the dynamic magnification factor.
- The stress spectra due to the hypothetical earthquakes are determined by Time History analysis in SAP 2000.
- The major stress cycles from this analysis are identified by rainflow cycle method, which are used for calculating cumulative damage ratio. The software J-Rain used to count the rainflow cycles
- The corrosivity class and the rate of corrosion are obtained from ISO Standard 9224 (1992)
- A set of maintenance strategies have been assumed
- A set of operating scenarios have been developed on the basis of different combinations of load and maintenance scenarios
- The cumulative damage ratio for each maintenance scenario is calculated by the Palmgren Miner's rule using the following formula

$$\sum_{i=1}^{n} \frac{n_i}{N_i} = D$$

- The residual life time is the time corresponding to cumulative damage ratio. D=1

1.2 SCOPE AND LIMITATION:

The limitation of this analysis are given below

- Some assumptions are made during the development of the model in SAP2000. So, the obtained result from the structural analysis can slightly vary from actuality.
- The corrosion in the bridge material is considered uniform to simplify the degradation mechanisms. Local corrosion in the joints and pitting in the coating protective system is neglected.
- The earthquake load and the time of occurrence of the three earthquakes are purely based on assumption.
- It is assumed that the corrosion resisting painting protects the bridge material from corrosive degradation for a period of ten years, which may not be the case.

CHAPTER 2
REVIEW OF THE RELATED LITERATURE

2.1 REVIEW OF THE FATIGUE THEORY:

Fatigue is the degradation of a material caused by repeatedly applied loads. It is the progressive and localized structural damage that occurs when a material is subjected to cyclic loading. Although, the cyclic loadings may not cause stress exceeding the extreme stress limit of the material, they will lead to crack formation, propagation and eventually fracture (Thun, 2006).

On the basis of resistance to fatigue damage, materials are divided into three categories: low-cycle fatigue, high-cycle fatigue and super-high cycle fatigue material. These classifications have been made from the results obtained from laboratory tests carried on either cracked or uncracked smooth bars specimens (High-Cycle Fatigue (HCF) Testing). Low-cycle fatigue (LCF) occurs when a material can sustain a small number of load cycles under a fatigue test, typically when the number of load cycles to failure is less than 10^3. High-cycle fatigue (HCF) occurs when a material is able to endure higher number of load cycles than 10^3 .The third kind of fatigue limits, which is the Super-high cycle fatigue, is not common type and its limit is number of 10^7 load cycles (Thun, 2006).It is observed the highway and railway bridges are generally high cycle fatigue structure as because these structure are capable of enduring load cycles more than the threshold amount 10^3 (Figure 2.1).

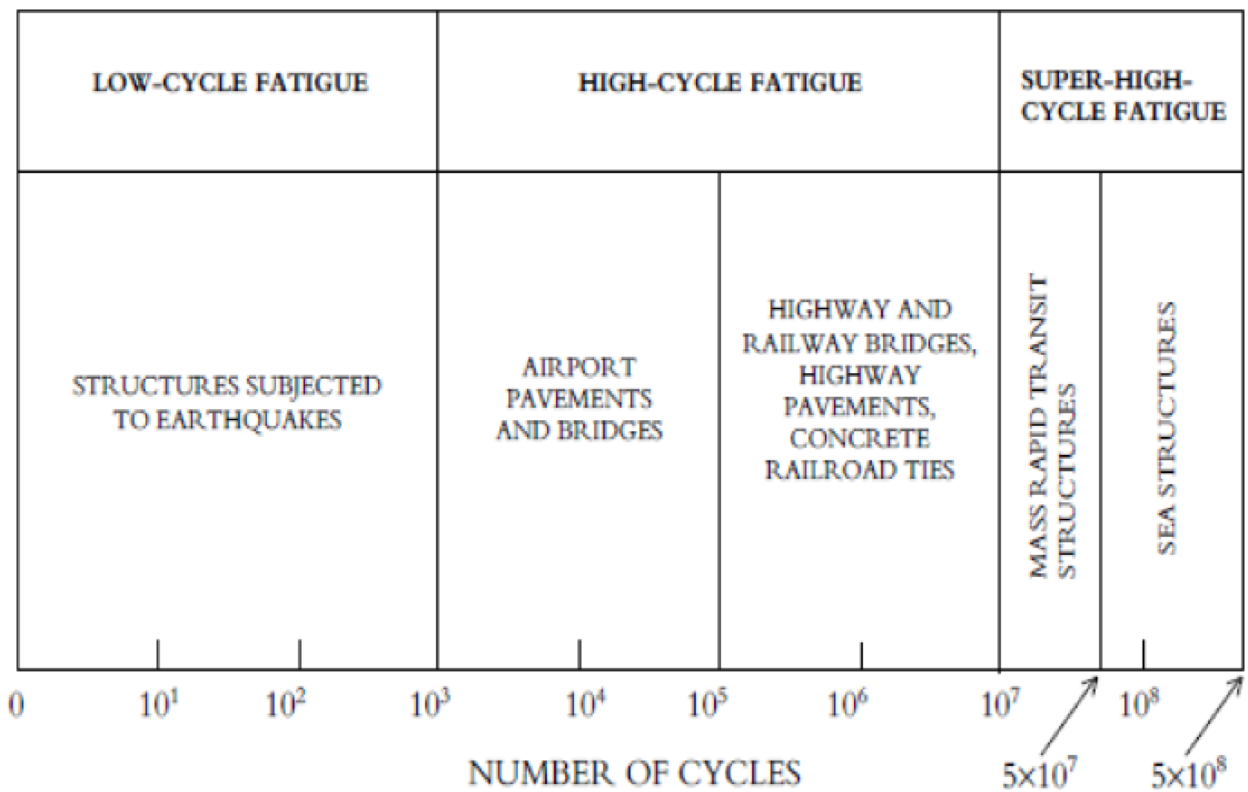

Figure 2.1: Fatigue categories (Thun 2006)

2.1.1 REVIEW OF S-N CURVE APPROACH:

If a structure is subjected to repeated number of stress cycles, which might be even lower than the extreme stress limit, micro-cracks will initiate in the structure. These cracks tend to become wider and more severe with further application of load cycles and cause sudden fracture and failure of the structure. If the stress amplitude of the cycles is higher, lower number of stress cycles causes failure and if the stress amplitude is lower, higher number of stress cycles are needed to cause failure. Therefore, any fatigue analysis approach has to take into consideration both the stress amplitudes and the number of stress cycles (Suguira & Kunitomo 2008)

One of the most widely used and effective approach in analyzing fatigue nature of failure of structure is the S-N curves approach. The S-N curve illustrates the co-relationship between stress amplitude and the number of load cycles that causes failure. The vertical axis of the S-N curve, plotted in log-log scale represents the stress range and the horizontal axis plotted also in log-log scale denotes the number of cycles to failure. The S-N curves are developed on the basis of laboratory tests, where stress cycles of constant amplitude are applied on specimen and the number of cycles until failure is counted (Maymon 1998). From the S-N curve it is evident that when the stress level decreases the number of load cycles that a material can endure increases. By reading the value of number of stress cycles on the horizontal axis of the S-N curve corresponding to the constant stress value, the fatigue endurance can be determined. However, in practical situation things are not that simple, because typically a structure is subjected to different values of load cycles during its life time and as such the S-N curve approach cannot be used directly to determine the fatigue strength of the structure. Therefore, the cumulative damage caused by all stress ranges should be estimated. This can be done by using the linear cumulative damage theory or Palmgren-Miner Rule.

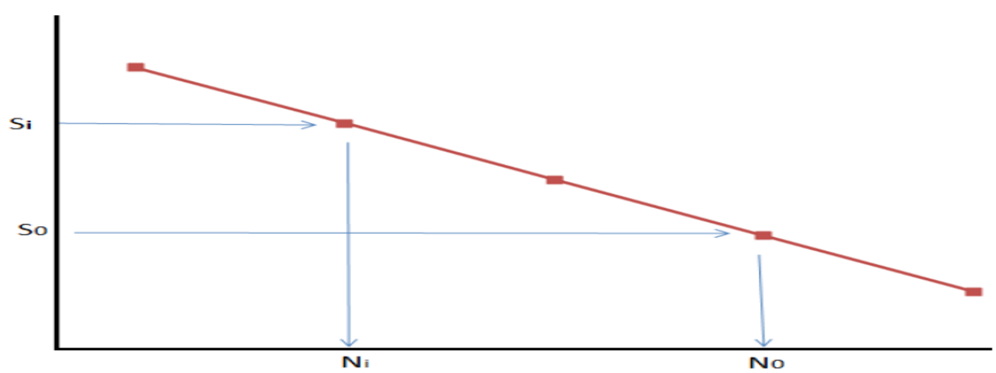

Figure 2.2: Typical S-N curve

For our analysis, the S-N curve for riveted element proposed by Pipinato, 2006 in the paper 'Fatigue tests on riveted steel elements taken from a railway bridge' has been adopted. This curve is a modification of the S-N curve for detail category C=63 given by Eurocode 3 EN 1993-1-9. The best fit equation of the proposed curve is

$$\log N = 13.835 - 3.784 \log \Delta\sigma$$
$$\Rightarrow N = 10^{13.835} . \Delta\sigma^{-3.784}$$

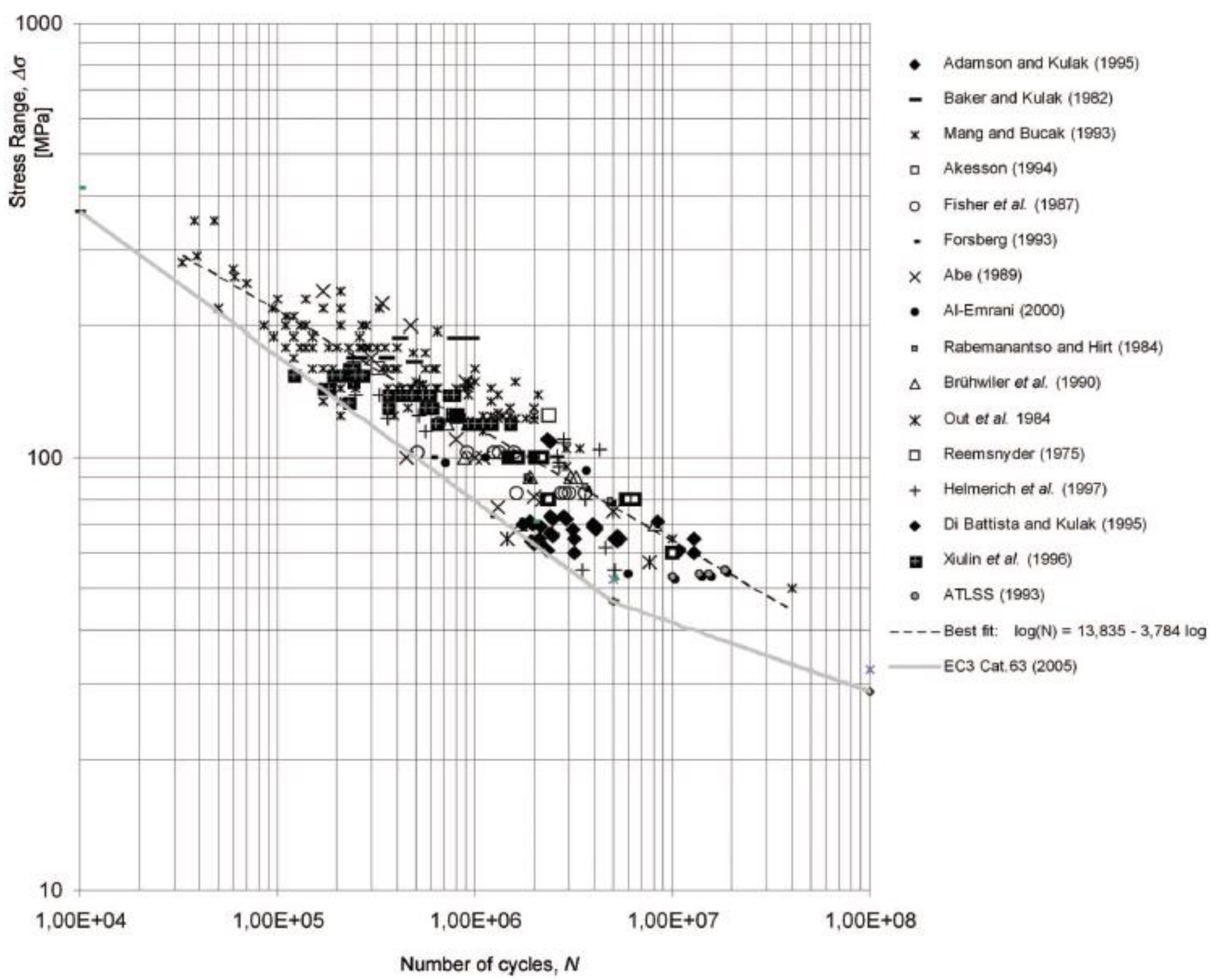

Figure 2.3: S-N curve for riveted elements

2.1.2 REVIEW OF THE PALMGREN-MINER's RULE:

From the above discussion, it is evident that if a structure is subjected to a constant value of loading, the number of cycles that causes failure for that constant stress range can be directly obtained from the S-N curve. When the number of the load cycles experienced by the structure during its life-time exceeds the number of load cycles obtained from S-N curves representing the enduring level of load cycles of the structure, fatigue cracks will develop and the structure will be considered failed in terms of fatigue. However, in practical situation things are more complicated owing to the fact that a structure is subjected to different amplitude of stress ranges over its life-time and as such the S-N curve approach cannot be used directly to determine the fatigue strength of the structure. In such cases, a cumulative hypothesis to assess fatigue damage due to the stress variations should be adopted.

One of most convenient and traditionally used approaches that addresses this cumulative damage theory is the Palmgren-Miner's rule. It is a fatigue damage accumulator theory was first introduced by Palmgren in 1924 and developed by Miner in 1945 (Thun 2006). This method suggest that if a structure is subjected to n_i cycles of stress range $\Delta\sigma_i$ and if N_i is the number of cycles that causes damage ratio for that constant stress range, than the contribution to failure for this stress range is n_i / N_i . The total cumulative damage is calculated by adding all the damage ratios corresponding to all stress ranges. Mathematically, according to the Palmgren-Miner's The cumulative damage ratio,

$$\sum_{i=1}^{n} \frac{n_i}{N_i} = D$$

Here, n_i =Number of load cycles corresponding to a certain stress level

N_i =The number of load cycles that causes failure for a specific stress level

D =Damage ratio

Although this rule is considered as non-conservative tool because it assumes that the damage will be accumulated linearly due to each loading cycles, it is still the most popular method to accumulate the total fatigue damage.

2.1.3 REVIEW OF THE RAINFALL CYCLES COUNTING METHOD:

If the stress acting on the structural member varies with time, it means that we have stress time history with different peaks and valleys amplitudes. Therefore, a proper cycle counting method should be adopted to determine the number of stress cycles which have been absorbed by the structure under dynamic loads. There are many different methods which have been introduced to count stress cycles, like Level-Crossing Counting, Peak Counting, Simple-Range Counting and Rainflow counting method (American Society for Testing and Materials 2011). Among all these, the Rainflow cycles counting method is considered to be the best method as compared to the other methods in terms of simplicity, accuracy and time consuming (Socie 1982).

Rainflow cycles counting method theory's depends on the hysteresis loops in the stress-strain behavior (Socie 1982), as shown in Fig. 2.4. As the figure illustrates, the strain will increase linearly from point A to point B, and when the load is removed at point B the strain will decrease until point C. When the member is reloaded the strain will increase linearly from point C to point D crossing its previous strain position before removing the load (point B). Therefore, all of events where the strain is reduced can be ignored like event BC, DE and FG.

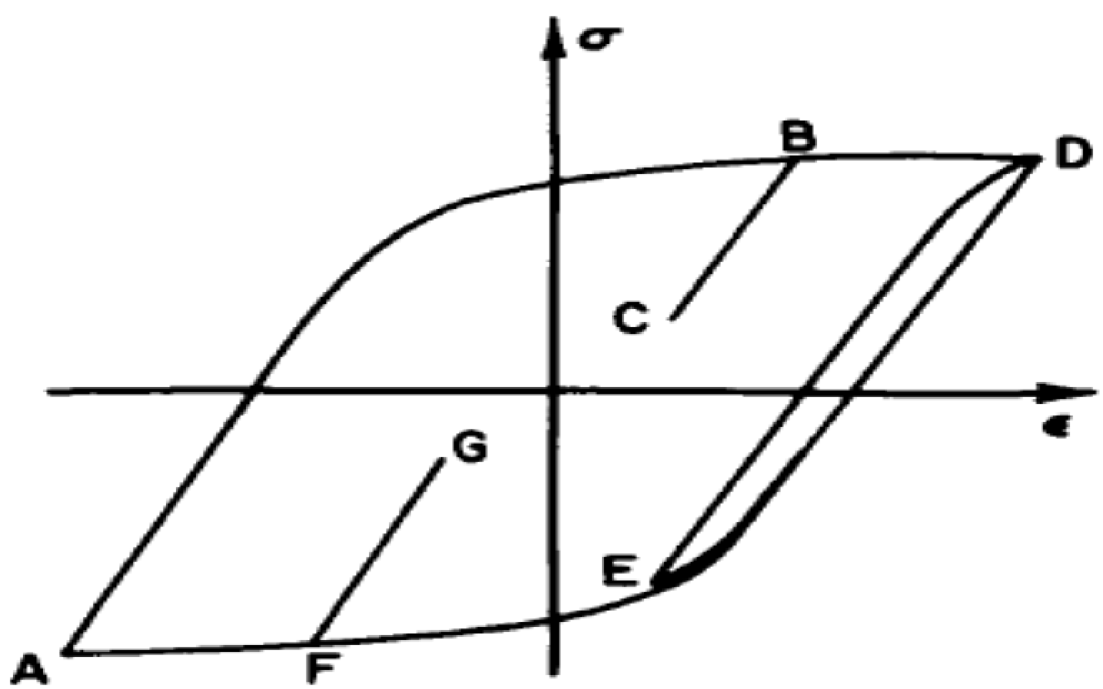

Figure 2.4: Hysteresis loops in the stress-strain behavior (Socie & Downing 1982)

The original name of this method is Pagoda Roofs method based on its graphical representation of the stress time which looks like a series of roofs when it is turned clockwise 90 degree. In the following a method of rainflow cycle counting has been described with example (Starns, 2004) (http://www.public.iastate.edu/~gkstarns/ME417).

1. Begin count at highest peak or deepest valley
2. Label each peak and valley with a letter
3. Turn the plot 90^0 clockwise; the peaks and valleys now may be imagined as rooftops.
4. Imagine a raindrop at the end of the right side of the first roof. Follow the drop of rain
5. Now let the raindrop roll down the slope of the roof toward the left and follow this drop
6. If the drop does not hit another rooftop immediately below it, then circle the node from which the drop started.
7. If the drop hits another rooftop immediately below it, follow the drop until it stops. Circle the node where it stopped.
8. Identify the largest and smallest loads in the interval, identified above
9. Record the maximum, minimum, mean and alternating loads of the uncircled node pairs in the interval- node pairs constitute a cycle.
10. Remove the uncircled nodes from the loading spectrum and plot the loading spectrum without these values
11. Repeat the process

Consider the following loading spectrum, one duty cycle is shown

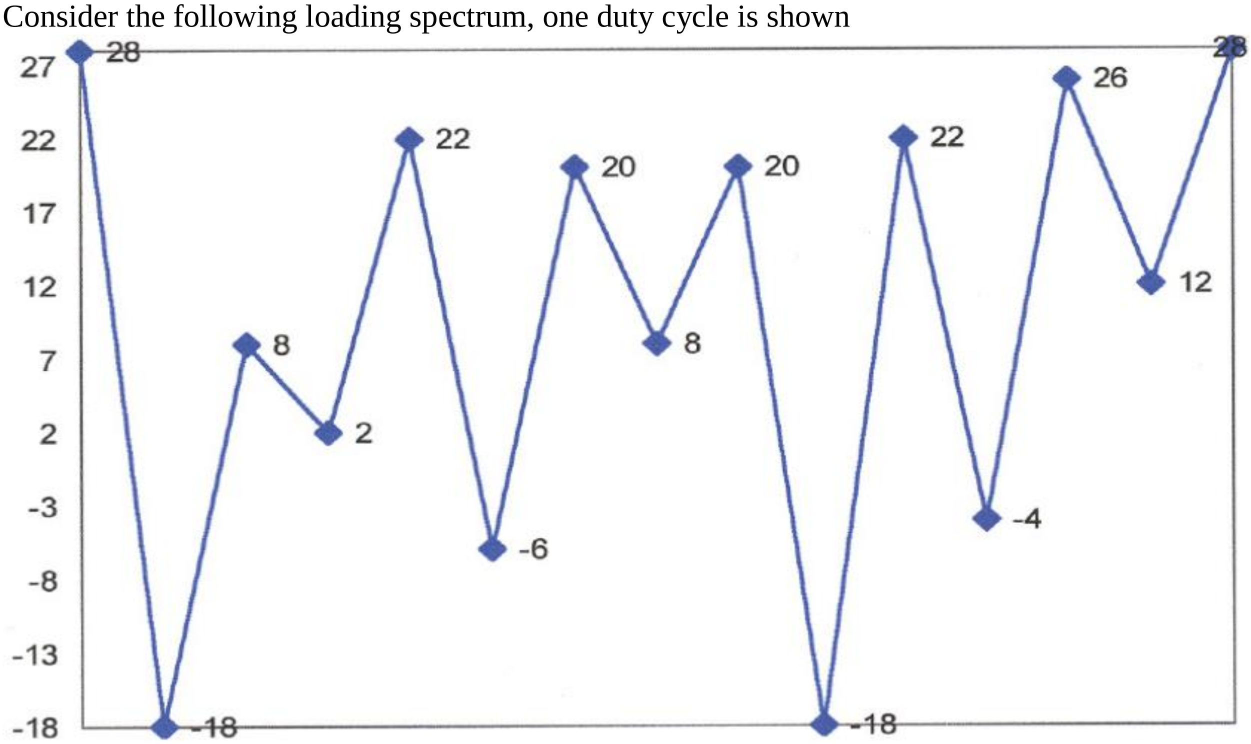

Figure 2.5: Loading spectrum, one duty cycle

Turn it clockwise 90 degree

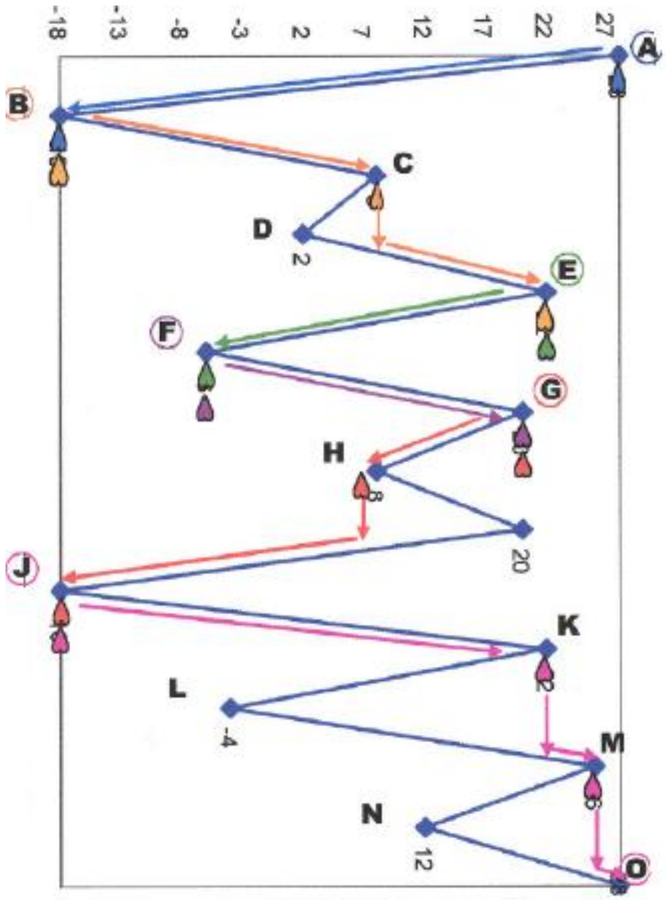

A	28
B	-18
C	8
D	2
E	22
F	-6
G	20
H	8
I	20
J	-18
K	22
L	-4
M	26
N	12
O	28

Figure 2.6: Loading spectrum, turned 90 degree clockwise

The blue rain drop rolls down roof AB and drips off node B without immediately hitting a rooftop below it-circle B.

The orange raindrop starts at B and rolls down roof BC, drips from C onto DE and drips off of E-circle E

The green drop starts at E, rolls down to F and drips off of F-circle F

The purple drops starts at F, rolls down to G and drips off of G-circle G

The red drop starts at G, rolls down to H, drips of H onto IJ, red drop rolls toward J and drips off of J-circle J

The uncircled nodes are CD, HI, KL, MN

Remove these nodes and plot the remaining nodes.

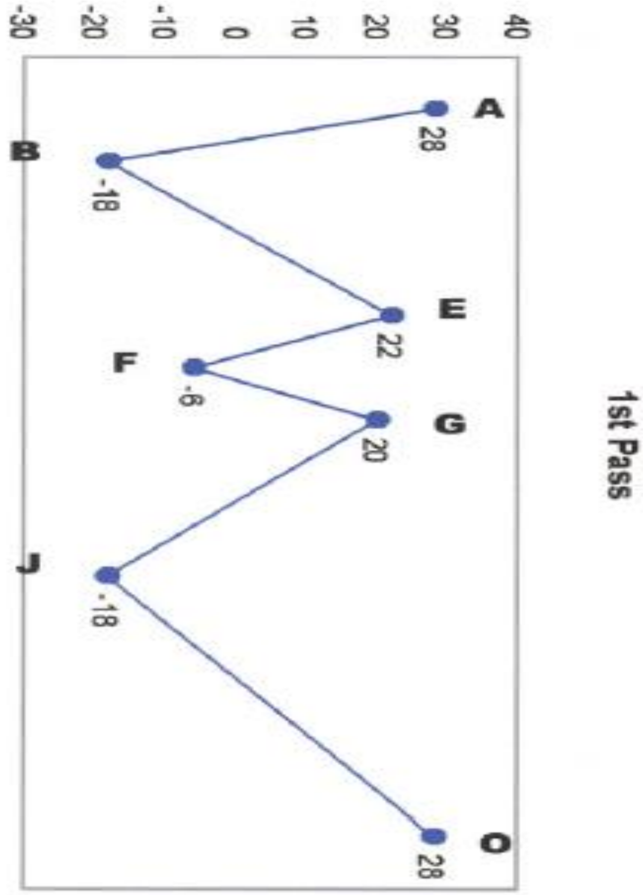

Figure 2.7: Loading spectrum after 1st pass

The procedure should be repeated until the last nodes left are those on the highest peak and lowest valley. After all the cycles are identified (node pairs), the maximum, minimum alternating and mean values of stresses need to be computed for each cycle.

Cycle	Maximum	Minimum	Mean	Alternating
CD	8	2	5	3
HI	20	8	14	6
KL	22	-4	9	13
MN	26	12	19	7
FG	20	-6	7	13
EB	22	-18	2	20
AJ	28	-18	5	23

Table 2.1: Stress cycles with maximum, minimum, mean and alternating

2.1.4 REVIEW OF THE RESERVOIR METHOD:

By the reservoir method the same result as the rainflow method can be found **Figure 2.8**. One of the advantages of this method is, it is better comprehensible. In this method, the stress-time diagram is filled with water like a reservoir, the water is let-out at the lowest point and the water column height gives the respective cycle with a range $\Delta\sigma_1$. The procedure is repeated at the next lower point and so on. The stress ranges are collected in classes and result in the cumulative frequency diagram, the stress spectrum. The counting method does not account for mean stresses or the R-ratio but this does not present a problem in life estimations in practice since these are based on an assessment of stress ranges (Kostesa, 1992).

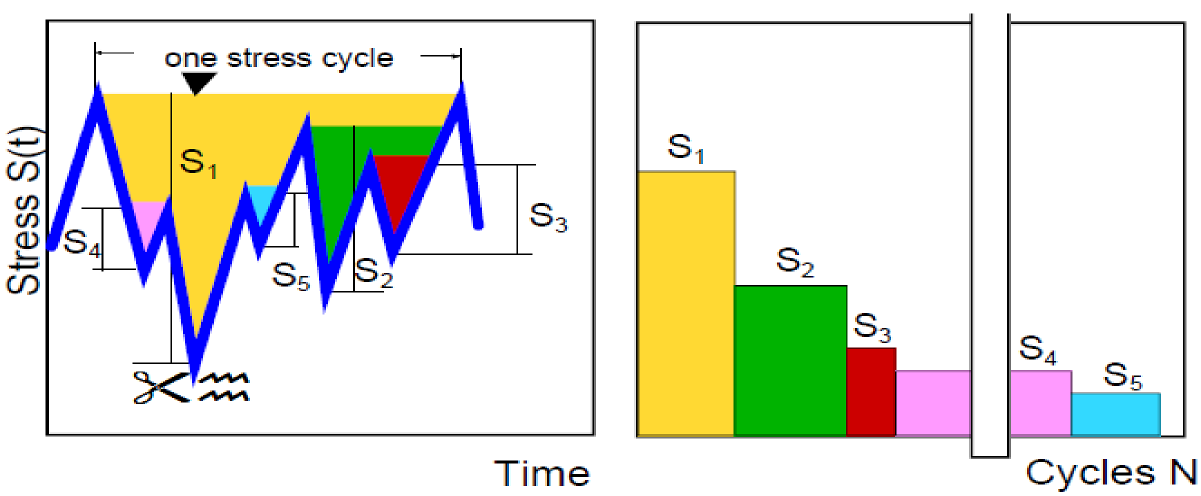

Figure 2. 8 Reservoir method

2.2 REVIEW OF THE CORROSION THEORY:

The durability of steel and other metal structures is considerably influced by the environmental conditions leading to corrosion and thus it is an important aspect for the design and rehabilitation of both new and historic construction. is From the structural point of view, the loss of thickness of the cross section due to corrosion attack leads to a smaller resistant area and increased stress, resulting in a decrease of fatigue resistance and hence the service life (Landolfo, 2010).

The corrosion phenomena of metals and alloys involve mainly two elements: the material and its environment. In particular, corrosion is defined as the deterioration of a material, usually a metal, which results from a reaction with its environment, causing the degradation of both (Landolfo, 2010). Atmospheric corrosion can be viewed as mainly an electrochemical process which is initiated by the formation of thin electrolyte films on the metal surface. This is followed by an anodic reaction invoving the dissolution of the metal in the electrolyte films and cathodic reactions, resulting in the oxidation reduction reaction.

$$M \rightarrow M^{n+} + ne^{-}$$

The rate of corrosion depends on a number of endogenous and exogenous factors. The endogenous factors such relates to the metal itself such as the physical and chemical homogeneity of the metal surface, its chemical composition, electrode potential, surface roughness etc. The exogenous factors are connected with the atmospheric condition such as humidity, temperature, presence of atmospheric pollutants like chloride and sulfate.

The corrosivity classification of some important metals as per EN 12500 (2000) is shown in the following table. This is based on: mass loss (g/m2) of the metals for one year field test exposure in the five corrosivity classes C1–C5, the order being from the least to the most corrosive

MASS LOSS g/m^2				Corrosiveness category	
Carbon Steel	Zinc	Copper	Aluminum		
≤10	≤0.7	≤ 0.9	Negligible	Very low	C1
10–200	0.7–5	0.9–5	≤0.6	Low	C2
200–400	5–15	5–12	0.6–2	Medium	C3
400–650	15–30	12–25	2–5	High	C4
650–1,500	30–60	25–50	5–10	Very high	C5

Table 2.2 Five corrosiveness categories (EN 12500/2000).

Corrosiveness category		Typical outdoor atmospheric environments
C1	Very low	Dry or cold zones; very low pollutants contamination; time of wetness very low, e.g., desert, Antarctic zone.
C2	Low	Temperate zone; low pollution (SO_2 [μg/m^3] < 12), e.g., rural areas and small towns. Dry or cold zones; short damp periods, e.g., desert, sub-artic zones.
C3	Medium	Temperate zones; medium pollutant contamination (12 < SO_2 [μg/m^3] < 40); low chloride influences, e.g., urban areas, coastal area characterized by low chloride deposition rate. Tropical zones with low pollution.
C4	High	Temperate zones; high pollution levels (40 < SO_2 [μg/m^3] < 80); important chloride influences, e.g., polluted urban areas, industrial areas, costal areas (no splashing zones), de-icing salt influence. Tropical zones with medium pollution level.
C5	Very high	Temperate zones; very high pollution levels (80 < SO_2 [μg/m^3] < 250); strong chloride deposition rates, e.g., industrial zones, coastal and sea areas (no splashing zones). Tropical zones with high pollution levels and/or strong chloride influences.

Table 2.3 Qualitative classification of corrosivity (EN 12500/2000).

As per ISO Standard 9224 (1992) the average corrosion rate of each material follows a bi-linear law. For the first 10 years of exposure the metal degrades at the average corrosion rate and after 10 years of exposure the rate of corrosion reduces and the metal surface degrades at steady state rate. During the first 10 years of atmospheric exposure, the corrosion depth is given by the formula:

$$d_1(t) = r_{av}.t; t < 10 years$$

Where

$d_1(t)$ = corrosion depth after the first 10 years of exposure (micrometers);

r_{av} = average corrosion rate (micrometers per year);

t = time at which the exposure ends.

After 10 years of exposure, the corrosion rate is assumed to be constant with time and the thickness loss is given by the formula:

$$d(t) = r_{av}.10 + r_{lin}(t-10); t \geq 10 years$$

Where

d(t) = corrosion depth for the considered time interval (micrometers);

r_{lin} = steady state corrosion rate (micrometers per year);

t=time in the linear region of the curve of uniform corrosion as function of time.

In the following table the average and steady state corrosion rates for different metals and corrosivity classes are shown

Metal	C1	C2	C3	C4	C5
Carbon Steel	$r_{av} \leq 0.5$	$0.5 < r_{av} \leq 5$	$5 < r_{av} \leq 12$	$12 < r_{av} \leq 30$	$30 < r_{av} \leq 100$
Weathering steel	$r_{av} \leq 0.1$	$0.1 < r_{av} \leq 2$	$2 < r_{av} \leq 8$	$8 < r_{av} \leq 15$	$15 < r_{av} \leq 80$
Zinc	$r_{av} \leq 0.1$	$0.1 < r_{av} \leq 0.5$	$0.5 < r_{av} \leq 2$	$2 < r_{av} \leq 4$	$4 < r_{av} \leq 10$
Copper	$r_{av} \leq 0.01$	$0.01 < r_{av} \leq 0.1$	$0.1 < r_{av} \leq 1.5$	$1.5 < r_{av} \leq 3$	$3 < r_{av} \leq 5$
Aluminium	$r_{av} \approx 0.01$	$r_{av} \leq 0.025$	$0.025 < r_{av} \leq 0.2$	-	-

Table 2.4 Average corrosion rate during first 10 years in micrometer/year (ISO 9224 (1992))

Metal	C1	C2	C3	C4	C5
Carbon Steel	$r_{av} \leq 0.1$	$0.1 < r_{av} \leq 1.5$	$1.5 < r_{av} \leq 6$	$6 < r_{av} \leq 20$	$20 < r_{av} \leq 90$
Weathering steel	$r_{av} \leq 0.1$	$0.1 < r_{av} \leq 1$	$1 < r_{av} \leq 5$	$5 < r_{av} \leq 10$	$10 < r_{av} \leq 80$
Zinc	$r_{av} \leq 0.05$	$0.05 < r_{av} \leq 0.5$	$0.5 < r_{av} \leq 2$	$2 < r_{av} \leq 4$	$4 < r_{av} \leq 10$
Copper	$r_{av} \leq 0.01$	$0.01 < r_{av} \leq 0.1$	$0.1 < r_{av} \leq 1$	$1 < r_{av} \leq 3$	$3 < r_{av} \leq 5$
Aluminium	negligible	$0.01 < r_{av} \leq 0.02$	$0.02 < r_{av} \leq 0.2$	-	-

Table 2.5 Steady state corrosion rate during first 10 years in micrometer/year (ISO 9224 (1992))

CHAPTER 3
SERVICE LIFE ASSESSMENT FOR DIFFERENT CASES AND COMPARISON OF RESULTS

3.1 HISTORICAL BACKGROUND OF THE BRIDGE:

In order to gain access and enhance administrative control over the annexed region of the unified Italy, the Italian Government had taken initiative to develop the railway network in the southern part of Italy in the second part of the nineteenth century. In 1870 the construction of the railway line Foggia-Cervaro-Napoli started, in which a large number of railway bridges of varying span were constructed. The bridge over river Gesso, built in Foggia County was one of those. The bridge was originally a multi-span arch stone bridge. A severe earthquake that occurred in the year 1962 caused considerable damage to the bridge, fatally impairing the structural safety. As a rehabilitation process, the multi-span arches have been substituted by three simple supported trussed beams rested on the original masonry piles, constituting the three –span steel bridge under examination (Figure 3.1). After reconstruction, the bridge was opened for traffic in thear 1966. The new bridge consists of a symmetric structure about the middle length of the intermediate span. Per span, the main girders are two riveted trusses 3.50 m high and 3.30 m apart, consisting of combined plates and L and C sections, as shown in Figure 3. In addition, the main trusses are connected with riveted built-up transverse secondary beams, a horizontal bracing system, and longitudinal secondary trussed beams, where the railway superstructure transmits the train loads.

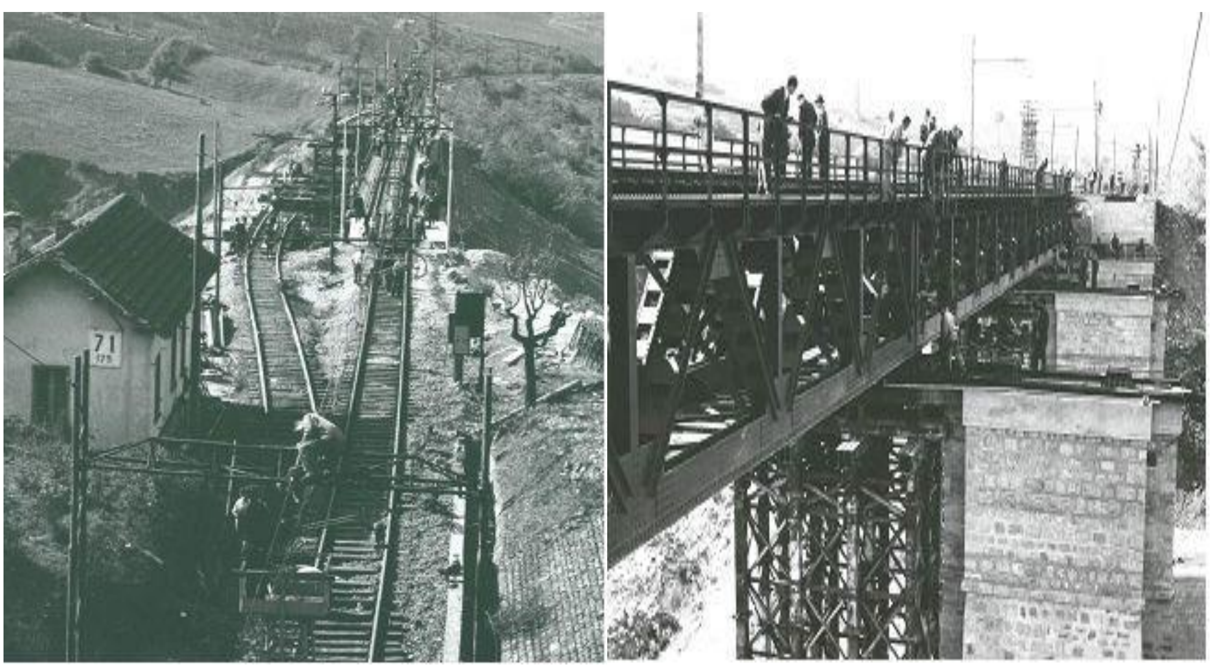

Figure 3.1: the bridge over the river Gesso after reconstruction

Recently, a research activity has been conducted in collaboration of the railway network owner (RFI) to assess the load bearing capacity, serviceability and future improvement of the bridge. As a part of this research work, The in situ dynamic measurements such as longitudinal, transverse and vertical mode of vibration testing were performed by RFI.. for the dynamic testing, The central bay of the bridge was instrumented with five pairs of accelerometers, having a sensitivity of 10 *V/g*, respectively placed at the bearings, at 1/3, 1/2 and 2/3 of the main girder length per span. The results are shown in Figure 3.2 in terms of modal shape and relevant fundamental periods.

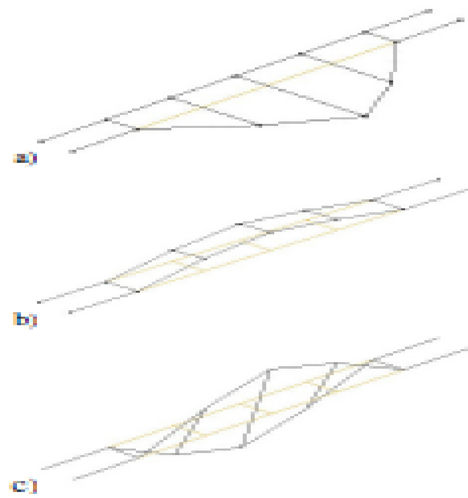

Fig 3.2: Measured fundamental modes of vibration: a) flexural in transverse direction (period 0.1250s); b) flexural in vertical direction (period 0.1250s); c) torsional (period 0.0819s)

3.2 MODELLING OF THE BRIDGE IN SAP2000:

A finite element model of the bridge has been developed in SAP 2000 on the basis of the geometric measurement obtained by the field survey and results from dynamic experiment (Fig. 3.3). The bridge truss has been modelled with beam elements. Although the structural system is a truss system, because of its large stiffness, all joints of the main girders are modelled as rigid connections.. Finally, for the development of the finite element model the following assumptions are made: (1) the structure is pinned to vertical supports; (2) the loads and reactions are applied only at joints; (3) in order to take into account the dynamic coupling between each span, the tracks and the wooden sleepers have modelled; (4) the lumped masses formulation has been assumed to characterize the inertial properties; (5) additional masses are introduced at the deck beams to account the presence of railway superstructures and secondary non-structural elements (as the handrails).

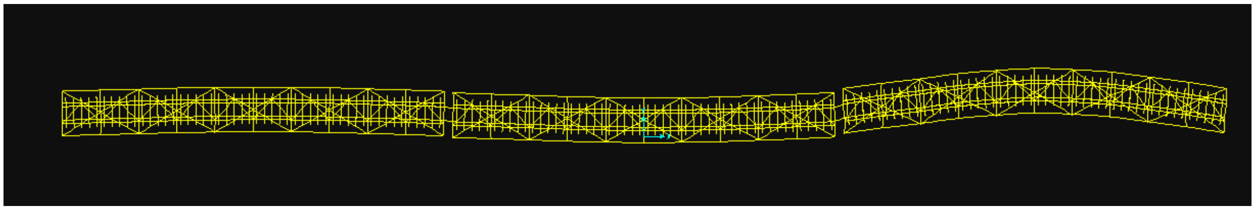

1st mode of vibration, flexural in transverse direction
Measured period 0.1587 second
Analytical period 0.145 second (variation -8.59%)

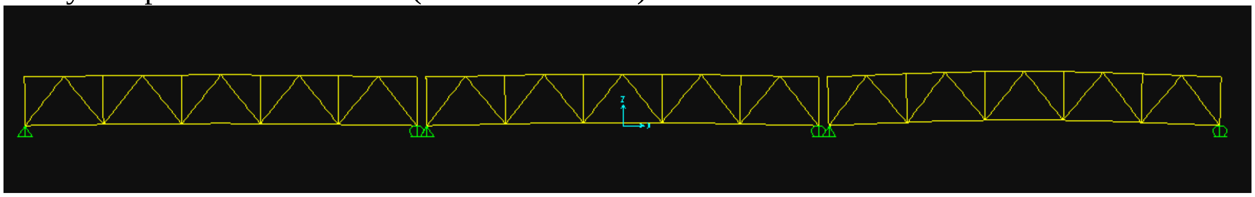

2nd mode of vibration in vertical direction
Measured period 0.125 second
Analytical period 0.1251 second (variation 0.06%)

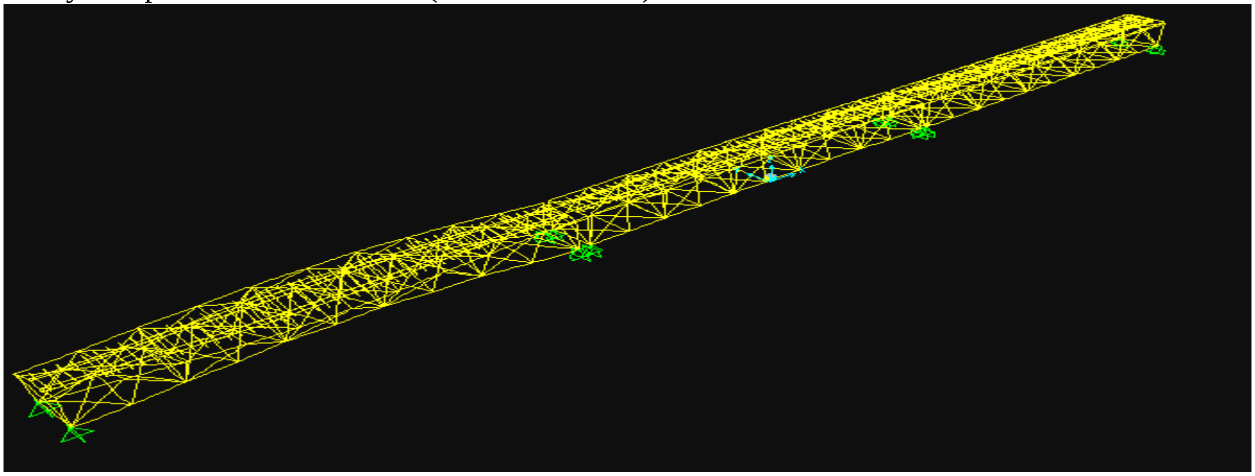

3rd mode of vibration , torsional
Measured period 0.0819 second
Analytical period 0.0766 second (variation – 6.55%)

Figure 3.3 The first three eigenperiods of the 3D finite element model

In order to assess the accuracy of the 3Dmodel to be used in the analysis, the modes of vibration obtained from software analysis were compared with those obtained from the field measurements. The first three eigenperiods of the 3D finite element model of the truss bridge and the corresponding mode shapes are shown in Fig. 3.3. From the comparison, it is obvious that, since the deviation of the analytical period from the experimental period is very insignificant, the

SAP model is valid to be used for further analysis. However, the slight variation from the experimental measurements is mainly due to the fact that the presence of masonry piles has been neglected in the numerical model

3.3 SERVICE LIFE ASSESSMENT:

The residual service life of the bridge has been calculated taking into account the fatigue resistance of the bridge. Fatigue occurs when the structure is subjected to cycles of loading and unloading. Although, the cyclic loadings may not cause stress exceeding the extreme stress limit of the material, they will lead to crack formation, propagation and eventually fracture (Thun, 2006).

The structural analysis shows that the longitudinal elements in the lower part of the main trussed Girders in the mid-span, as shown in Fig. 3.4 (element 20 in the model), is subjected to higher tensile stresses .The mid-span has been used as an indicator of fatigue life because overall maximum moment occurs in that region.

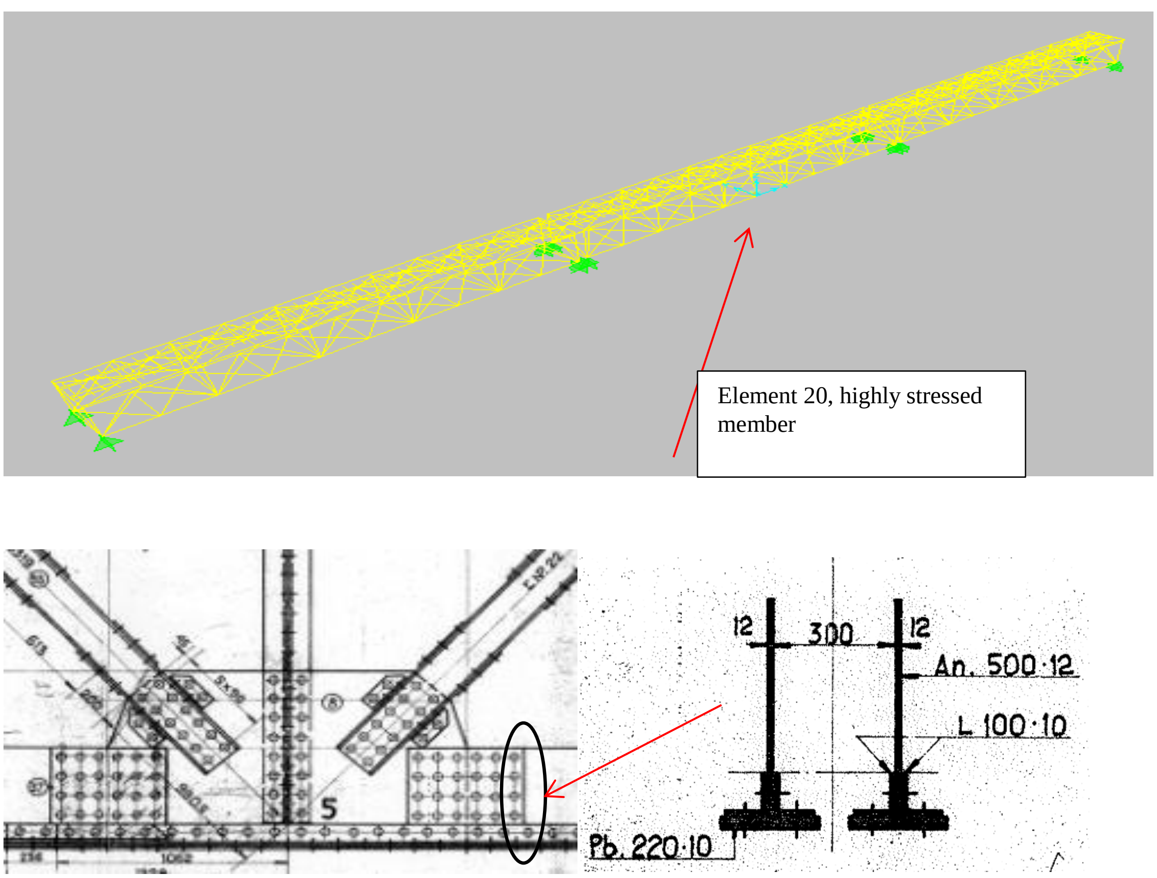

Figure 3.4 The member verified for fatigue and cross section of that member

The durability of this part of the bridge having a total cross-sectional area of 0.024 square meter has been assessed considering different combinations of train load, earthquake load, operating condition (corrosion) and maintenance program. For each combination, The total accumulated fatigue damage(D) has been calculated by Palmgren-Miner's Rule at the interval of every 10 years since the bridge construction (1966). Obviously, The residual life-time is the time corresponding to D=1.

3.4 TRAIN LOAD:

Four types of train loading are considered in this analysis:

-Condition A, it is assumed for the future, the same railway load acting till now will act on the bridge (as provided by RFI)

Type of the train	Trains per day	Axles per train	Axles per day	Speed in km/h	Load in kN
Express	7	66	462	150	9300
Through	6	46	276	140	5450
Goods	1	76	76	100	16800
Mixed (passenger+goods)	1	54	54	120	9762

Table 3.1: Railway Load; Track frequency (RFI)

-Condition B, it is assumed that the design coded railway loads have been applied from the bridge erection;

Type of the train	Trains per day	Axles per train	Axles per day	Speed in km/h	Load in kN
Express	15	66	990	150	9300
Through	30	46	1380	140	5450
Goods	5	76	380	100	16800
Mixed (passenger+goods)	5	54	270	120	9762

Table 3.2: Railway Load; Track frequency (Italian code)

-Condition C, it is assumed only passenger trains having the frequency as required by RFI;

Type of the train	Trains per day	Axles per train	Axles per day	Speed in km/h	Load in kN
Express or Passenger	15	66	990	150	9300

Table 3.3: Railway Load; considering all trains are passenger trains (RFI)

-Condition D, it is assumed only passenger trains having the frequency as given by Italian code.

Type of the train	Trains per day	Axles per train	Axles per day	Speed in km/h	Load in kN
Express or Passenger	55	66	3630	150	9300

Table 3.4: Railway Load; considering all trains are passenger trains (Italian code)

The axial force acting in the member due to the passage of each train is calculated by a multistep static analysis and taken into account the dynamic magnification factor. The dynamic magnification factor is calculated using the following formula

$$\phi_{real} = 1 + \phi' + 0.5 * \phi''; \phi_{real} \leq 2$$

$$\phi' = \frac{k}{1 - k + k^4}; k = \frac{v}{2 * L * n_0}$$

$$\phi'' = 0.1 * \alpha * (56 * e^{-(L/10)^2} - 50 * (\frac{n_0 * L}{80} - 1) * e^{-(L/20)^2})$$

$$\alpha = v / 22; v \leq 22 m / \sec$$

$$\alpha = 1; v > 22 m / \sec$$

Where, L= span length

n_0 = fundamental frequency

V= speed in m/sec. For example, in case of passenger train, the calculated dynamic magnification factor is 1.09

Type of the train	Velocity in mps, V	Span length, L	constant, K	ϕ′	0.5*ϕ″	ϕ real
Express	41.65	28.32	0.22626	0.291	0.05	1.34
Through	38.88	28.32	0.21121	0.267	0.05	1.32
Goods	27.77	28.32	0.15086	0.178	0.05	1.23
Mixed (passenger goods)	33.32	28.32	0.18101	0.221	0.05	1.27

Table 3.5: Dynamic magnification factor for different trains

After calculating the axial force, the stress can be found by dividing the force with the area. Then using the rain flow cycle counting method, the stress cycle can be determined and the stress cycle histogram can be obtained. By this histogram, the accumulated damage can be calculated using Palmgren-Miner's Rule.

3.4.1 EXPRESS OR PASSENGER TRAIN:

In the following diagram the load pattern of passenger train is shown

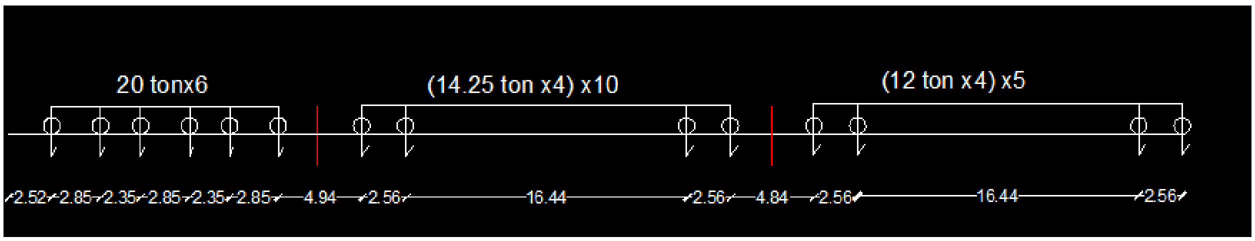

Figure 3.5 Load diagram of the express train

Due to passage of a single Express train, the different magnitude of axial force acting in different time in the member which is being checked for fatigue life (member 20), is shown in the following figure:

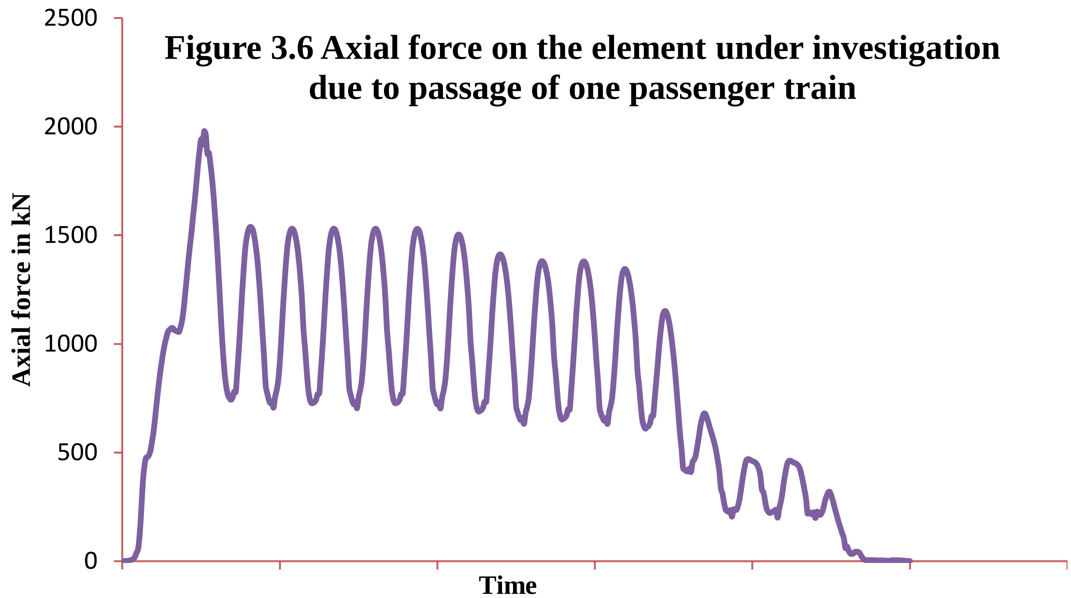

Figure 3.6 Axial force on the element under investigation due to passage of one passenger train

And the different axial stress (assuming the initial cross-sectional area) acting on the same member
in different time during the passage of a single passenger train is shown below

Figure 3. 7 Stress on the element under investigation due to passage of one passenger train

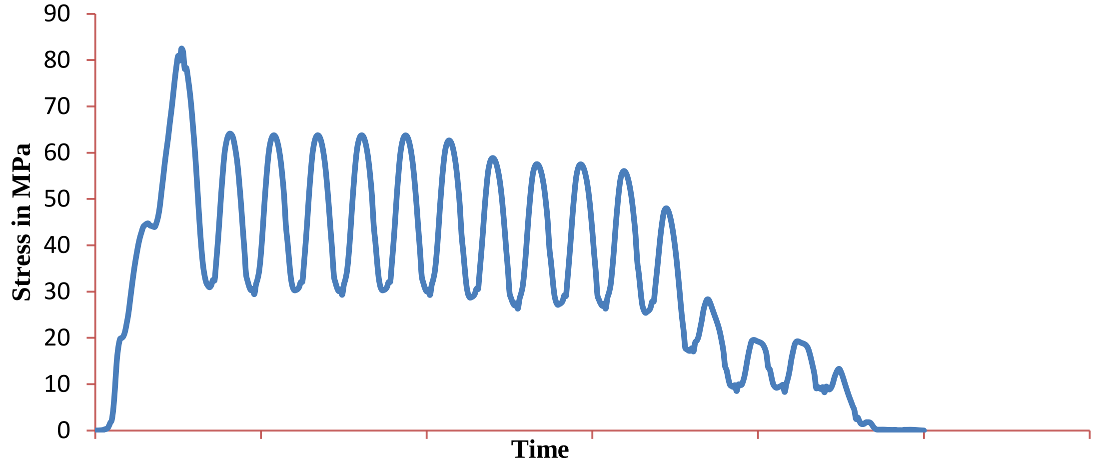

In the following table the major stress cycles acting on the member during the passage of a single passenger train, computed according to rainflow cycle counting method has been shown

Axial Force Range, ΔN in kN	Stress cycle, Δσ	Frequency
1992	83	1
816	34	6
720	30	4
552	23	1
264	11	3
120	5	1

Table 3.6: Major stress cycles observed during the passage of a single passenger train

3.4.2 THROUGH TRAIN:

In the following diagram the load pattern of through train is shown

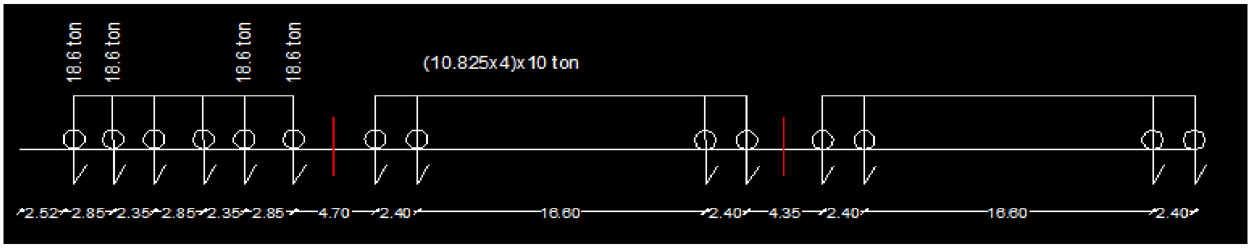

Figure 3.8 Load diagram of the through train

Due to passage of a single Express train, the different magnitude of axial force acting in different time in the member which is being checked for fatigue life (member 20), is shown in the following figure:

Fig 3.9 Axial force in the member under investigation in different time during the passage of a single train

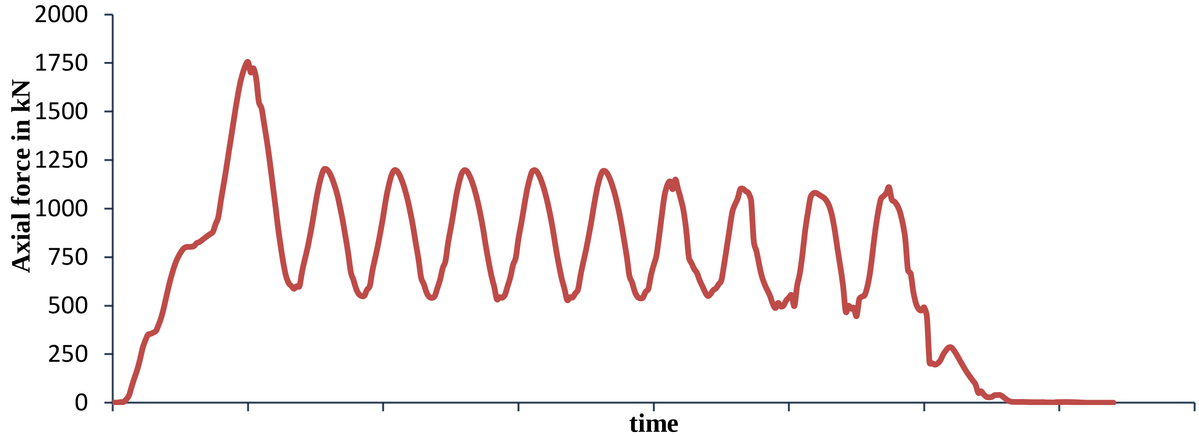

And the different axial stress (assuming the initial cross-sectional area) acting on the same member in different time during the passage of a single through train is shown below

Fig 3.10 Stress in the member under investigation in different time during the passage of a single through train

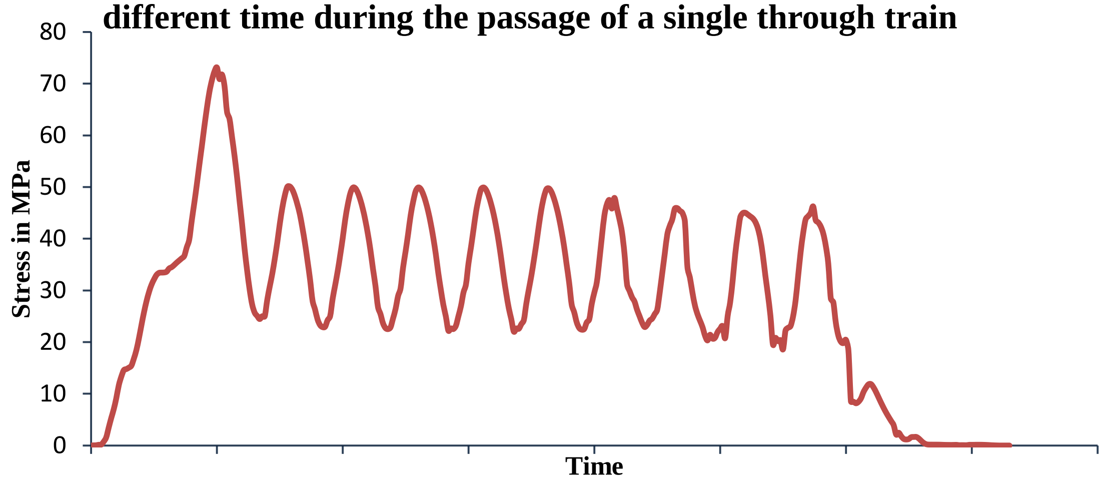

In the following table the major stress cycles acting on the member during the passage of a single through train, computed according to rainflow cycle counting method has been shown

Axial force range, ΔN in kN	Stress cycle, Δσ	Frequency
1752	73	1
672	28	5
624	26	4
96	4	1

Table 3.7: Major stress cycles observed during the passage of a single through train

3.4.3 GOODS TRAIN:

In the following diagram the load pattern of Goods train is shown

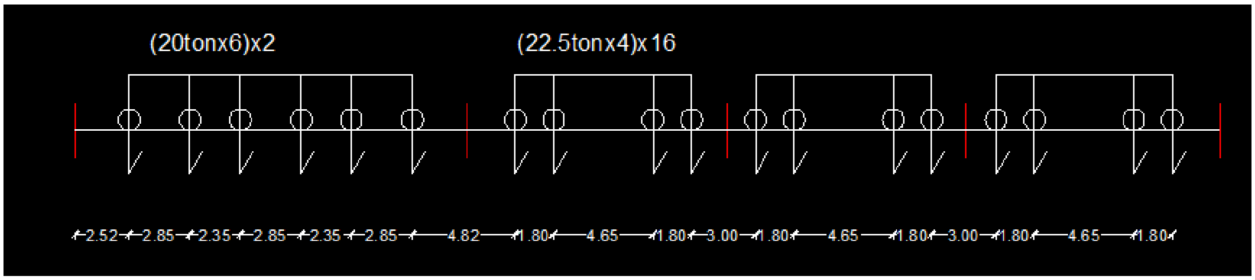

Figure 3.11 Load diagram of the goods train

Due to passage of a single Goods train, the different magnitude of axial force acting in different time in the member which is being checked for fatigue life (member 20), is shown in the following figure:

Fig 3. 12 Axial force in the member under under investigation in different time due to passage of a single goods train

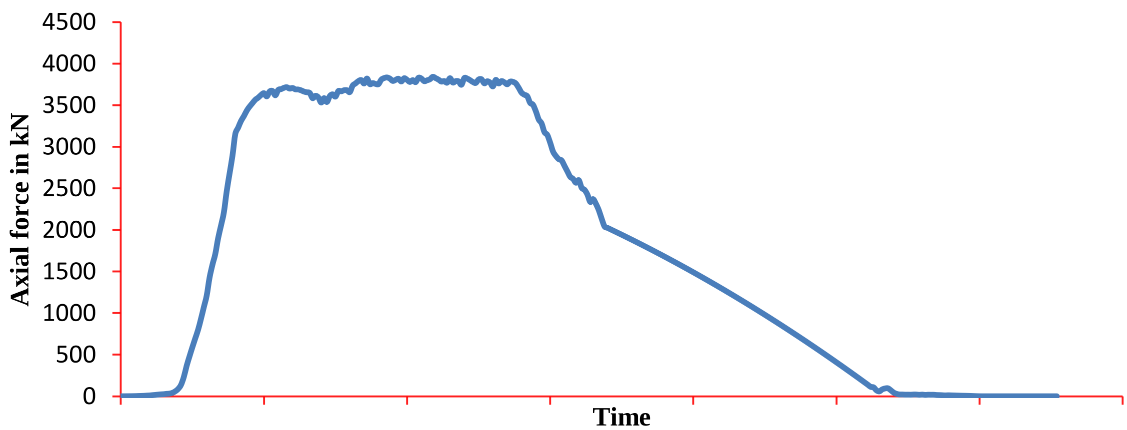

And the different axial stress (assuming the initial cross-sectional area) acting on the same member in different time during the passage of a single goods train is shown below

Fig 3.13 Stress in the member under investigation in different time due to passage of a single goods train

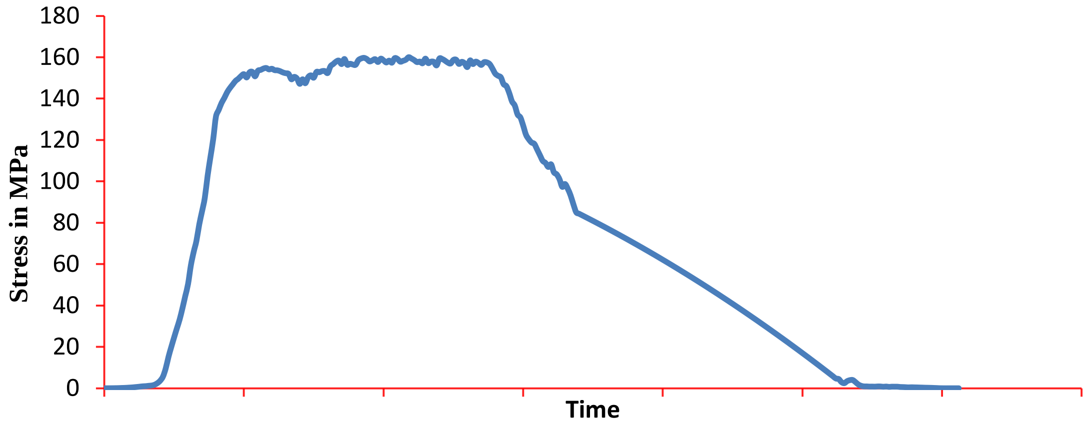

In the following table the major stress cycles acting on the member during the passage of a single goods train, computed according to rainflow cycle counting method has been shown

Axial force range, ΔN in kN	Stress cycle, Δσ	Frequency
3792	158	1

Table 3.8: Major stress cycles observed during the passage of a single goods train

3.4.4 MIXED (PASSENGER+GOODS)TRAIN:

In the following diagram the load pattern of Mixed train is shown

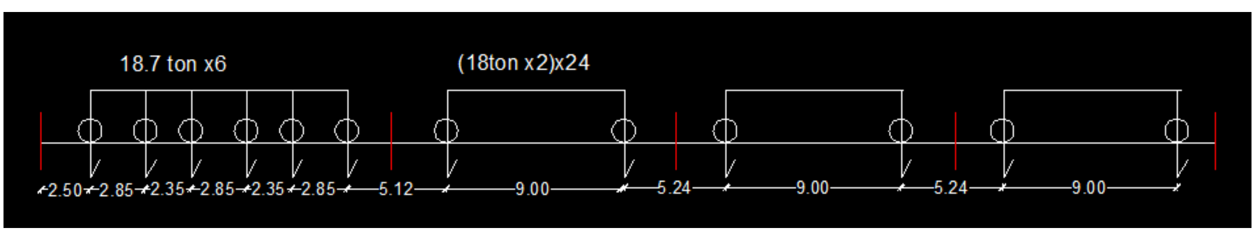

Figure 3.14 Load diagram of the mixed train

Due to passage of a single Mixed train, the different magnitude of axial force acting in different time in the member which is being checked for fatigue life (member 20), is shown in the following figure:

Fig 3.15 Axial force acting in the member under investigation in different time during the passage of a single mixed train

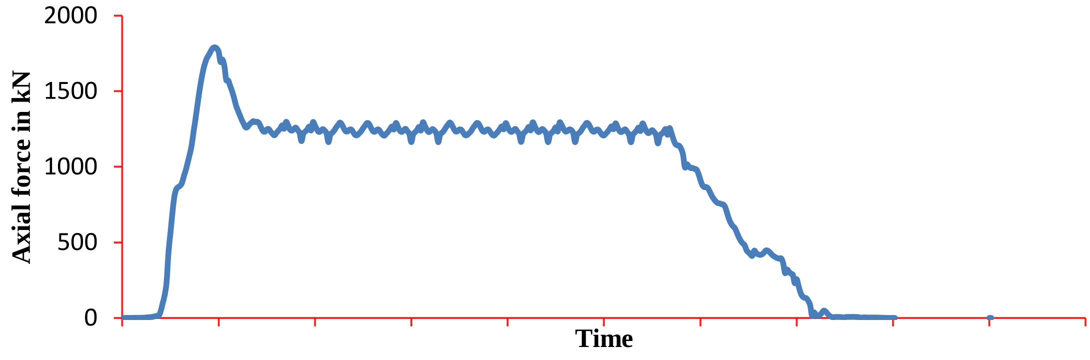

And the different axial stress (assuming the initial cross-sectional area) acting on the same member in different time during the passage of a single Mixed train is shown below

Fig 3.16 Stress in the member under investigation in different time due to passage of a single Mixed train

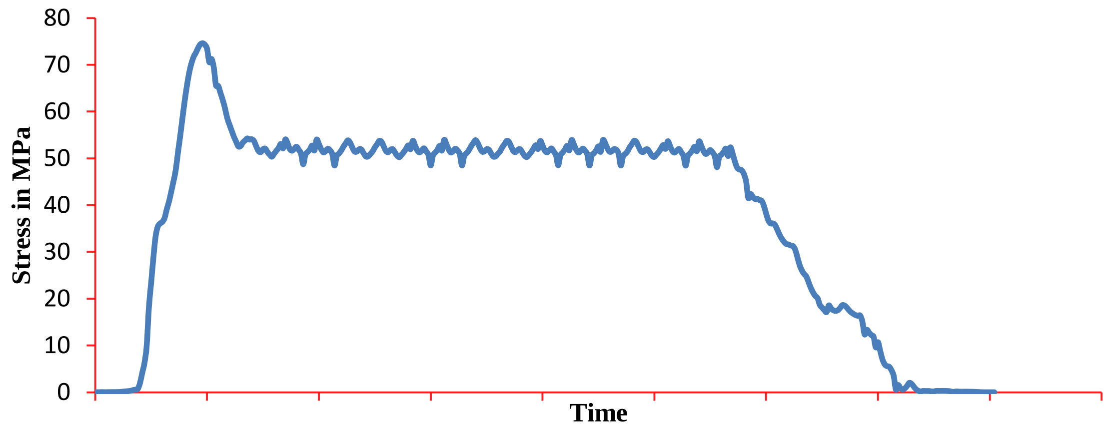

In the following table the major stress cycles acting on the member during the passage of a single Mixed train, computed according to rainflow cycle counting method has been shown

Axial force range, ΔN in kN	Stress cycle, Δσ	Frequency
1800	75	1
120	5	8
96	4	7

Table 3.9: Major stress cycles observed during the passage of a single Mixed train

3.5 EARTHQUAKE LOAD:

For the purpose of this analysis, it is assumed that the bridge will be subjected to three hypothetical earthquake events. The first earthquake will occur 60 years after the bridge had been put into service (1966 A.D.) that is in the year 2026. The second earthquake will occur 90 years after that is in the year 2056. And the third earthquake will occur 120 years after that is in the year 2096.The magnitude and the effect of these earthquakes on the member under investigation have been illustrated in the following.

3.5.1 EARTHQUAKE 1:

The accelerogram of artificial earthquake 1 is shown in the following figure. It can be noted that the peak ground acceleration is almost 10 m/sec^2 (1g).

Fig 3.17 Accelerogram of earthquake 1

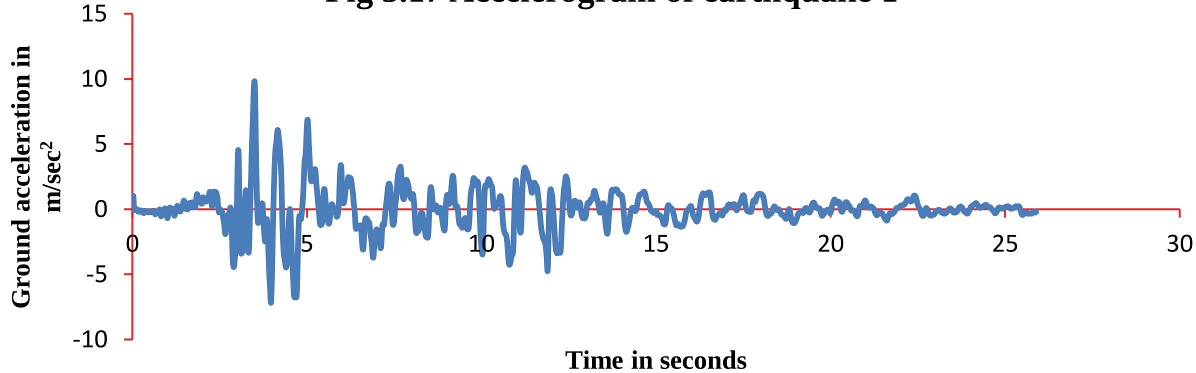

A time history analysis is performed in SAP2000 and the resulting axial force acting in different time on the member under investigation is shown below

Fig 3.18 Axial force in the member under investigation due to Earthquake 1

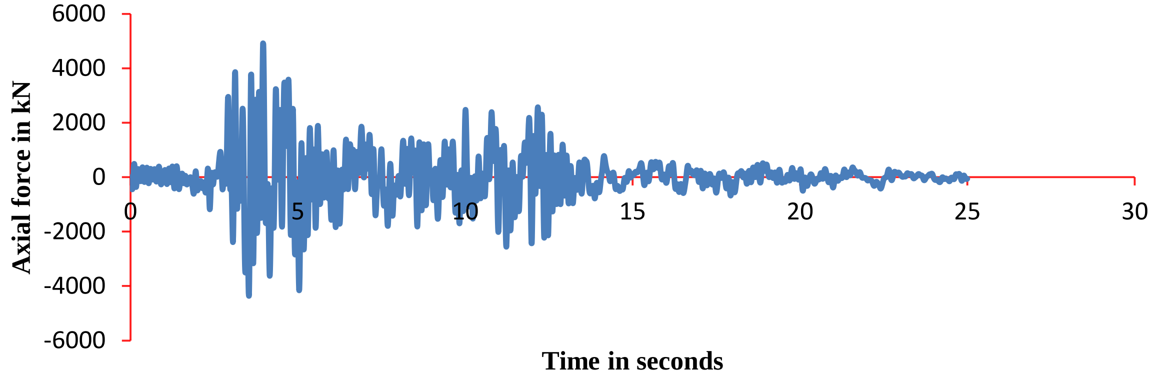

Assuming initial cross/sectional area, the Stress acting in different time on the member under investigation due to this earthquake is shown below

Fig 3.19Stress acting in the member under investigation due to earthquake 1

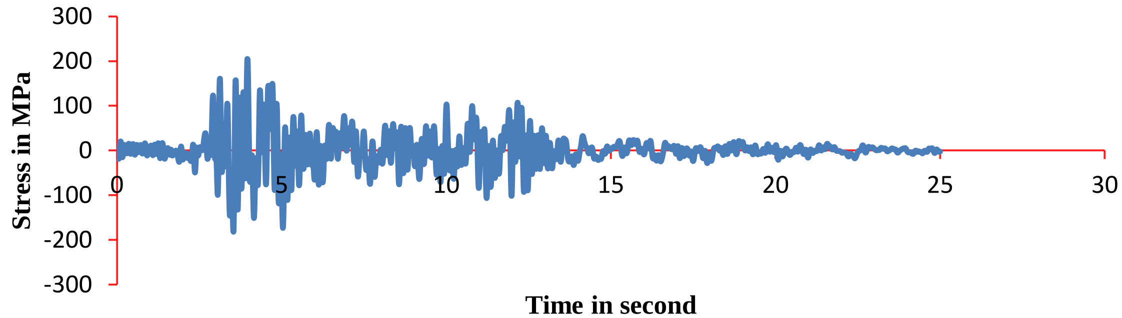

Using rainflow cycle counting method number of cycles and corresponding stress ranges have been determined and the rainflow stress histogram has been constructed which is shown below

Fig 3.20 Rainflow Histogram for earthquake 1 (member 20)

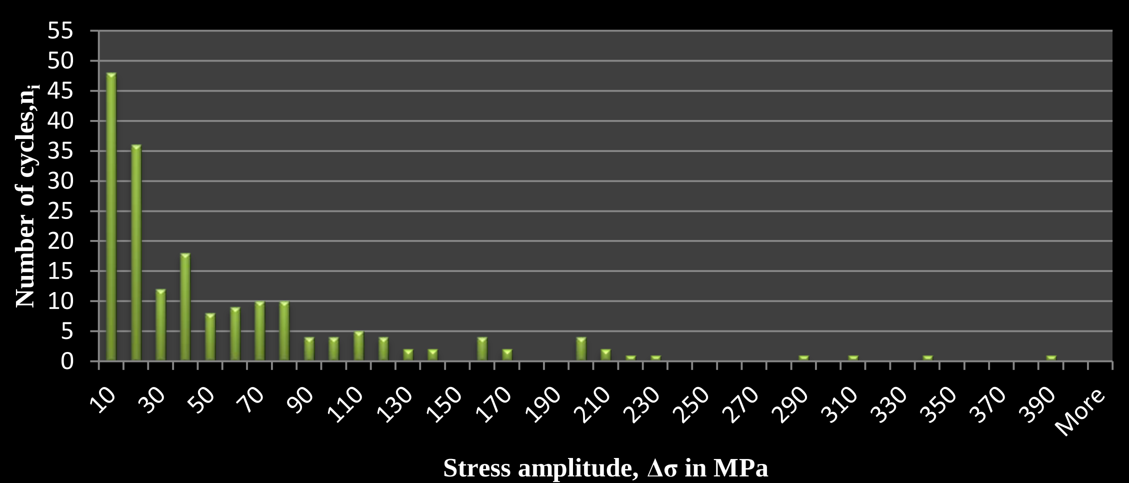

3.5.2 EARTHQUAKE 2:

The accelerogram of artificial earthquake 2 is shown in the following figure. It can be noted that the peak ground acceleration is almost 9.8 m/sec^2 (1g).

Fig 3.21 Accelerogram of earthquake 2

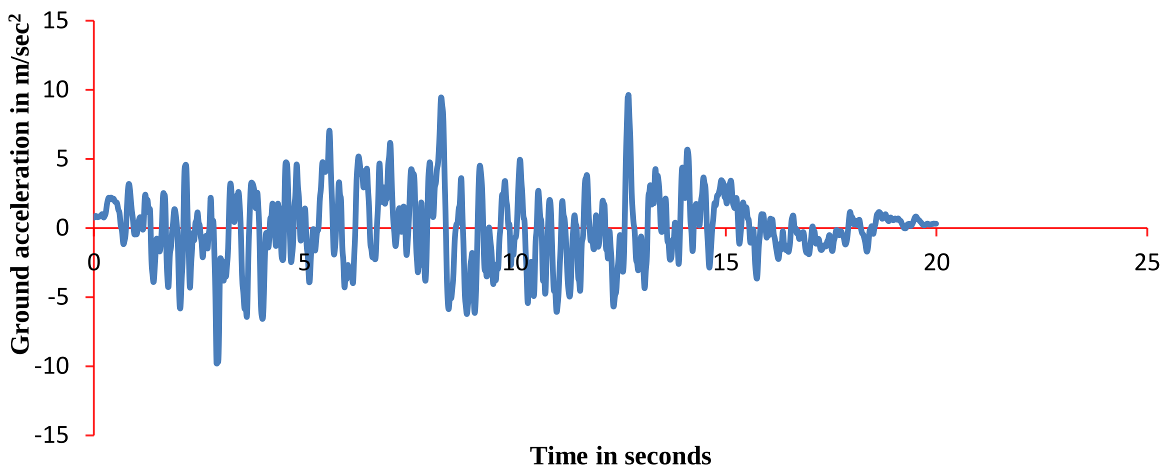

A time history analysis is performed in SAP2000 and the resulting axial force acting in different time on the member under investigation is shown below

fig 3.22 Axial force acting in the member under investigation due to earthquake 2

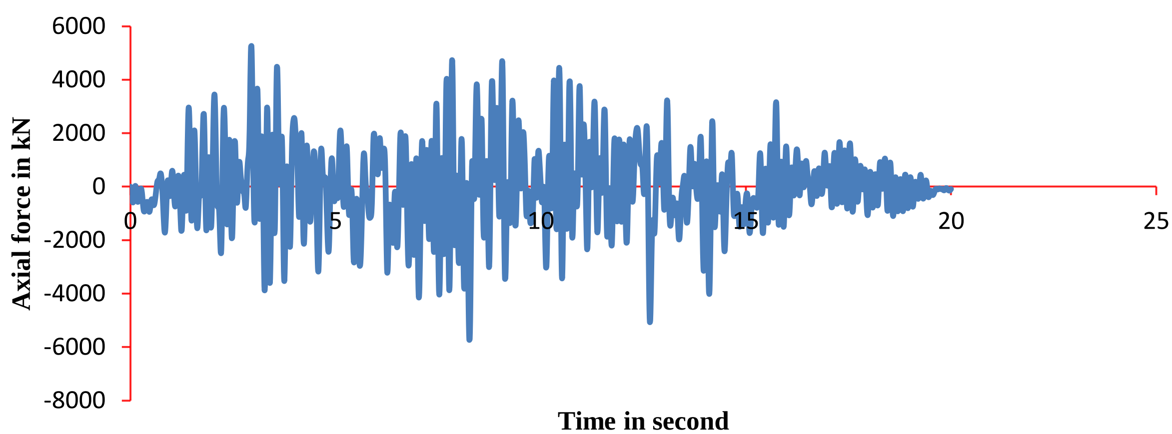

Assuming initial cross/sectional area (0.024 square meter), the Stress acting in different time on the member under investigation due to this earthquake is shown below

fig 3.23 Stress acting in the member under investigation due to earthquake 2

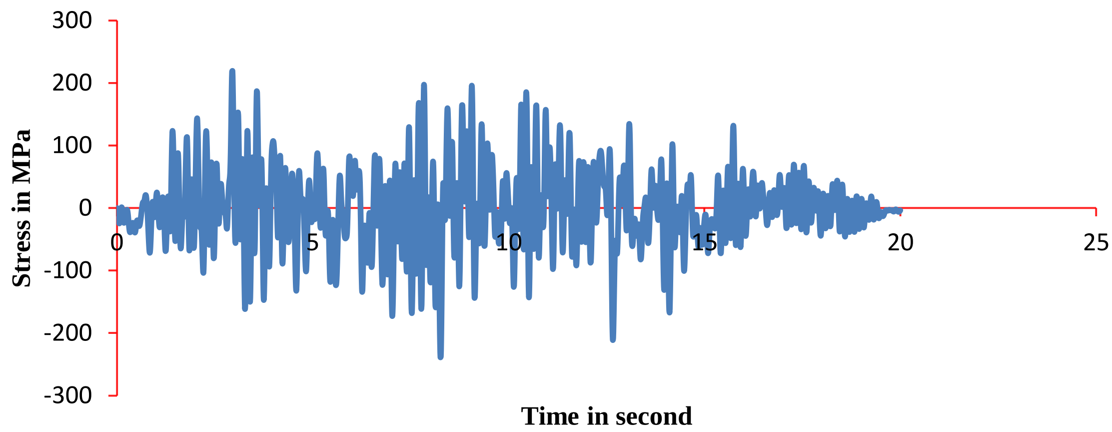

Using rainflow cycle counting method number of cycles and corresponding stress ranges have been determined and the rainflow stress histogram has been constructed which is shown below

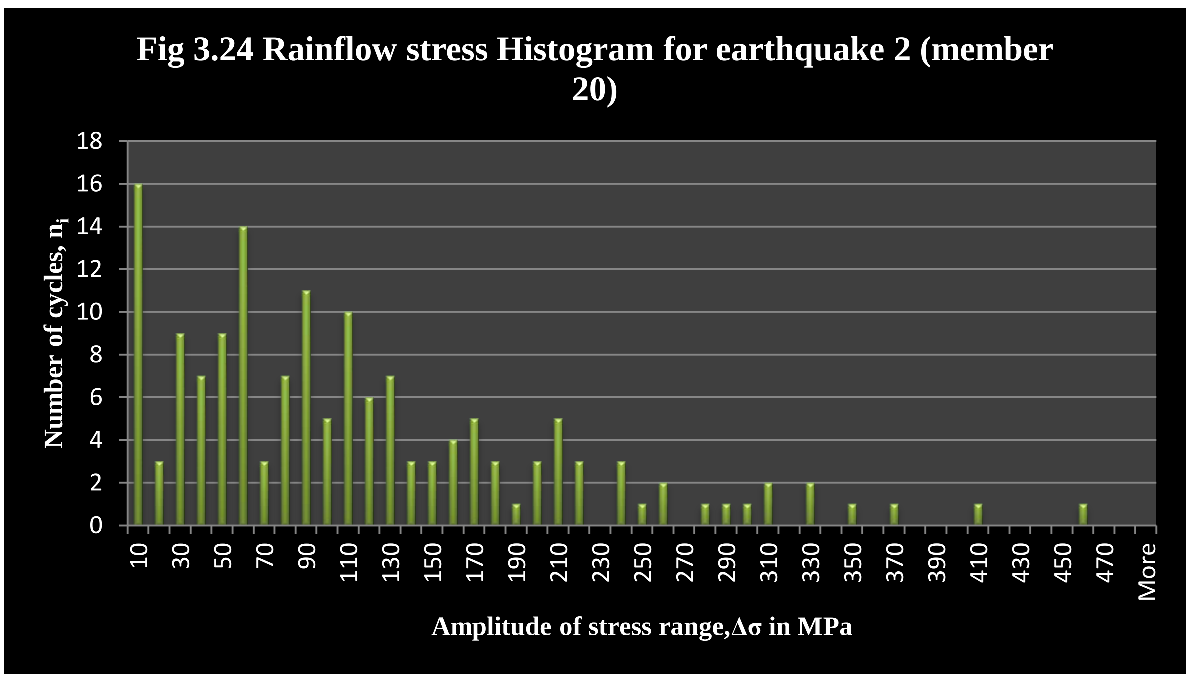

3.5.3 EARTHQUAKE 3:

The accelerogram of earthquake 2 is shown in the following figure. It can be noted that the peak ground acceleration is almost 9.8 m/sec^2 (1g).

fig 3.25 Accelerogram of Earthquake 3

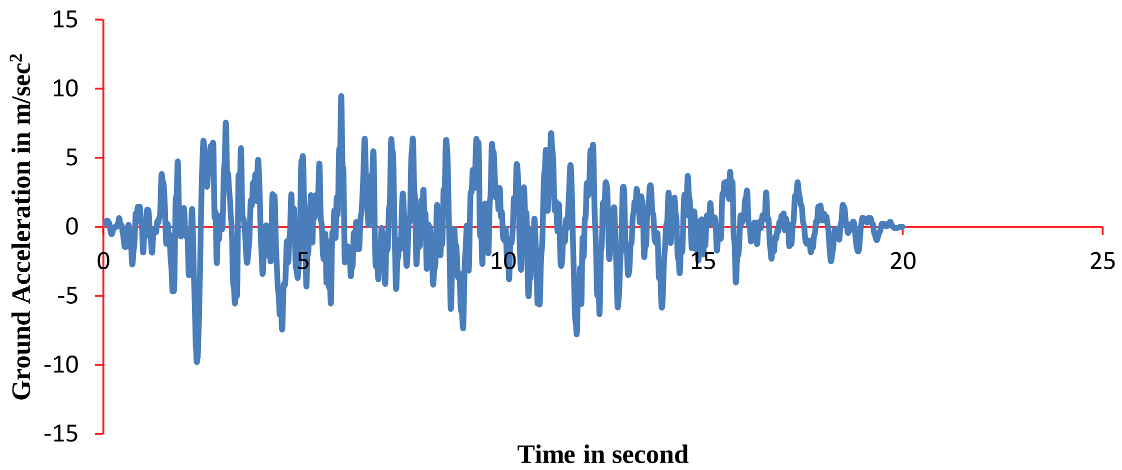

A time history analysis is performed in SAP2000 and the resulting axial force acting in different time on the member under investigation is shown below

fig 3.26 Axial force acting in the member under investigation due to earthquake 3

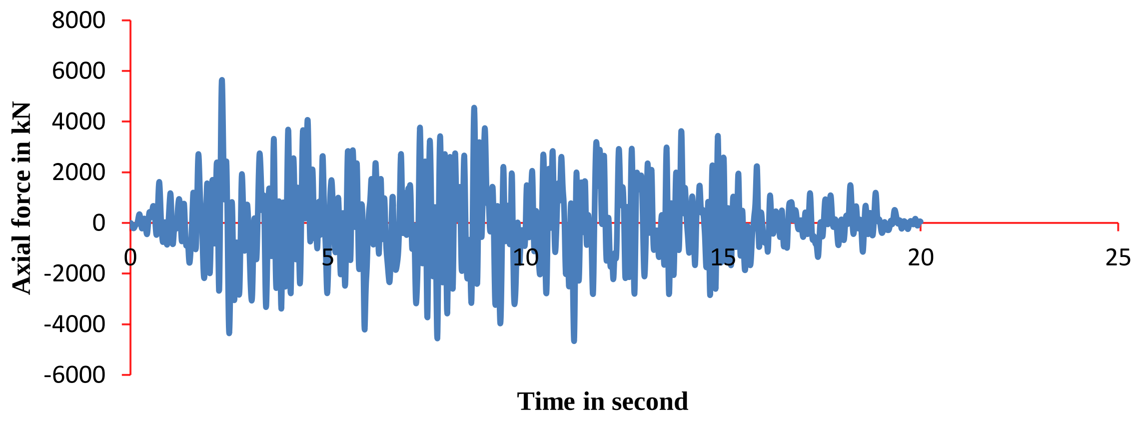

Assuming initial cross/sectional area (0.024 square meter), the Stress acting in different time on the member under investigation due to this earthquake is shown below

Fig 3.27 Stress acting in the member under investigation due to earthquake 3

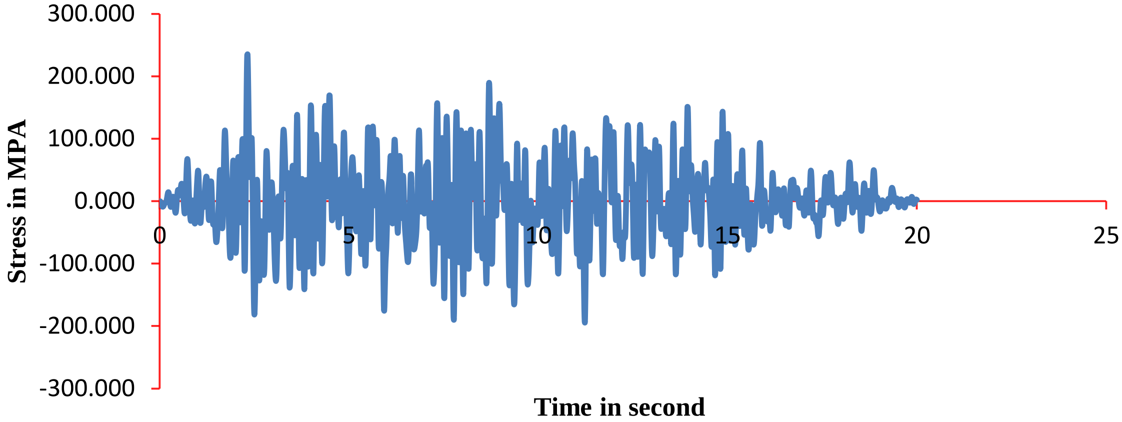

Using rainflow cycle counting method number of cycles and corresponding stress ranges have been determined and the rainflow stress histogram has been constructed which is shown below

Fig 3.28 Rain flow stress Histogram for earthquake 3 (member 20)

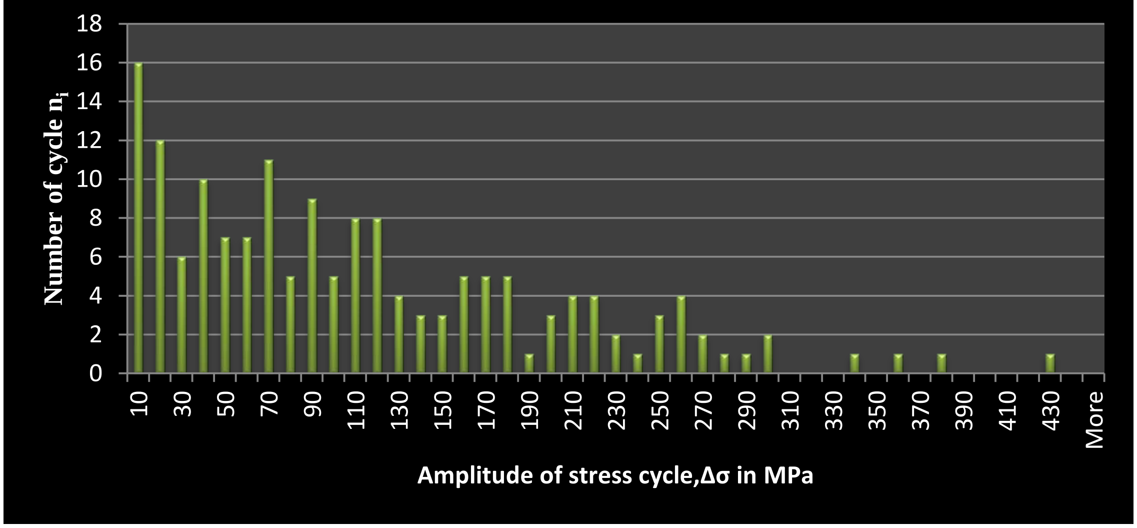

3.6 ATMOSPHERIC CONDITION; CORROSION:

The corrosion phenomena of metals and alloys involve mainly two elements: the material and its environment. In particular, corrosion is defined as the deterioration of a material, usually a metal, which results from a reaction with its environment, causing the degradation of both (Landolfo, 2010).

From the structural point of view, the loss of thickness of the cross section due to corrosion attack leads to a smaller resistant area and increased stress, resulting in a decrease of fatigue resistance and hence the service life. To investigate the effect of corrosion in the service life of our bridge only uniform corrosion of the component is considered, local corrosion in the connections, pitting in the coating protective and fatigue damage have been neglected.

The corrosiveness of atmosphere has been selected according to the qualitative procedure provided in EN 12500 (2000) and the structure environment corresponds to a medium corrosivity class C3. As for deterioration model at material level, the dose-response function that describes the evolution of the degradation with time has been selected according to the ISO Standard 9224 (1992). Such model expresses that the average corrosion rate of each material follows a bi-linear law. During the first 10 years of atmospheric exposure, the corrosion depth is given by the formula:

$$d_1(t) = r_{av}.t; t < 10 years$$

Where

$d_1(t)$ = corrosion depth after the first 10 years of exposure (micrometers);

r_{av} = average corrosion rate (micrometers per year);

t = time at which the exposure ends.

After 10 years of exposure, the corrosion rate is assumed to be constant with time and the thickness loss is given by the formula:

$$d(t) = r_{av}.10 + r_{lin}(t - 10); t \geq 10 years$$

Where

d(t) = corrosion depth for the considered time interval (micrometers);

r_{lin} = steady state corrosion rate (micrometers per year);

t=time in the linear region of the curve of uniform corrosion as function of time.

Reference values for material are reported in ISO 9224 (1992). As for the case study under investigation, the average corrosion rate of 12 µm/year and the steady state corrosion rate of 6 µm/year have been selected. For this rates, the thickness loss for corrosion of carbon steel in C3 corrosiveness class with respect to time is shown in the following figure

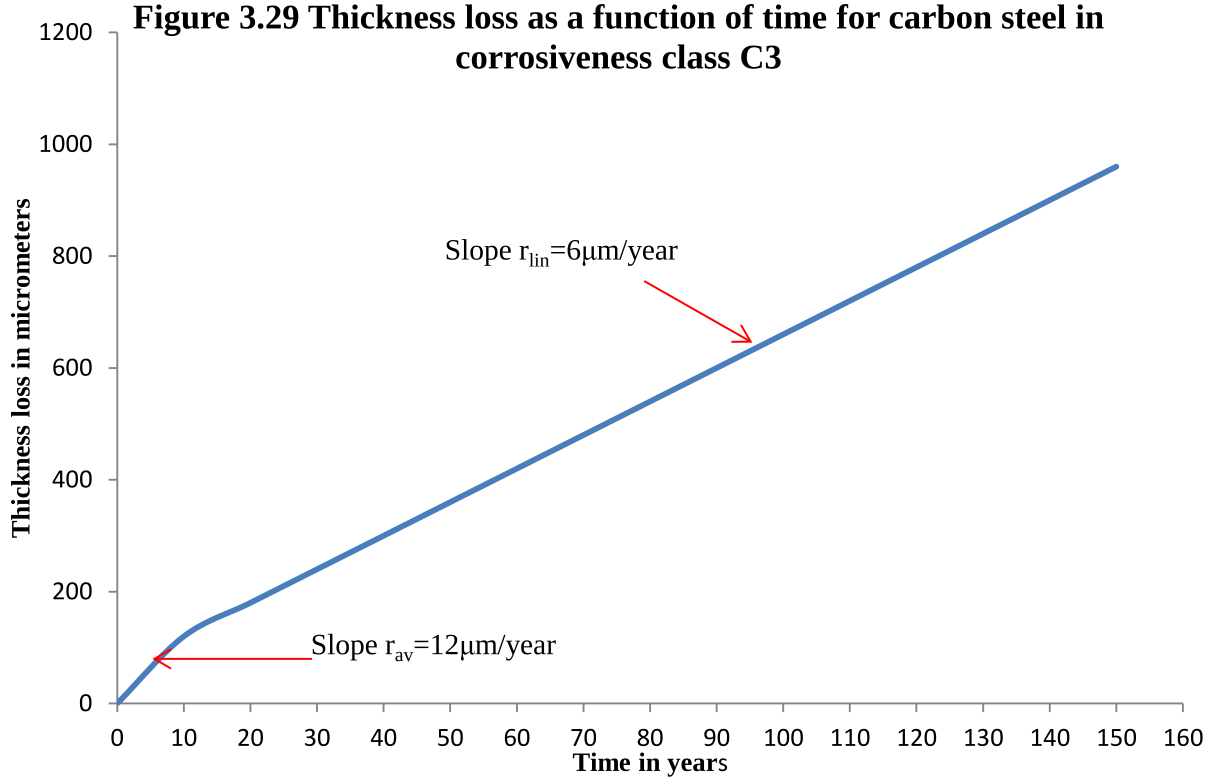

Figure 3.29 Thickness loss as a function of time for carbon steel in corrosiveness class C3

3.7 MAINTENANCE SCENARIO:

In this analysis three maintenance scenarios have been assumed:

1) No maintenance;
2) Painting every 10 years carried out into the first 30 years from bridge construction, but no further maintenance intervention after that;
3) Painting every 30 years;

For the purpose of this analysis, in compliance with the information provided by RFI ,it is assumed that every maintenance intervention is capable of protecting the bridge material from corrosive degradation for a period of ten years.

3. 7.1 NO MAINTENANCE:

For this scenario, it is assumed that maintenance operation such as painting is never carried out since the bridge had been put into service. However in the light of the information provided by RFI, for the first 10 years after the bridge had been put into service (1966 to 1976), since the bridge is new and painted, it is quite justified to assume that no deterioration in the bridge material had occurred due to corrosion. After that period, the material corroded at the average corrosion rate r_{av}=12 µm/year for the first 10 years (1976 to 1986) and then onwards it continued to corrode at the linear corrosion rate r_{lin}=6 µm/year. According to this maintenance scenario, the thickness loss due to corrosion is shown in the following figure:

Figure 3. 30Thickness loss due to corrosion in different year under no maintenance scenario

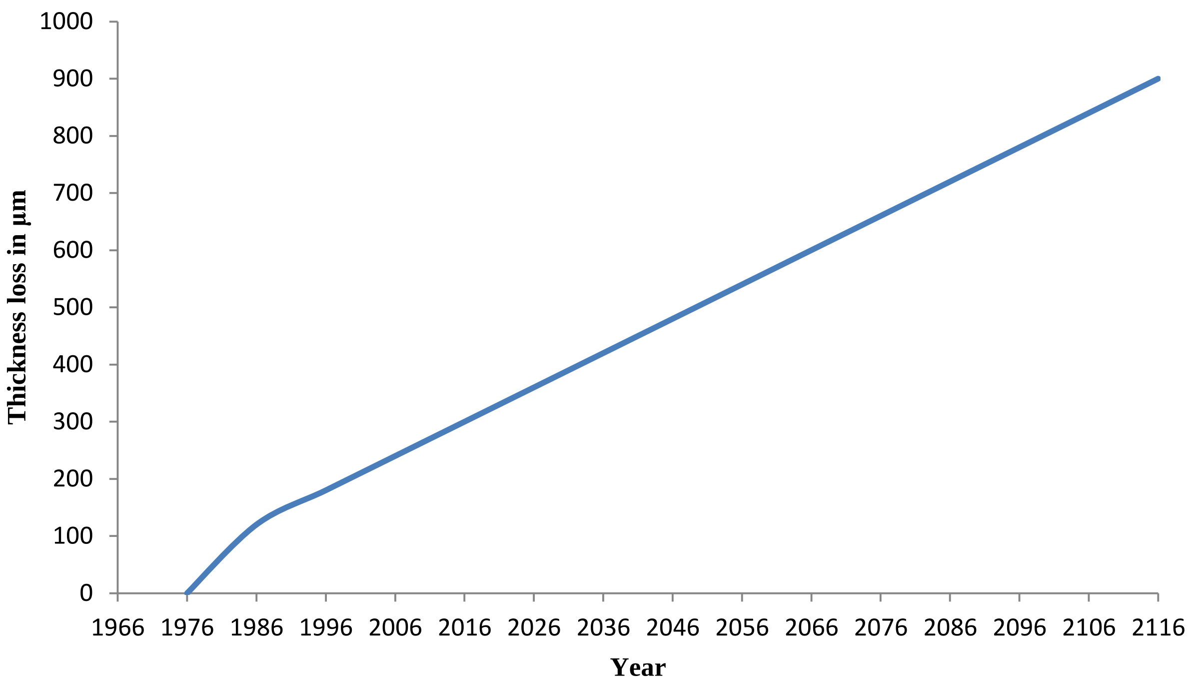

3. 7.2 PAINTING EVERY 10 YEARS FOR THE FIRST THIRTY YEAR:

Under this maintenance scenario, it is assumed that, corrosion protective painting woks are carried out in every 10 years for the first 30 years from bridge construction, but no further maintenance was done after that. So, for the first 10 years after the bridge had been put into service (1966 to 1976), since the bridge is new, there was no thickness loss due to corrosion. 10

years after that (in the year 1976), the first painting was done and it is presumed that, this maintenance intervention protected the bridge from corrosion for the next 10 years. So, for that period (1976-186), no material degradation had occurred due to corrosion. The second painting was provided 10 years after the first painting (i.e. in the year 1986). Similarly, that painting would protect the bridge material from corrosion for the next 10 years (1986-1996).The third maintenance intervention done 10 years after that (i.e. in the year 1996) would provide protection from corrosion for the next 10years (from 1996 to2006) in the same manner. So, the corrosion would initiate 40 years after the bridge construction (2006), and the bridge material would lose thickness at the rate of 12 μm/year for the first 10 years (2006-2016) and then onwards it continued to corrode at the linear corrosion rate r_{lin}=6 μm/year. According to this maintenance scenario, the thickness loss due to corrosion is shown in the following figure:

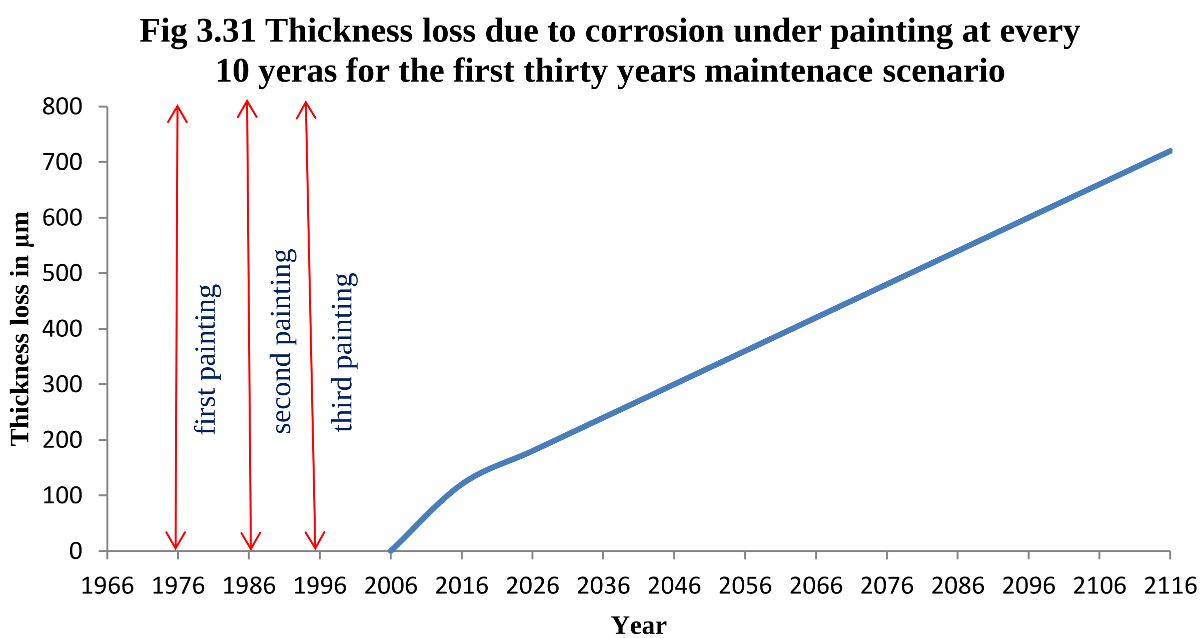

3. 7.3 PAINTING EVERY 30 YEARS:

Under this maintenance scenario, it is assumed that, corrosion protective painting woks are carried out in every 30 years interval from the year the bridge had been put into service. So, first painting was done 30 years after the bridge construction, i.e. in the year 1996, second painting was provided 60 years after the bridge construction, i.e. in the year 2026 and so on. For the first 10 years after the bridge had been put into service (1966 to 1976), since the bridge is new, there was no thickness loss due to corrosion. . So, the corrosion would start 10 years after the bridge construction (i.e. in the year 1976), and the bridge material would lose thickness at the average corrosion rate of r_{av}=12 μm/year for the first 10 years (1976 to 1986) and then for the next 10 years (1986-1996) it would corrode at the linear corrosion rate r_{lin}=6 μm/year. The first maintenance intervention after 30years of bridge construction (i.e. in the year 1996) would protect the corrosive deterioration of the bridge material for the next 10 years (1996-2006). After this period the bridge material would corrode at the linear corrosion rate of r_{lin}=6 μm/year for the next 20 years (2006-2026) until the second painting is provided in the year 2026. Then onwards it would follow the similar pattern of corrosion as described before. The thickness loss due to corrosion under this maintenance scenario is shown in the following figure:

Figure 3. 32 Thickness loss due to corrosion uder painting every 30years maintenance scenario

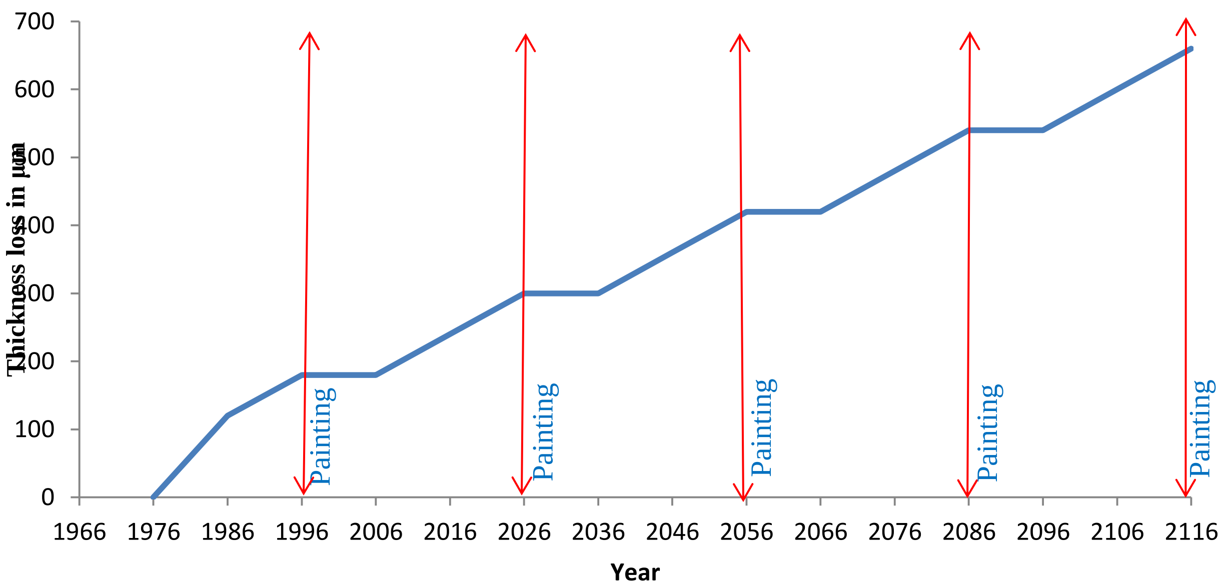

3.8 OPERATING SCENARIOS:

Hence, combining all the examined variables (train loads, earthquake load, corrosion and maintenance), a total number of 16 operating scenarios have been analyzed and the fatigue capacity has been verified at every 10 years interval for a period of 150 years from the year of bridge construction. The details of each operating scenario are given.

Category	Railway loads	Earthquake load	Corrosion phenomenon	Maintenance plan
A1	Mixed Track (According to RFI)	Yes, at 60, 90 and 120 years after construction	No corrosion	No maintenance
A2	Mixed Track (According to RFI)	Yes, at 60, 90 and 120 years after construction	Corrosion at specified rate	No maintenance
A3	Mixed Track (According to RFI)	Yes, at 60, 90 and 120 years after construction	Corrosion at specified rate	First 30years
A4	Mixed Track (According to RFI)	Yes, at 60, 90 and 120 years after construction	Corrosion at specified rate	Every thirty years
B1	Mixed Track (According to Italian code)	Yes, at 60, 90 and 120 years after construction	No corrosion	No maintenance
B2	Mixed Track (According to Italian code)	Yes, at 60, 90 and 120 years after construction	Corrosion at specified rate	No maintenance
B3	Mixed Track (According to Italian code)	Yes, at 60, 90 and 120 years after construction	Corrosion at specified rate	First 30years
B4	Mixed Track (According to Italian code)	Yes, at 60, 90 and 120 years after construction	Corrosion at specified rate	Every thirty years
C1	Passenger Trains (According to RFI)	Yes, at 60, 90 and 120 years after construction	No corrosion	No maintenance
C2	Passenger Trains (According to RFI)	Yes, at 60, 90 and 120 years after construction	Corrosion at specified rate	No maintenance
C3	Passenger Trains (According to RFI)	Yes, at 60, 90 and 120 years after construction	Corrosion at specified rate	First 30years
C4	Passenger Trains (According to RFI)	Yes, at 60, 90 and 120 years after construction	Corrosion at specified rate	Every thirty years
D1	Passenger Trains (According to Italian code)	Yes, at 60, 90 and 120 years after construction	No corrosion	No maintenance
D2	Passenger Trains (According to Italian code)	Yes, at 60, 90 and 120 years after construction	Corrosion at specified rate	No maintenance
D3	Passenger Trains (According to Italian code)	Yes, at 60, 90 and 120 years after construction	Corrosion at specified rate	First 30years
D4	Passenger Trains (According to Italian code)	Yes, at 60, 90 and 120 years after construction	Corrosion at specified rate	Every thirty years

Table 3.10: Operating Scenarios

3.8.0 PALMGREN MINER'S RULE; SELECTION OF S-N CURVE:

According to the Palmgren-Miner's The cumulative damage ratio,

$$\sum_{i=1}^{n} \frac{n_i}{N_i} = D$$

Here, n_i =Number of load cycles corresponding to a certain stress level

N_i =The number of load cycles that causes failure for a specific stress level

D =Damage ratio

The values of Ni can be obtained from the appropriate S-N curve. For our analysis, the S-N curve for riveted element proposed by Pipinato, 2006 in the paper 'Fatigue tests on riveted steel elements taken from a railway bridge' has been adopted. This curve is a modification of the S-N curve for detail category C=63 given by Eurocode 3 EN 1993-1-9. The best fit equation of the proposed curve is

$$\log N = 13.835 - 3.784 \log \Delta\sigma$$
$$\Rightarrow N = 10^{13.835} . \Delta\sigma^{-3.784}$$

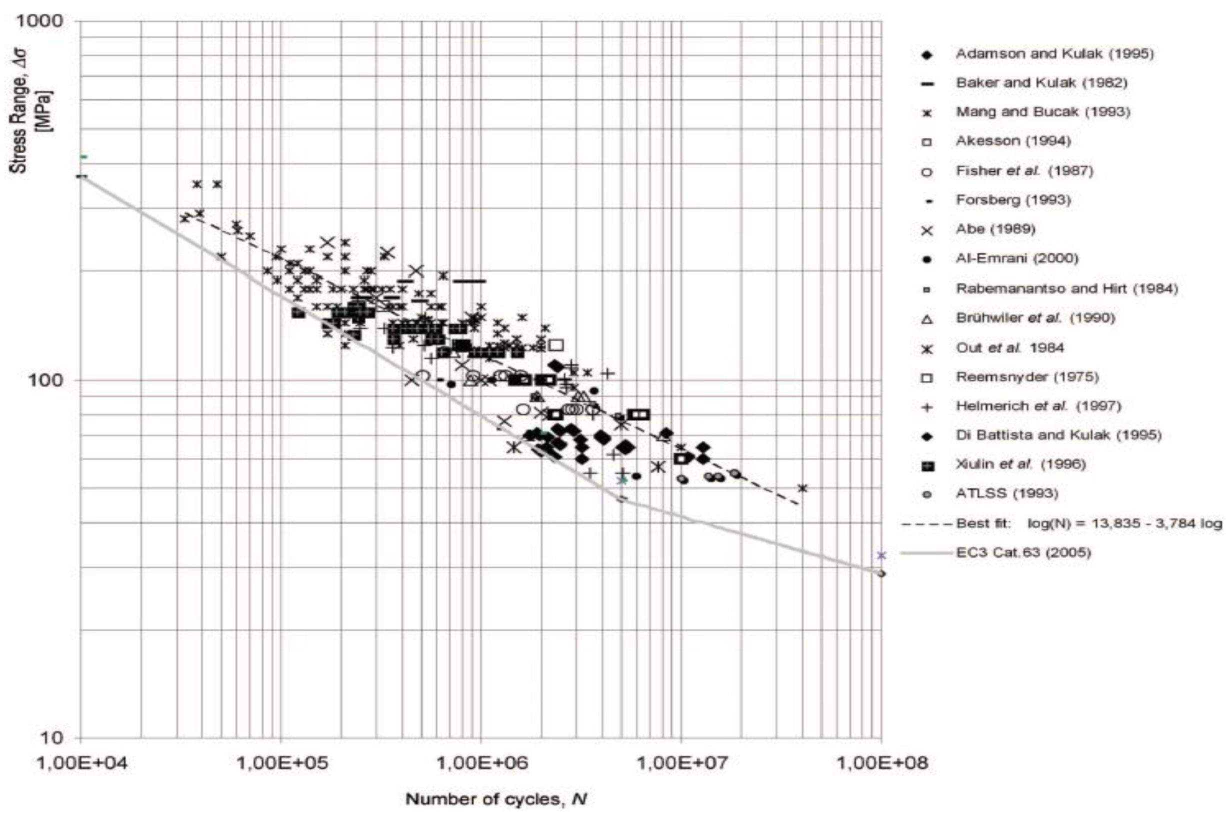

Figure 3.33: Selected S-N curve

3.8.1 OPERATING SCENARIO A1:

Under this operating condition passenger, goods, through and mixed train loads are applied according to the frequency specified by RFI. Three Earthquakes events of magnitude described before are applied at 60, 90 and 120 years from year of bridge construction (i.e. in the year 2026, 2056 and2086). It is also assumed that there is no degradation of bridge material due to corrosion and there is no maintenance program carried out. For this operating scenario, the damage ratio for the first 10 years after the bridge construction is shown in the following table

Axial force range in kN, ΔN	Area of the cross-section in sqm, A	Stress range in MPa, $\Delta\sigma$	Total cycles in 10 years n_i	Number of cycles to failure, N_i	n_i/N_i
3792	0.024	158	3650	327553.0012	0.01114323
1992	0.024	83	25550	3742902.364	0.00682625
1800	0.024	75	3650	5492476.145	0.00066455
1752	0.024	73	21900	6083959.261	0.00359963
816	0.024	34	153300	109618480.6	0.00139849
720	0.024	30	102000	176024521.4	0.00057946
672	0.024	28	109500	228535677.8	0.00047914
624	0.024	26	87600	302510777.1	0.00028958
552	0.024	23	25550	481085058.1	5.3109E-05
264	0.024	11	76650	7840975184	9.7756E-06
120	0.024	5	54750	1.54916E+11	3.5342E-07
96	0.024	4	47450	3.60417E+11	1.3165E-07
				Total damage ratio in 1st ten years=	**0.0250437**

Table 3.11: Damage ratio for first 10 years (1966-1976) under A1

Similarly, for every 10 years the same damage ratio will be found. The damage ratio for the earthquakes can be calculated from the rainflow histogram .Assuming no reduction in the cross-sectional area, the calculated damage ratio for the first earthquake, which will occur in the year 2026 is 0.00332. The calculated damage ratio for the second earthquake, which will occur in the year 2056 is 0.00997. The calculated damage ratio for the third earthquake, which will occur in the year 2086 is 0.009.

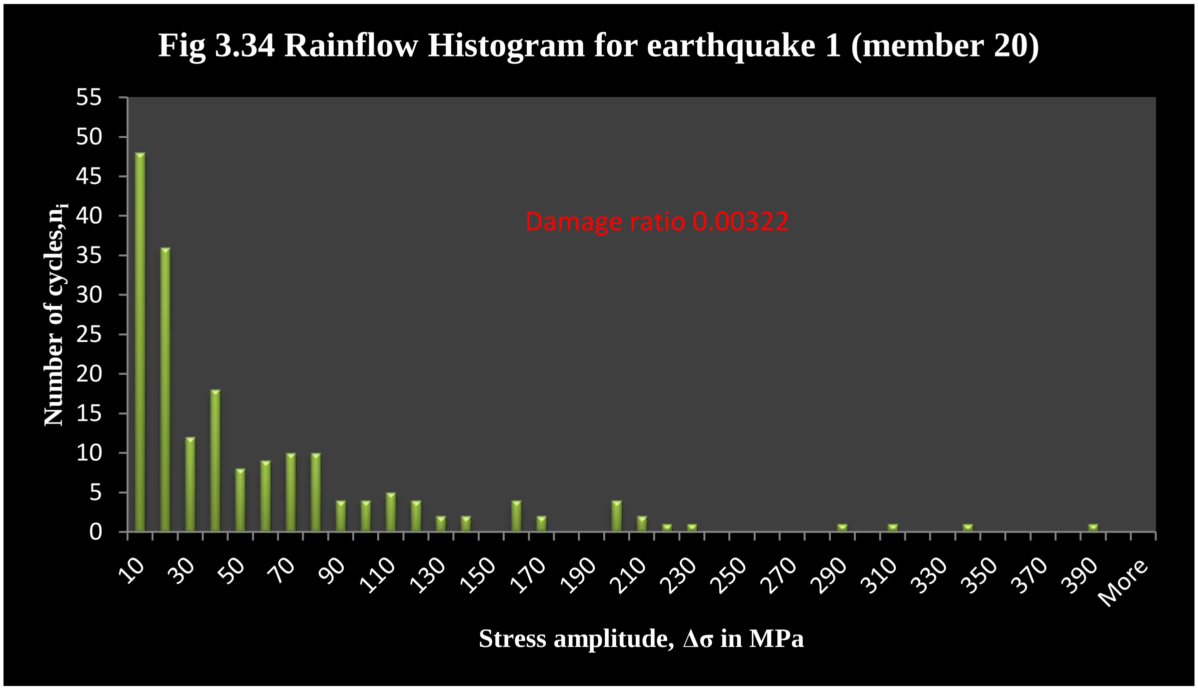

Figure 3.34: Rainflow histogram for the first earthquake in 2026, under scenario A1

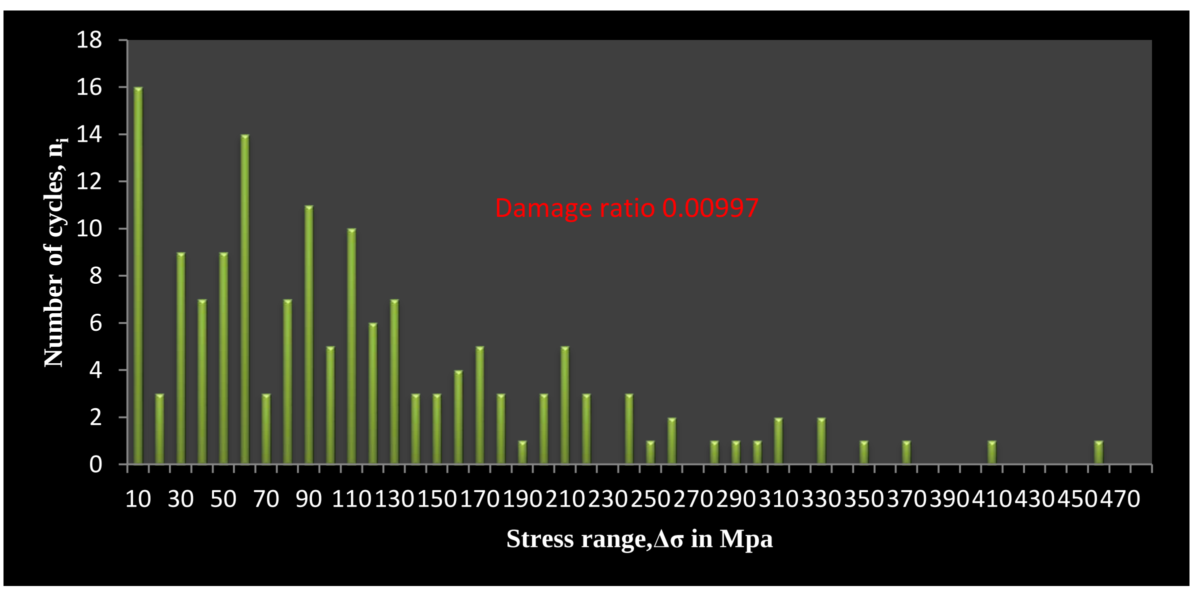

Figure 3.35: Rainflow histogram for the second earthquake in 2056, under scenario A1

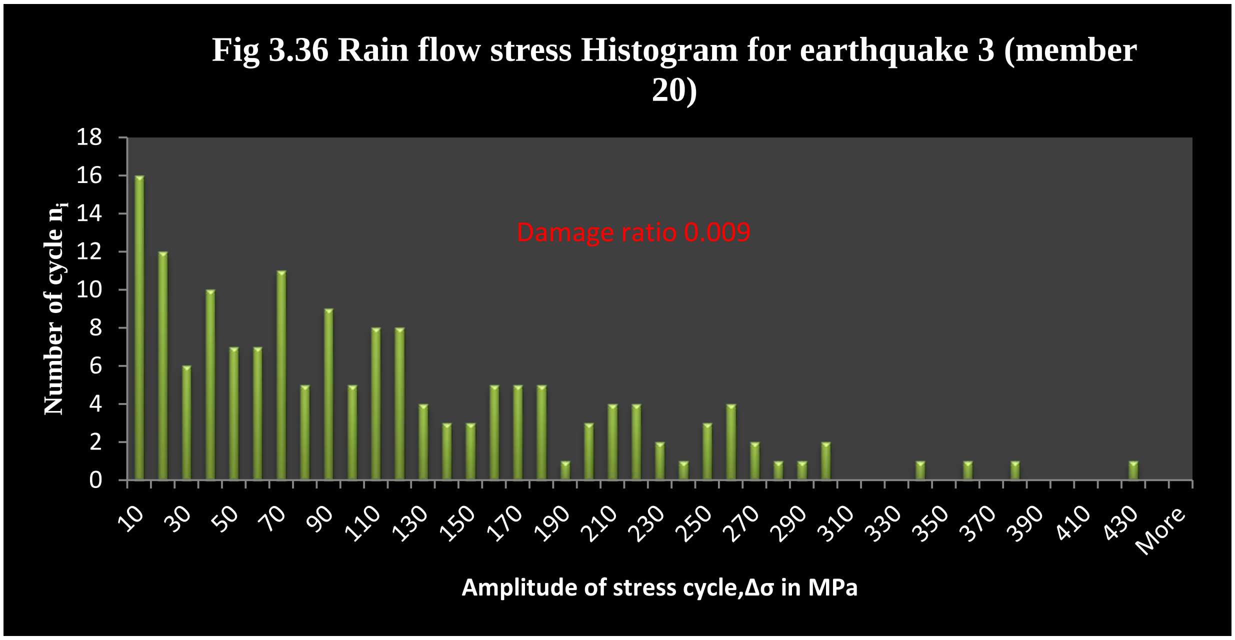

Figure 3.36: Rainflow histogram for the the earthquake in 2056, under scenario A1

In the following table and figure, the cumulative damage ratio from the year 1966 to 2116 for operating scenario A1 is shown

Year	Time period, years	Damage ratio	cumulative time, years	cumulative Damage ratio, D
1966-1976	10	0.0250437	10	0.0250437
1976-1986	10	0.0250437	20	0.0500874
1986-1996	10	0.0250437	30	0.0751311
1996-2006	10	0.0250437	40	0.1001748
2006-2016	10	0.0250437	50	0.1252185
2016-2026	10	0.0250437	60	0.1502622
2026 (EQ 1)	-	0.00322	60	0.1534822
2026-2036	10	0.0250437	70	0.1785259
2036-2046	10	0.0250437	80	0.2035696
2046-2056	10	0.0250437	90	0.2286133
2056(EQ 2)	-	0.00997	90	0.2385833
2056-2066	10	0.0250437	100	0.263627
2066-2076	10	0.0250437	110	0.2886707
2076-2086	10	0.0250437	120	0.3137144
2086(EQ 3)	-	0.009	120	0.3227144
2086-2096	10	0.0250437	130	0.3477581
2096-2106	10	0.0250437	140	0.3728018
2106-2116	10	0.0250437	150	0.3978455

Table 3.12: Cumulative damage ratio for A1

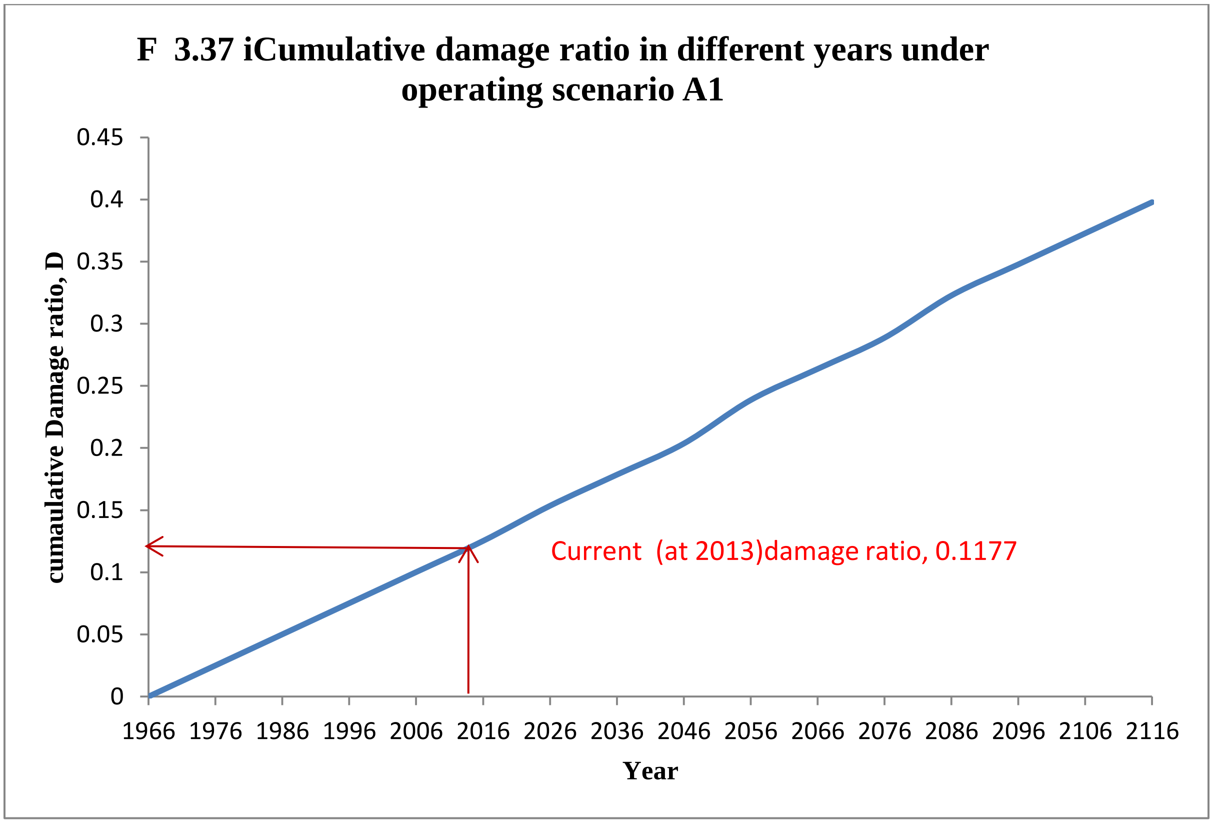

From the figure,

At current period, (2013) the cumulative damage ratio is 0.1177

The service life of the bridge is 377 years

The residual service life is 330 years

3.8.2 OPERATING SCENARIO A2:

Under this operating condition passenger, goods, through and mixed train loads are applied according to the frequency specified by RFI. Three Earthquakes events of magnitude described before are applied at 60, 90 and 120 years from year of bridge construction (i.e. in the year 2026, 2056 and2086). It is also assumed that there is thickness loss of bridge material due to corrosion and there is no maintenance program carried out. For this operating scenario, the damage ratio due to train load for the first 10 years, after the bridge construction is 0.0250437 as calculated before. The damage ratio in other decades are shown in the following tables

Axial force range in kN, ΔN	Average cross-sectional Area in sqm A	Stress range in MPa, $\Delta\sigma$	Total cycles in 10 years n_i	Number of cycles to failure, N_i	n_i/N_i
3792	0.0238	159.33	3650	317343.38	0.0115017
1992	0.0238	83.70	25550	3626238.5	0.0070459
1800	0.0238	75.63	3650	5321279.2	0.0006859
1752	0.0238	73.61	21900	5894326.2	0.0037154
816	0.0238	34.29	153300	106201743	0.0014435
720	0.0238	30.25	102000	170537950	0.0005981
672	0.0238	28.24	109500	221412368	0.0004946
624	0.0238	26.22	87600	293081711	0.0002989
552	0.0238	23.19	25550	466089947	5.482E-05
264	0.0238	11.09	76650	7.597E+09	1.009E-05
120	0.0238	5.04	54750	1.501E+11	3.648E-07
96	0.0238	4.03	47450	3.492E+11	1.359E-07
Total damage ratio from 1976 to1986 =					0.0258494

Table 3.13: Damage ratio from 1976 to 1986 under operating scenario A2

Axial force range in kN, ΔN	Average cross-sectional Area in sqm A	Stress range in MPa, $\Delta\sigma$	Total cycles in 10 years n_i	Number of cycles to failure, N_i	n_i/N_i
3792	0.0235	161.36	3650	302470.51	0.0120673
1992	0.0235	84.77	25550	3456288.2	0.0073923
1800	0.0235	76.60	3650	5071887.7	0.0007197
1752	0.0235	74.55	21900	5618077.8	0.0038981
816	0.0235	34.72	153300	101224404	0.0015145
720	0.0235	30.64	102000	162545378	0.0006275
672	0.0235	28.60	109500	211035473	0.0005189
624	0.0235	26.55	87600	279345901	0.0003136
552	0.0235	23.49	25550	444245790	5.751E-05
264	0.0235	11.23	76650	7.241E+09	1.059E-05
120	0.0235	5.11	54750	1.431E+11	3.827E-07
96	0.0235	4.09	47450	3.328E+11	1.426E-07
Total damage ratio from 1986 to 1996 =					0.0271205

Table 3.14: Damage ratio from 1986 to 1996 under operating scenario A2

Axial force range in kN, ΔN	Average cross-sectional Area in sqm, A	Stress range in MPa, $\Delta\sigma$	Total cycles in 10 years n_i	Number of cycles to failure, N_i	n_i/N_i
3792	0.0233	162.75	3650	292844.48	0.012464
1992	0.0233	85.49	25550	3346293	0.0076353
1800	0.0233	77.25	3650	4910476.6	0.0007433
1752	0.0233	75.19	21900	5439284.4	0.0040263
816	0.0233	35.02	153300	98002972	0.0015642
720	0.0233	30.90	102000	157372426	0.0006481
672	0.0233	28.84	109500	204319339	0.0005359
624	0.0233	26.78	87600	270455811	0.0003239
552	0.0233	23.69	25550	430107816	5.94E-05
264	0.0233	11.33	76650	7.01E+09	1.093E-05
120	0.0233	5.15	54750	1.385E+11	3.953E-07
96	0.0233	4.12	47450	3.222E+11	1.473E-07
				Total damage ratio from 1996 to2006 =	0.0280119

Table 3.15: Damage ratio from 1996 to 2006 under operating scenario A2

Axial force range in kN, ΔN	Average cross-sectional Area in sqm, A	Stress range in MPa, $\Delta\sigma$	Total cycles in 10 years n_i	Number of cycles to failure, N_i	n_i/N_i
3792	0.0231	164.16	3650	283445.77	0.0128772
1992	0.0231	86.23	25550	3238895.2	0.0078885
1800	0.0231	77.92	3650	4752877	0.000768
1752	0.0231	75.84	21900	5264712.9	0.0041598
816	0.0231	35.32	153300	94857608	0.0016161
720	0.0231	31.17	102000	152321625	0.0006696
672	0.0231	29.09	109500	197761798	0.0005537
624	0.0231	27.01	87600	261775649	0.0003346
552	0.0231	23.90	25550	416303691	6.137E-05
264	0.0231	11.43	76650	6.785E+09	1.13E-05
120	0.0231	5.19	54750	1.341E+11	4.084E-07
96	0.0231	4.16	47450	3.119E+11	1.521E-07
				Total damage ratio from 2006 to2016 =	0.0289408

Table 3.16: Damage ratio from 2006 to 2016 under operating scenario A2

Axial force range in kN, ΔN	Average cross-sectional Area in sqm, A	Stress range in MPa, Δσ	Total cycles in 10 years n_i	Number of cycles to failure, N_i	n_i/N_i
3792	0.0229	165.59	3650	274270.89	0.013308
1992	0.0229	86.99	25550	3134055.1	0.0081524
1800	0.0229	78.60	3650	4599030.7	0.0007936
1752	0.0229	76.51	21900	5094298.9	0.0042989
816	0.0229	35.63	153300	91787154	0.0016702
720	0.0229	31.44	102000	147391113	0.000692
672	0.0229	29.34	109500	191360429	0.0005722
624	0.0229	27.25	87600	253302209	0.0003458
552	0.0229	24.10	25550	402828320	6.343E-05
264	0.0229	11.53	76650	6.566E+09	1.167E-05
120	0.0229	5.24	54750	1.297E+11	4.221E-07
96	0.0229	4.19	47450	3.018E+11	1.572E-07
Total damage ratio from 2016 to2026 =					0.0299089

Table 3.17: Damage ratio from 2016 to 2026 under operating scenario A2

Axial force range in kN, ΔN	Average cross-sectional Area in sqm, A	Stress range in MPa, Δσ	Total cycles in 10 years n_i	Number of cycles to failure, N_i	n_i/N_i
3792	0.0227	167.05	3650	265316.4	0.0137572
1992	0.0227	87.75	25550	3031733.4	0.0084275
1800	0.0227	79.30	3650	4448879.9	0.0008204
1752	0.0227	77.18	21900	4927978.5	0.004444
816	0.0227	35.95	153300	88790455	0.0017265
720	0.0227	31.72	102000	142579037	0.0007154
672	0.0227	29.60	109500	185112827	0.0005915
624	0.0227	27.49	87600	245032311	0.0003575
552	0.0227	24.32	25550	389676641	6.557E-05
264	0.0227	11.63	76650	6.351E+09	1.207E-05
120	0.0227	5.29	54750	1.255E+11	4.363E-07
96	0.0227	4.23	47450	2.919E+11	1.625E-07
Total damage ratio from 2026 to2036 =					0.0309183

Table 3.18: Damage ratio from 2026 to 2036 under operating scenario A2

Axial force range in kN, ΔN	Average cross-sectional Area in sqm, A	Stress range in MPa, Δσ	Total cycles in 10 years n_i	Number of cycles to failure, N_i	n_i/N_i
3792	0.0225	168.53	3650	256578.87	0.0142256
1992	0.0225	88.53	25550	2931890.9	0.0087145
1800	0.0225	80.00	3650	4302367.4	0.0008484
1752	0.0225	77.87	21900	4765688	0.0045953
816	0.0225	36.27	153300	85866367	0.0017853
720	0.0225	32.00	102000	137883558	0.0007398
672	0.0225	29.87	109500	179016606	0.0006117
624	0.0225	27.73	87600	236962794	0.0003697
552	0.0225	24.53	25550	376843630	6.78E-05
264	0.0225	11.73	76650	6.142E+09	1.248E-05
120	0.0225	5.33	54750	1.213E+11	4.512E-07
96	0.0225	4.27	47450	2.823E+11	1.681E-07
Total damage ratio from 2036 to2046 =					0.0319712

Table 3.19: Damage ratio from 2036 to 2046 under operating scenario A2

Axial force range in kN, ΔN	Average cross-sectional Area in sqm, A	Stress range in MPa, Δσ	Total cycles in 10 years n_i	Number of cycles to failure, N_i	n_i/N_i
3792	0.0223	170.04	3650	248054.92	0.0147145
1992	0.0223	89.33	25550	2834488.9	0.009014
1800	0.0223	80.72	3650	4159436	0.0008775
1752	0.0223	78.57	21900	4607364.4	0.0047533
816	0.0223	36.59	153300	83013752	0.0018467
720	0.0223	32.29	102000	133302850	0.0007652
672	0.0223	30.13	109500	173069394	0.0006327
624	0.0223	27.98	87600	229090518	0.0003824
552	0.0223	24.75	25550	364324294	7.013E-05
264	0.0223	11.84	76650	5.938E+09	1.291E-05
120	0.0223	5.38	54750	1.173E+11	4.667E-07
96	0.0223	4.30	47450	2.729E+11	1.738E-07
Total damage ratio from 2046 to2056 =					0.0330698

Table 3.20: Damage ratio from 2046 to 2056 under operating scenario A2

Axial force range in kN, ΔN	Average cross-sectional Area in sqm, A	Stress range in MPa, Δσ	Total cycles in 10 years n_i	Number of cycles to failure, N_i	n_i/N_i
3792	0.0221	171.58	3650	239741.16	0.0152248
1992	0.0221	90.14	25550	2739488.8	0.0093266
1800	0.0221	81.45	3650	4020029.2	0.000908
1752	0.0221	79.28	21900	4452944.9	0.0049181
816	0.0221	36.92	153300	80231480	0.0019107
720	0.0221	32.58	102000	128835099	0.0007917
672	0.0221	30.41	109500	167268836	0.0006546
624	0.0221	28.24	87600	221412368	0.0003956
552	0.0221	24.98	25550	352113676	7.256E-05
264	0.0221	11.95	76650	5.739E+09	1.336E-05
120	0.0221	5.43	54750	1.134E+11	4.829E-07
96	0.0221	4.34	47450	2.638E+11	1.799E-07
Total damage ratio from 2056 to2066 =					0.0342166

Table 3.21: Damage ratio from 2056 to 2066 under operating scenario A2

Axial force range in kN, ΔN	Average cross-sectional Area in sqm, A	Stress range in MPa, Δσ	Total cycles in 10 years n_i	Number of cycles to failure, N_i	n_i/N_i
3792	0.0219	173.15	3650	231634.25	0.0157576
1992	0.0219	90.96	25550	2646852.2	0.009653
1800	0.0219	82.19	3650	3884090.8	0.0009397
1752	0.0219	80.00	21900	4302367.4	0.0050902
816	0.0219	37.26	153300	77518430	0.0019776
720	0.0219	32.88	102000	124478505	0.0008194
672	0.0219	30.68	109500	161612594	0.0006775
624	0.0219	28.49	87600	213925248	0.0004095
552	0.0219	25.21	25550	340206855	7.51E-05
264	0.0219	12.05	76650	5.545E+09	1.382E-05
120	0.0219	5.48	54750	1.096E+11	4.998E-07
96	0.0219	4.38	47450	2.549E+11	1.862E-07
Total damage ratio from 2066 to2076 =					0.0354142

Table 3.22: Damage ratio from 2066 to 2076 under operating scenario A2

Axial force range in kN, ΔN	Average cross-sectional Area in sqm, A	Stress range in MPa, Δσ	Total cycles in 10 years n_i	Number of cycles to failure, N_i	n_i/N_i
3792	0.0217	174.75	3650	223730.85	0.0163142
1992	0.0217	91.80	25550	2556541.2	0.009994
1800	0.0217	82.95	3650	3751565	0.0009729
1752	0.0217	80.74	21900	4155569.9	0.00527
816	0.0217	37.60	153300	74873489	0.0020475
720	0.0217	33.18	102000	120231279	0.0008484
672	0.0217	30.97	109500	156098347	0.0007015
624	0.0217	28.76	87600	206626084	0.000424
552	0.0217	25.44	25550	328598943	7.775E-05
264	0.0217	12.17	76650	5.356E+09	1.431E-05
120	0.0217	5.53	54750	1.058E+11	5.174E-07
96	0.0217	4.42	47450	2.462E+11	1.927E-07
Total damage ratio from 2076 to 2086 =					0.0366652

Table 3.23: Damage ratio from 2076 to 2086 under operating scenario A2

Axial force range in kN, ΔN	Average cross-sectional Area in sqm, A	Stress range in MPa, Δσ	Total cycles in 10 years n_i	Number of cycles to failure, N_i	n_i/N_i
3792	0.0215	176.37	3650	216027.67	0.016896
1992	0.0215	92.65	25550	2468518	0.0103503
1800	0.0215	83.72	3650	3622396.4	0.0010076
1752	0.0215	81.49	21900	4012491.2	0.005458
816	0.0215	37.95	153300	72295551	0.0021205
720	0.0215	33.49	102000	116091645	0.0008786
672	0.0215	31.26	109500	150723789	0.0007265
624	0.0215	29.02	87600	199511827	0.0004391
552	0.0215	25.67	25550	317285089	8.053E-05
264	0.0215	12.28	76650	5.171E+09	1.482E-05
120	0.0215	5.58	54750	1.022E+11	5.359E-07
96	0.0215	4.47	47450	2.377E+11	1.996E-07
Total damage ratio from 2086 to 2096 =					0.0379726

Table 3.24: Damage ratio from 2086 to 2096 under operating scenario A2

Axial force range in kN, ΔN	Average cross-sectional Area in sqm, A	Stress range in MPa, Δσ	Total cycles in 10 years n_i	Number of cycles to failure, N_i	n_i/N_i
3792	0.0213	178.03	3650	208521.42	0.0175042
1992	0.0213	93.52	25550	2382745.1	0.0107229
1800	0.0213	84.51	3650	3496530	0.0010439
1752	0.0213	82.25	21900	3873070.3	0.0056544
816	0.0213	38.31	153300	69783518	0.0021968
720	0.0213	33.80	102000	112057842	0.0009102
672	0.0213	31.55	109500	145486632	0.0007526
624	0.0213	29.30	87600	192579446	0.0004549
552	0.0213	25.92	25550	306260473	8.343E-05
264	0.0213	12.39	76650	4.992E+09	1.536E-05
120	0.0213	5.63	54750	9.862E+10	5.552E-07
96	0.0213	4.51	47450	2.294E+11	2.068E-07
Total damage ratio from 2086 to 2096 =					0.0393395

Table 3.25: Damage ratio from 2096 to 2106 under operating scenario A2

Axial force range in kN, ΔN	Average cross-sectional Area in sqm, A	Stress range in MPa, Δσ	Total cycles in 10 years n_i	Number of cycles to failure, N_i	n_i/N_i
3792	0.0211	179.72	3650	201208.84	0.0181404
1992	0.0211	94.41	25550	2299185.3	0.0111126
1800	0.0211	85.31	3650	3373911.2	0.0010818
1752	0.0211	83.03	21900	3737246.7	0.0058599
816	0.0211	38.67	153300	67336300	0.0022766
720	0.0211	34.12	102000	108128118	0.0009433
672	0.0211	31.85	109500	140384604	0.00078
624	0.0211	29.57	87600	185825934	0.0004714
552	0.0211	26.16	25550	295520315	8.646E-05
264	0.0211	12.51	76650	4.817E+09	1.591E-05
120	0.0211	5.69	54750	9.516E+10	5.753E-07
96	0.0211	4.55	47450	2.214E+11	2.143E-07
Total damage ratio from 2106 to 2116 =					0.0407693

Table 3.26: Damage ratio from 2106 to 2116 under operating scenario A2

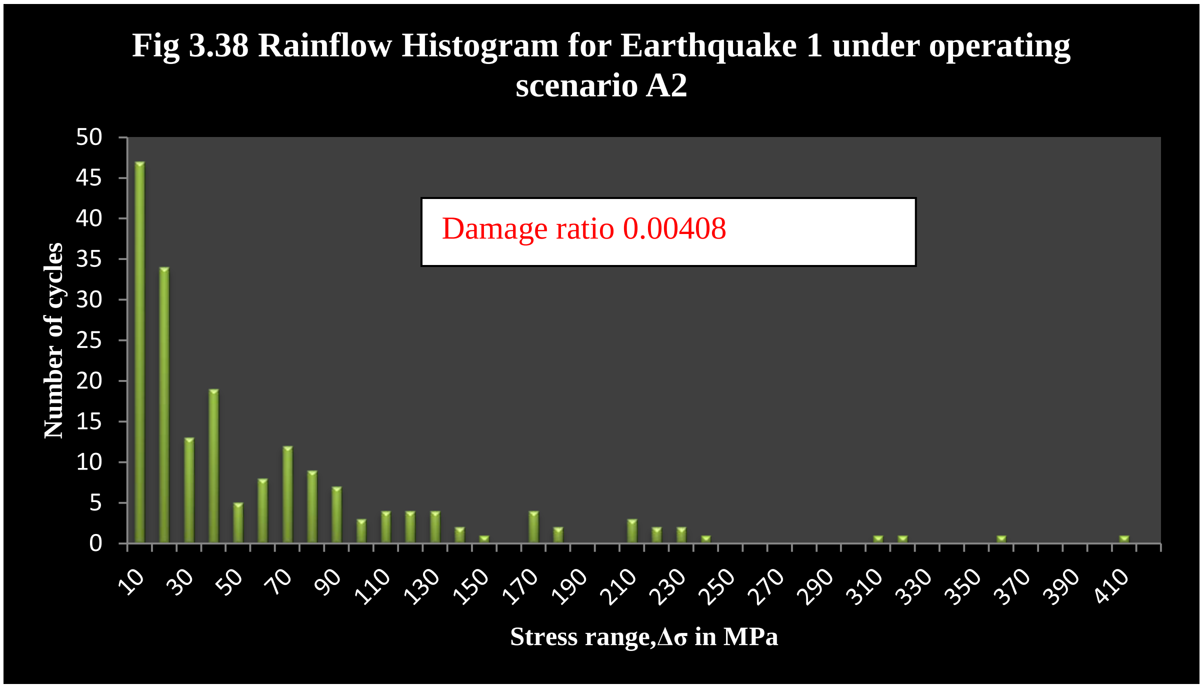

Figure 3. 38: Damage ratio for earthquake 1 in the year 2026 under operating scenario A2

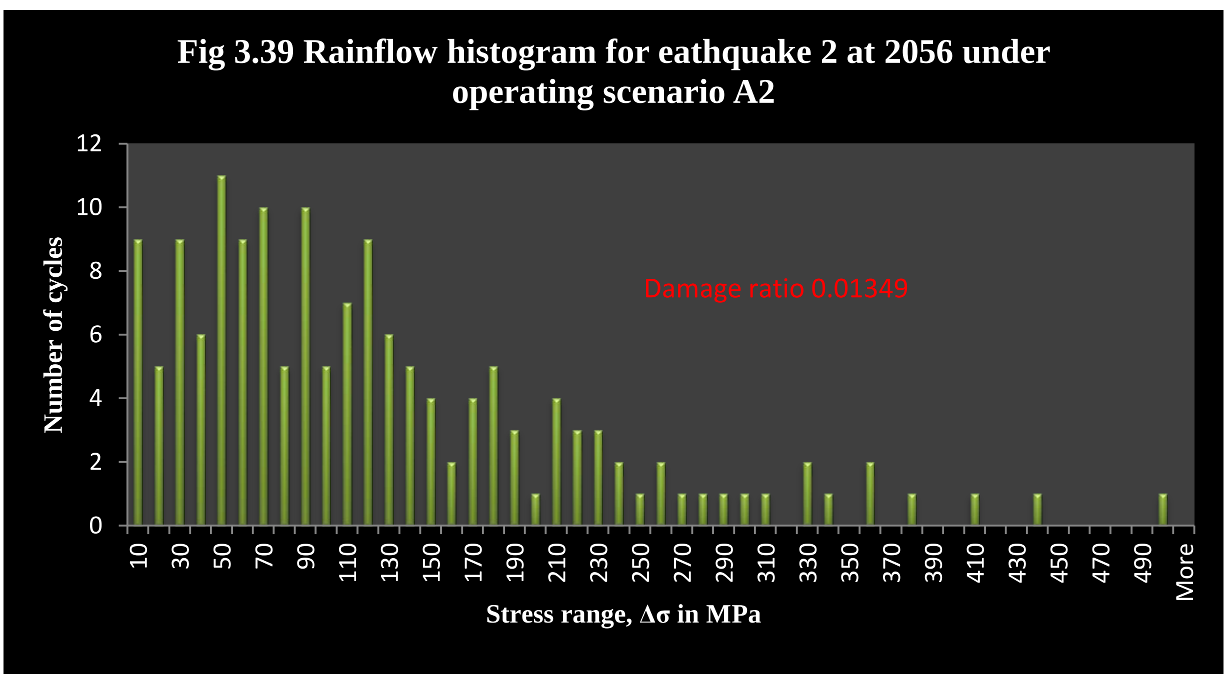

Figure 3.39 : Damage ratio for earthquake 2 in the year 2056 under operating scenario A2

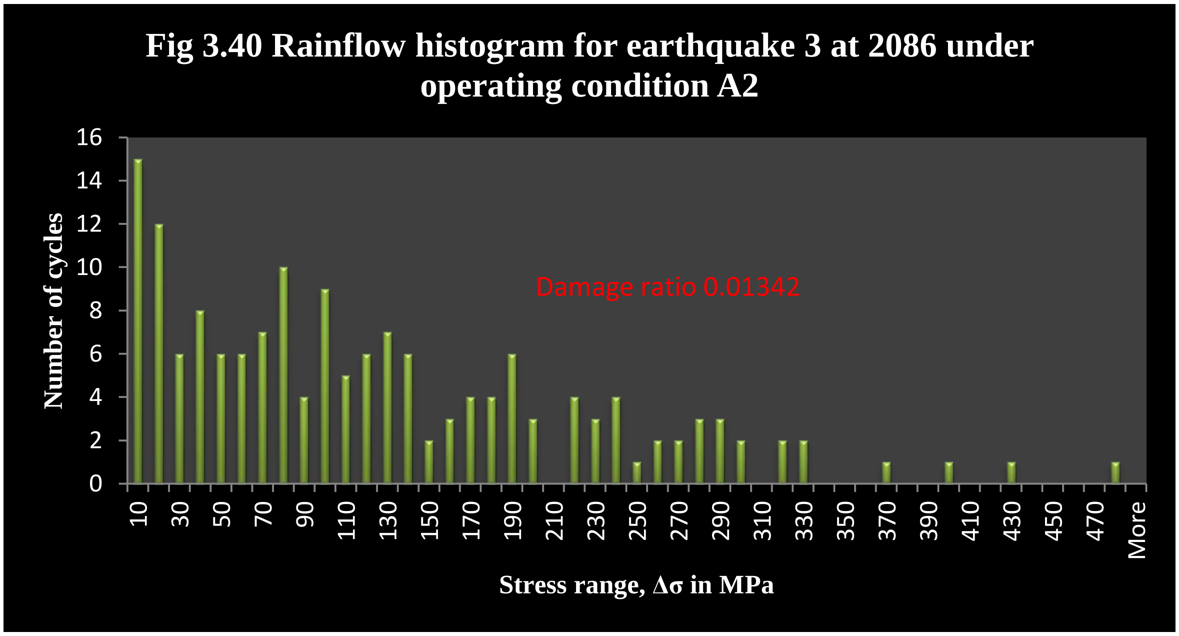

Figure 3.40 : Damage ratio for earthquake 3 in the year 2086 under operating scenario A2

In the following table and figure, the cumulative damage ratio from the year 1966 to 2116 for operating scenario A2 is shown

Year	Time period, years	Damage ratio	cumulative time, years	cumulative Damage ratio
1966-1976	10	0.0250437	10	0.0250437
1976-1986	10	0.02584941	20	0.0508931
1986-1996	10	0.02712046	30	0.0780136
1996-2006	10	0.02801193	40	0.1060255
2006-2016	10	0.02894077	50	0.1349663
2016-2026	10	0.02990889	60	0.1648752
2026 (EQ 1)	-	0.00408	60	0.1689552
2026-2036	10	0.03091833	70	0.1998735
2036-2046	10	0.03197122	80	0.2318447
2046-2056	10	0.03306985	90	0.2649145
2056(EQ 2)	-	0.01349	90	0.2784045
2056-2066	10	0.03421665	100	0.3126212
2066-2076	10	0.03541419	110	0.3480354
2076-2086	10	0.03666521	120	0.3847006
2086(EQ 3)	-	0.01342	120	0.3981206
2086-2096	10	0.03797263	130	0.4360932
2096-2106	10	0.03933955	140	0.4754328
2106-2116	10	0.04076928	150	0.516202

Table 3.27: Cumulative damage ratio for A2

Fig 3.41 Cumulative damage ratio for operating condition A2

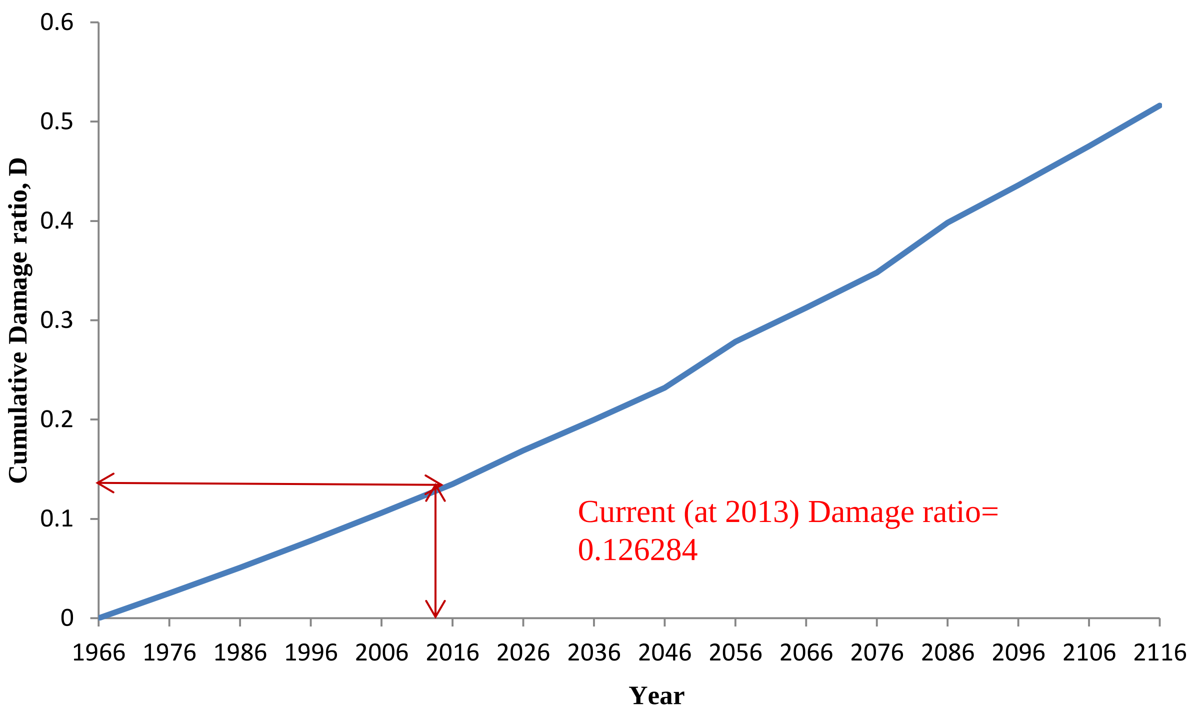

From the figure,

At current period, (2013) the cumulative damage ratio is 0.126284

3.8.3 OPERATING SCENARIO A3:

Under this operating condition passenger, goods, through and mixed train loads are applied according to the frequency specified by RFI. Three Earthquakes events of magnitude described before are applied at 60, 90 and 120 years from year of bridge construction (i.e. in the year 2026, 2056 and2086). It is also assumed that a total number of three corrosion protective paintings are provide at the interval of every ten years for the first thirty years from the year of bridge construction and the thickness loss of bridge material due to corrosion initiates after forty years of bridge construction, i.e. in the year 2006 .For this operating scenario, the damage ratio due to train load for the first 10 (1966-76) years, after the bridge construction is 0.0250437 as calculated before. The damage ratio due to train load for the next three decades (1976-1986, 1986-1996 and 1996-2006) are also 0.0250437 as calculated before. The damage ratio in other decades are shown in the following tables

Axial force range, ΔN	Average cross-sectional Area A	Stress range, Δσ	Total cycles in 10 years n_i	Number of cycles to failure, N_i	n_i/N_i
3792	0.0238	159.33	3650	317343.38	0.0115017
1992	0.0238	83.70	25550	3626238.5	0.0070459
1800	0.0238	75.63	3650	5321279.2	0.0006859
1752	0.0238	73.61	21900	5894326.2	0.0037154
816	0.0238	34.29	153300	106201743	0.0014435
720	0.0238	30.25	102000	170537950	0.0005981
672	0.0238	28.24	109500	221412368	0.0004946
624	0.0238	26.22	87600	293081711	0.0002989
552	0.0238	23.19	25550	466089947	5.482E-05
264	0.0238	11.09	76650	7.597E+09	1.009E-05
120	0.0238	5.04	54750	1.501E+11	3.648E-07
96	0.0238	4.03	47450	3.492E+11	1.359E-07
Total damage ratio from 2006 to2016 =					0.0258494

Table 3.28: Damage ratio from 2006 to 2016 under operating scenario A3

Axial force range, ΔN	Average cross-sectional Area A	Stress range, Δσ	Total cycles in 10 years n_i	Number of cycles to failure, N_i	n_i/N_i
3792	0.0235	161.36	3650	302470.51	0.0120673
1992	0.0235	84.77	25550	3456288.2	0.0073923
1800	0.0235	76.60	3650	5071887.7	0.0007197
1752	0.0235	74.55	21900	5618077.8	0.0038981
816	0.0235	34.72	153300	101224404	0.0015145
720	0.0235	30.64	102000	162545378	0.0006275
672	0.0235	28.60	109500	211035473	0.0005189
624	0.0235	26.55	87600	279345901	0.0003136
552	0.0235	23.49	25550	444245790	5.751E-05
264	0.0235	11.23	76650	7.241E+09	1.059E-05
120	0.0235	5.11	54750	1.431E+11	3.827E-07
96	0.0235	4.09	47450	3.328E+11	1.426E-07
Total damage ratio from 2016 to2026 =					0.0271205

Table 3.29: Damage ratio from 2016 to 2026 under operating scenario A3

Axial force range, ΔN	Average cross-sectional Area A	Stress range, Δσ	Total cycles in 10 years n_i	Number of cycles to failure, N_i	n_i/N_i
3792	0.0233	162.75	3650	292844.48	0.012464
1992	0.0233	85.49	25550	3346293	0.0076353
1800	0.0233	77.25	3650	4910476.6	0.0007433
1752	0.0233	75.19	21900	5439284.4	0.0040263
816	0.0233	35.02	153300	98002972	0.0015642
720	0.0233	30.90	102000	157372426	0.0006481
672	0.0233	28.84	109500	204319339	0.0005359
624	0.0233	26.78	87600	270455811	0.0003239
552	0.0233	23.69	25550	430107816	5.94E-05
264	0.0233	11.33	76650	7.01E+09	1.093E-05
120	0.0233	5.15	54750	1.385E+11	3.953E-07
96	0.0233	4.12	47450	3.222E+11	1.473E-07
Total damage ratio from 2026 to2036 =					0.0280119

Table 3.30: Damage ratio from 2026 to 2036 under operating scenario A3

Axial force range, ΔN	Average cross-sectional Area A	Stress range, Δσ	Total cycles in 10 years n_i	Number of cycles to failure, N_i	n_i/N_i
3792	0.0231	164.16	3650	283445.77	0.0128772
1992	0.0231	86.23	25550	3238895.2	0.0078885
1800	0.0231	77.92	3650	4752877	0.000768
1752	0.0231	75.84	21900	5264712.9	0.0041598
816	0.0231	35.32	153300	94857608	0.0016161
720	0.0231	31.17	102000	152321625	0.0006696
672	0.0231	29.09	109500	197761798	0.0005537
624	0.0231	27.01	87600	261775649	0.0003346
552	0.0231	23.90	25550	416303691	6.137E-05
264	0.0231	11.43	76650	6.785E+09	1.13E-05
120	0.0231	5.19	54750	1.341E+11	4.084E-07
96	0.0231	4.16	47450	3.119E+11	1.521E-07
Total damage ratio from 2036 to2046 =					0.0289408

Table 3.31: Damage ratio from 2036 to 2046 under operating scenario A3

Axial force range in kN, ΔN	Average cross-sectional Area in sqm, A	Stress range in MPa, Δσ	Total cycles in 10 years n_i	Number of cycles to failure, N_i	n_i/N_i
3792	0.0229	165.59	3650	274270.89	0.013308
1992	0.0229	86.99	25550	3134055.1	0.0081524
1800	0.0229	78.60	3650	4599030.7	0.0007936
1752	0.0229	76.51	21900	5094298.9	0.0042989
816	0.0229	35.63	153300	91787154	0.0016702
720	0.0229	31.44	102000	147391113	0.000692
672	0.0229	29.34	109500	191360429	0.0005722
624	0.0229	27.25	87600	253302209	0.0003458
552	0.0229	24.10	25550	402828320	6.343E-05
264	0.0229	11.53	76650	6.566E+09	1.167E-05
120	0.0229	5.24	54750	1.297E+11	4.221E-07
96	0.0229	4.19	47450	3.018E+11	1.572E-07
				Total damage ratio from 2046 to2056 =	0.0299089

Table 3.32: Damage ratio from 2046 to 2056 under operating scenario A3

Axial force range in kN, ΔN	Average cross-sectional Area in sqm, A	Stress range in MPa, Δσ	Total cycles in 10 years n_i	Number of cycles to failure, N_i	n_i/N_i
3792	0.0227	167.05	3650	265316.4	0.0137572
1992	0.0227	87.75	25550	3031733.4	0.0084275
1800	0.0227	79.30	3650	4448879.9	0.0008204
1752	0.0227	77.18	21900	4927978.5	0.004444
816	0.0227	35.95	153300	88790455	0.0017265
720	0.0227	31.72	102000	142579037	0.0007154
672	0.0227	29.60	109500	185112827	0.0005915
624	0.0227	27.49	87600	245032311	0.0003575
552	0.0227	24.32	25550	389676641	6.557E-05
264	0.0227	11.63	76650	6.351E+09	1.207E-05
120	0.0227	5.29	54750	1.255E+11	4.363E-07
96	0.0227	4.23	47450	2.919E+11	1.625E-07
				Total damage ratio from 2056 to2066 =	0.0309183

Table 3.33: Damage ratio from 2056 to 2066 under operating scenario A3

Axial force range in kN, ΔN	Average cross-sectional Area in sqm, A	Stress range in MPa, $\Delta\sigma$	Total cycles in 10 years n_i	Number of cycles to failure, N_i	n_i/N_i
3792	0.0225	168.53	3650	256578.87	0.0142256
1992	0.0225	88.53	25550	2931890.9	0.0087145
1800	0.0225	80.00	3650	4302367.4	0.0008484
1752	0.0225	77.87	21900	4765688	0.0045953
816	0.0225	36.27	153300	85866367	0.0017853
720	0.0225	32.00	102000	137883558	0.0007398
672	0.0225	29.87	109500	179016606	0.0006117
624	0.0225	27.73	87600	236962794	0.0003697
552	0.0225	24.53	25550	376843630	6.78E-05
264	0.0225	11.73	76650	6.142E+09	1.248E-05
120	0.0225	5.33	54750	1.213E+11	4.512E-07
96	0.0225	4.27	47450	2.823E+11	1.681E-07
				Total damage ratio from 2066 to2076 =	0.0319712

Table 3.34: Damage ratio from 2066 to 2076 under operating scenario A3

Axial force range in kN, ΔN	Average cross-sectional Area in sqm, A	Stress range in MPa, $\Delta\sigma$	Total cycles in 10 years n_i	Number of cycles to failure, N_i	n_i/N_i
3792	0.0223	170.04	3650	248054.92	0.0147145
1992	0.0223	89.33	25550	2834488.9	0.009014
1800	0.0223	80.72	3650	4159436	0.0008775
1752	0.0223	78.57	21900	4607364.4	0.0047533
816	0.0223	36.59	153300	83013752	0.0018467
720	0.0223	32.29	102000	133302850	0.0007652
672	0.0223	30.13	109500	173069394	0.0006327
624	0.0223	27.98	87600	229090518	0.0003824
552	0.0223	24.75	25550	364324294	7.013E-05
264	0.0223	11.84	76650	5.938E+09	1.291E-05
120	0.0223	5.38	54750	1.173E+11	4.667E-07
96	0.0223	4.30	47450	2.729E+11	1.738E-07
				Total damage ratio from 2076 to 2086 =	0.0330698

Table 3.35: Damage ratio from 2076 to 2086 under operating scenario A3

Axial force range in kN, ΔN	Average cross-sectional Area in sqm, A	Stress range in MPa, Δσ	Total cycles in 10 years n_i	Number of cycles to failure, N_i	n_i/N_i
3792	0.0221	171.58	3650	239741.16	0.0152248
1992	0.0221	90.14	25550	2739488.8	0.0093266
1800	0.0221	81.45	3650	4020029.2	0.000908
1752	0.0221	79.28	21900	4452944.9	0.0049181
816	0.0221	36.92	153300	80231480	0.0019107
720	0.0221	32.58	102000	128835099	0.0007917
672	0.0221	30.41	109500	167268836	0.0006546
624	0.0221	28.24	87600	221412368	0.0003956
552	0.0221	24.98	25550	352113676	7.256E-05
264	0.0221	11.95	76650	5.739E+09	1.336E-05
120	0.0221	5.43	54750	1.134E+11	4.829E-07
96	0.0221	4.34	47450	2.638E+11	1.799E-07
Total damage ratio from 2086 to 2096 =					0.0342166

Table 3.36: Damage ratio from 2086 to 2096 under operating scenario A3

Axial force range in kN, ΔN	Average cross-sectional Area in sqm, A	Stress range in MPa, Δσ	Total cycles in 10 years n_i	Number of cycles to failure, N_i	n_i/N_i
3792	0.0219	173.15	3650	231634.25	0.0157576
1992	0.0219	90.96	25550	2646852.2	0.009653
1800	0.0219	82.19	3650	3884090.8	0.0009397
1752	0.0219	80.00	21900	4302367.4	0.0050902
816	0.0219	37.26	153300	77518430	0.0019776
720	0.0219	32.88	102000	124478505	0.0008194
672	0.0219	30.68	109500	161612594	0.0006775
624	0.0219	28.49	87600	213925248	0.0004095
552	0.0219	25.21	25550	340206855	7.51E-05
264	0.0219	12.05	76650	5.545E+09	1.382E-05
120	0.0219	5.48	54750	1.096E+11	4.998E-07
96	0.0219	4.38	47450	2.549E+11	1.862E-07
Total damage ratio from 2096 to 2106 =					0.0354142

Table 3.37: Damage ratio from 2096 to 2106 under operating scenario A3

Axial force range in kN, ΔN	Average cross-sectional Area in sqm, A	Stress range in MPa, $\Delta\sigma$	Total cycles in 10 years n_i	Number of cycles to failure, N_i	n_i/N_i
3792	0.0217	174.75	3650	223730.85	0.0163142
1992	0.0217	91.80	25550	2556541.2	0.009994
1800	0.0217	82.95	3650	3751565	0.0009729
1752	0.0217	80.74	21900	4155569.9	0.00527
816	0.0217	37.60	153300	74873489	0.0020475
720	0.0217	33.18	102000	120231279	0.0008484
672	0.0217	30.97	109500	156098347	0.0007015
624	0.0217	28.76	87600	206626084	0.000424
552	0.0217	25.44	25550	328598943	7.775E-05
264	0.0217	12.17	76650	5.356E+09	1.431E-05
120	0.0217	5.53	54750	1.058E+11	5.174E-07
96	0.0217	4.42	47450	2.462E+11	1.927E-07
Total damage ratio from 2106 to 2116 =					0.0366652

Table 3.38: Damage ratio from 2106 to 2116 under operating scenario A3

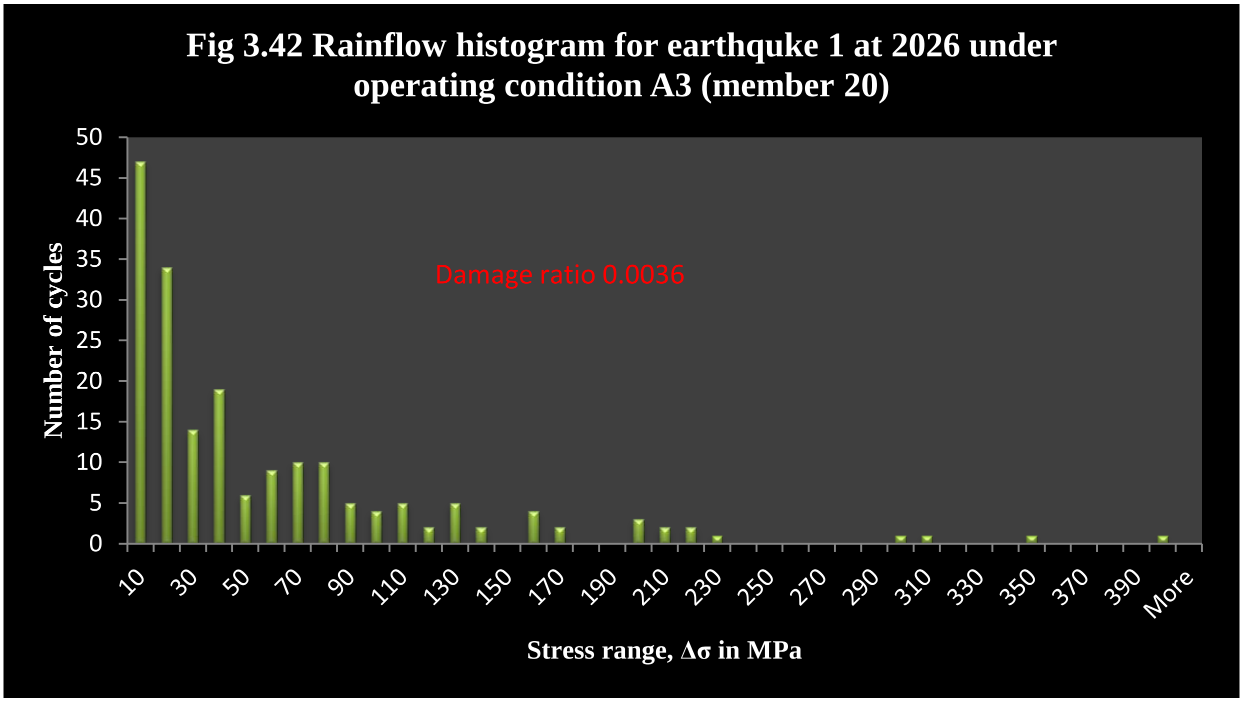

Figure 3.42 : Damage ratio for earthquake 1 in the year 2026 under operating scenario A3

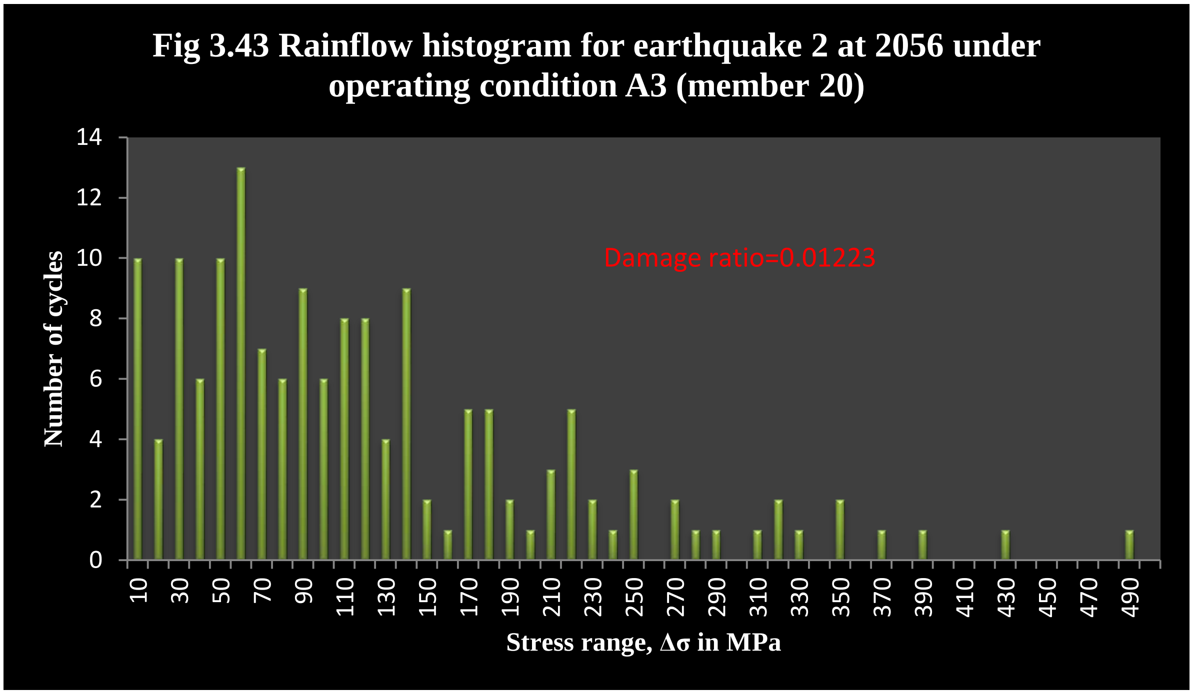

Figure 3.43 : Damage ratio for earthquake 2 in the year 2056 under operating scenario A3

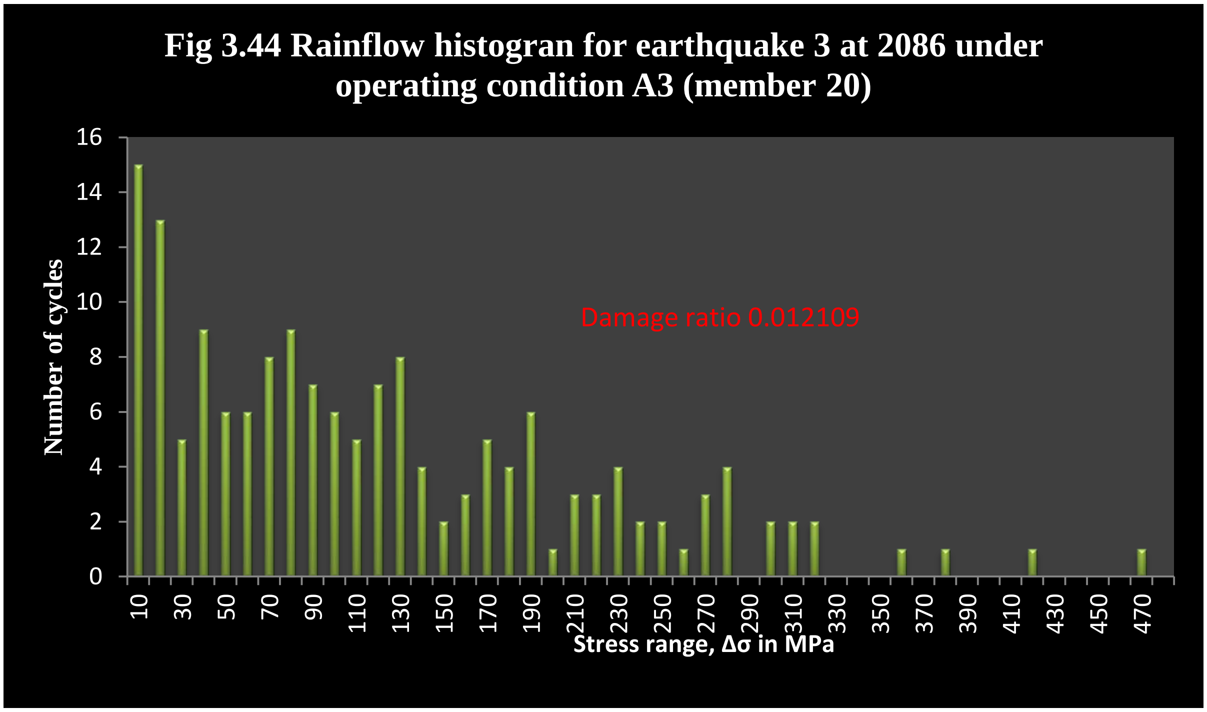

Figure 3.44: Damage ratio for earthquake 3 in the year 2086 under operating scenario A3

In the following table and figure, the cumulative damage ratio from the year 1966 to 2116 for operating scenario A3 is shown

Year	Time period, years	Damage ratio	cumulative time, years	cumulative Damage ratio
1966-1976	10	0.0250437	10	0.0250437
1976-1986	10	0.0250437	20	0.0500874
1986-1996	10	0.0250437	30	0.0751311
1996-2006	10	0.0250437	40	0.1001748
2006-2016	10	0.0258494	50	0.1260242
2016-2026	10	0.0271205	60	0.1531447
2026 (EQ 1)	-	0.0036	60	0.1567447
2026-2036	10	0.0280119	70	0.1847566
2036-2046	10	0.0289408	80	0.2136974
2046-2056	10	0.0299089	90	0.2436063
2056(EQ 2)	-	0.01223	90	0.2558363
2056-2066	10	0.0309183	100	0.2867546
2066-2076	10	0.0319712	110	0.3187258
2076-2086	10	0.0330698	120	0.3517956
2086(EQ 3)	-	0.012109	120	0.3639046
2086-2096	10	0.0342166	130	0.3981213
2096-2106	10	0.0354142	140	0.4335355
2106-2116	10	0.0366652	150	0.4702007

Table 3.39: Cumulative Damage ratio under operating scenario A3

Fig 3.45 Cumulative damage ratio for operating condition A3

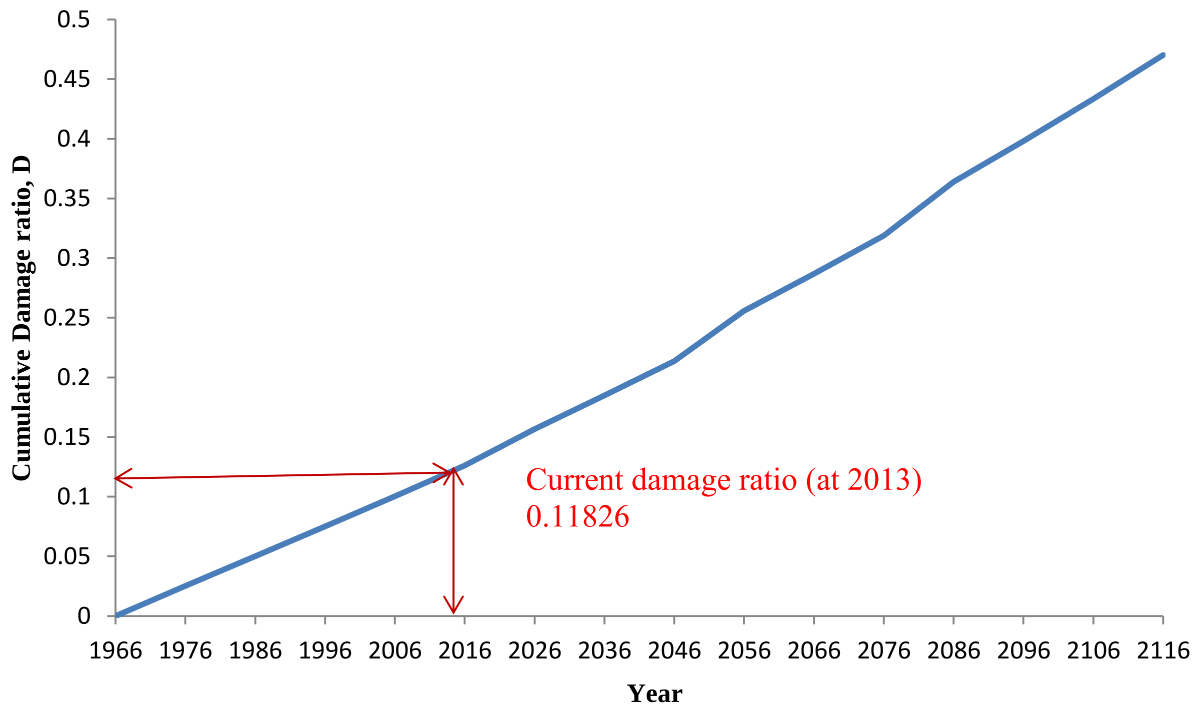

3.8.4 OPERATING SCENARIO A4:

Under this operating condition passenger, goods, through and mixed train loads are applied according to the frequency specified by RFI. Three Earthquakes events of magnitude described before are applied at 60, 90 and 120 years from year of bridge construction (i.e. in the year 2026, 2056 and2086). It is also assumed that corrosion protective paintings are provide at the interval of every thirty years from the year of bridge construction and the thickness loss of bridge material due to corrosion initiated after 10 years of bridge construction, i.e. in the year1976 and continues as described before in paragraph 3.6.3 .For this operating scenario, the damage ratio due to train load for the first 10 (1966-76) years, after the bridge construction is 0.0250437 as calculated before. The damage ratio in other decades are shown in the following tables

Axial force range, ΔN	Average cross-sectional Area A	Stress range, Δσ	Total cycles in 10 years n_i	Number of cycles to failure, N_i	n_i/N_i
3792	0.0238	159.33	3650	317343.38	0.0115017
1992	0.0238	83.70	25550	3626238.5	0.0070459
1800	0.0238	75.63	3650	5321279.2	0.0006859
1752	0.0238	73.61	21900	5894326.2	0.0037154
816	0.0238	34.29	153300	106201743	0.0014435
720	0.0238	30.25	102000	170537950	0.0005981
672	0.0238	28.24	109500	221412368	0.0004946
624	0.0238	26.22	87600	293081711	0.0002989
552	0.0238	23.19	25550	466089947	5.482E-05
264	0.0238	11.09	76650	7.597E+09	1.009E-05
120	0.0238	5.04	54750	1.501E+11	3.648E-07
96	0.0238	4.03	47450	3.492E+11	1.359E-07
Total damage ratio from 1976 to 1986 =					0.0258494

Table 3.40: Damage ratio from 1976 to 1986 under operating scenario A4

Axial force range, ΔN	Average cross-sectional Area A	Stress range, Δσ	Total cycles in 10 years n_i	Number of cycles to failure, N_i	n_i/N_i
3792	0.0235	161.36	3650	302470.51	0.0120673
1992	0.0235	84.77	25550	3456288.2	0.0073923
1800	0.0235	76.60	3650	5071887.7	0.0007197
1752	0.0235	74.55	21900	5618077.8	0.0038981
816	0.0235	34.72	153300	101224404	0.0015145
720	0.0235	30.64	102000	162545378	0.0006275
672	0.0235	28.60	109500	211035473	0.0005189
624	0.0235	26.55	87600	279345901	0.0003136
552	0.0235	23.49	25550	444245790	5.751E-05
264	0.0235	11.23	76650	7.241E+09	1.059E-05
120	0.0235	5.11	54750	1.431E+11	3.827E-07
96	0.0235	4.09	47450	3.328E+11	1.426E-07
Total damage ratio from 1986 to1996 =					0.0271205

Table 3.41: Damage ratio from 1986 to 1996 under operating scenario A4

Axial force range, ΔN	Average cross-sectional Area A	Stress range, Δσ	Total cycles in 10 years n_i	Number of cycles to failure, N_i	n_i/N_i
3792	0.0234	162.05	3650	297628.87	0.0122636
1992	0.0234	85.13	25550	3400963.4	0.0075126
1800	0.0234	76.92	3650	4990702.1	0.0007314
1752	0.0234	74.87	21900	5528149.3	0.0039615
816	0.0234	34.87	153300	99604106	0.0015391
720	0.0234	30.77	102000	159943516	0.0006377
672	0.0234	28.72	109500	207657430	0.0005273
624	0.0234	26.67	87600	274874414	0.0003187
552	0.0234	23.59	25550	437134752	5.845E-05
264	0.0234	11.28	76650	7.125E+09	1.076E-05
120	0.0234	5.13	54750	1.408E+11	3.889E-07
96	0.0234	4.10	47450	3.275E+11	1.449E-07
				Total damage ratio from 1996 to2006 =	0.0275616

Table 3.42: Damage ratio from 1996 to 2006 under operating scenario A4

Axial force range, ΔN	Average cross-sectional Area A	Stress range, Δσ	Total cycles in 10 years n_i	Number of cycles to failure, N_i	n_i/N_i
3792	0.0233	162.75	3650	292844.48	0.012464
1992	0.0233	85.49	25550	3346293	0.0076353
1800	0.0233	77.25	3650	4910476.6	0.0007433
1752	0.0233	75.19	21900	5439284.4	0.0040263
816	0.0233	35.02	153300	98002972	0.0015642
720	0.0233	30.90	102000	157372426	0.0006481
672	0.0233	28.84	109500	204319339	0.0005359
624	0.0233	26.78	87600	270455811	0.0003239
552	0.0233	23.69	25550	430107816	5.94E-05
264	0.0233	11.33	76650	7.01E+09	1.093E-05
120	0.0233	5.15	54750	1.385E+11	3.953E-07
96	0.0233	4.12	47450	3.222E+11	1.473E-07
				Total damage ratio from 2006 to2016 =	0.0280119

Table 3.43: Damage ratio from 2006 to 2016 under operating scenario A4

Axial force range, ΔN	Average cross-sectional Area A	Stress range, $\Delta\sigma$	Total cycles in 10 years n_i	Number of cycles to failure, N_i	n_i/N_i
3792	0.0231	164.16	3650	283445.77	0.0128772
1992	0.0231	86.23	25550	3238895.2	0.0078885
1800	0.0231	77.92	3650	4752877	0.000768
1752	0.0231	75.84	21900	5264712.9	0.0041598
816	0.0231	35.32	153300	94857608	0.0016161
720	0.0231	31.17	102000	152321625	0.0006696
672	0.0231	29.09	109500	197761798	0.0005537
624	0.0231	27.01	87600	261775649	0.0003346
552	0.0231	23.90	25550	416303691	6.137E-05
264	0.0231	11.43	76650	6.785E+09	1.13E-05
120	0.0231	5.19	54750	1.341E+11	4.084E-07
96	0.0231	4.16	47450	3.119E+11	1.521E-07
Total damage ratio from 2016 to2026 =					0.0289408

Table 3.44: Damage ratio from 2016 to 2026 under operating scenario A4

Axial force range, ΔN	Average cross-sectional Area A	Stress range, $\Delta\sigma$	Total cycles in 10 years n_i	Number of cycles to failure, N_i	n_i/N_i
3792	0.023	164.87	3650	278830.56	0.0130904
1992	0.023	86.61	25550	3186157.9	0.0080191
1800	0.023	78.26	3650	4675488.3	0.0007807
1752	0.023	76.17	21900	5178990.2	0.0042286
816	0.023	35.48	153300	93313090	0.0016429
720	0.023	31.30	102000	149841449	0.0006807
672	0.023	29.22	109500	194541743	0.0005629
624	0.023	27.13	87600	257513288	0.0003402
552	0.023	24.00	25550	409525229	6.239E-05
264	0.023	11.48	76650	6.675E+09	1.148E-05
120	0.023	5.22	54750	1.319E+11	4.152E-07
96	0.023	4.17	47450	3.068E+11	1.547E-07
Total damage ratio from 2026 to2036 =					0.0294198

Table 3.45: Damage ratio from 2026 to 2036 under operating scenario A4

Axial force range, ΔN	Average cross-sectional Area A	Stress range, Δσ	Total cycles in 10 years n_i	Number of cycles to failure, N_i	n_i/N_i
3792	0.0229	165.59	3650	274270.89	0.013308
1992	0.0229	86.99	25550	3134055.1	0.0081524
1800	0.0229	78.60	3650	4599030.7	0.0007936
1752	0.0229	76.51	21900	5094298.9	0.0042989
816	0.0229	35.63	153300	91787154	0.0016702
720	0.0229	31.44	102000	147391113	0.000692
672	0.0229	29.34	109500	191360429	0.0005722
624	0.0229	27.25	87600	253302209	0.0003458
552	0.0229	24.10	25550	402828320	6.343E-05
264	0.0229	11.53	76650	6.566E+09	1.167E-05
120	0.0229	5.24	54750	1.297E+11	4.221E-07
96	0.0229	4.19	47450	3.018E+11	1.572E-07
				Total damage ratio from 2036 to2046 =	0.0299089

Table 3.46: Damage ratio from 2036 to 2046 under operating scenario A4

Axial force range in kN, ΔN	Average cross-sectional Area in sqm, A	Stress range in MPa, Δσ	Total cycles in 10 years n_i	Number of cycles to failure, N_i	n_i/N_i
3792	0.0227	167.05	3650	265316.4	0.0137572
1992	0.0227	87.75	25550	3031733.4	0.0084275
1800	0.0227	79.30	3650	4448879.9	0.0008204
1752	0.0227	77.18	21900	4927978.5	0.004444
816	0.0227	35.95	153300	88790455	0.0017265
720	0.0227	31.72	102000	142579037	0.0007154
672	0.0227	29.60	109500	185112827	0.0005915
624	0.0227	27.49	87600	245032311	0.0003575
552	0.0227	24.32	25550	389676641	6.557E-05
264	0.0227	11.63	76650	6.351E+09	1.207E-05
120	0.0227	5.29	54750	1.255E+11	4.363E-07
96	0.0227	4.23	47450	2.919E+11	1.625E-07
				Total damage ratio from 2046 to2056 =	0.0309183

Table 3.47: Damage ratio from 2046 to 2056 under operating scenario A4

Axial force range in kN, ΔN	Average cross-sectional Area in sqm, A	Stress range in MPa, $\Delta\sigma$	Total cycles in 10 years n_i	Number of cycles to failure, N_i	n_i/N_i
3792	0.0226	167.79	3650	260920.73	0.0139889
1992	0.0226	88.14	25550	2981504.7	0.0085695
1800	0.0226	79.65	3650	4375172.4	0.0008343
1752	0.0226	77.52	21900	4846333.5	0.0045189
816	0.0226	36.11	153300	87319406	0.0017556
720	0.0226	31.86	102000	140216837	0.0007274
672	0.0226	29.73	109500	182045943	0.0006015
624	0.0226	27.61	87600	240972701	0.0003635
552	0.0226	24.42	25550	383220615	6.667E-05
264	0.0226	11.68	76650	6.246E+09	1.227E-05
120	0.0226	5.31	54750	1.234E+11	4.437E-07
96	0.0226	4.25	47450	2.871E+11	1.653E-07
Total damage ratio from 2056 to2066 =					0.0314392

Table 3.48: Damage ratio from 2056 to 2066 under operating scenario A4

Axial force range in kN, ΔN	Average cross-sectional Area in sqm, A	Stress range in MPa, $\Delta\sigma$	Total cycles in 10 years n_i	Number of cycles to failure, N_i	n_i/N_i
3792	0.0225	168.53	3650	256578.87	0.0142256
1992	0.0225	88.53	25550	2931890.9	0.0087145
1800	0.0225	80.00	3650	4302367.4	0.0008484
1752	0.0225	77.87	21900	4765688	0.0045953
816	0.0225	36.27	153300	85866367	0.0017853
720	0.0225	32.00	102000	137883558	0.0007398
672	0.0225	29.87	109500	179016606	0.0006117
624	0.0225	27.73	87600	236962794	0.0003697
552	0.0225	24.53	25550	376843630	6.78E-05
264	0.0225	11.73	76650	6.142E+09	1.248E-05
120	0.0225	5.33	54750	1.213E+11	4.512E-07
96	0.0225	4.27	47450	2.823E+11	1.681E-07
Total damage ratio from 2066 to2076 =					0.0319712

Table 3.49: Damage ratio from 2066 to 2076 under operating scenario A4

Axial force range in kN, ΔN	Average cross-sectional Area in sqm, A	Stress range in MPa, $\Delta\sigma$	Total cycles in 10 years n_i	Number of cycles to failure, N_i	n_i/N_i
3792	0.0223	170.04	3650	248054.92	0.0147145
1992	0.0223	89.33	25550	2834488.9	0.009014
1800	0.0223	80.72	3650	4159436	0.0008775
1752	0.0223	78.57	21900	4607364.4	0.0047533
816	0.0223	36.59	153300	83013752	0.0018467
720	0.0223	32.29	102000	133302850	0.0007652
672	0.0223	30.13	109500	173069394	0.0006327
624	0.0223	27.98	87600	229090518	0.0003824
552	0.0223	24.75	25550	364324294	7.013E-05
264	0.0223	11.84	76650	5.938E+09	1.291E-05
120	0.0223	5.38	54750	1.173E+11	4.667E-07
96	0.0223	4.30	47450	2.729E+11	1.738E-07
				Total damage ratio from 2076 to 2086 =	0.0330698

Table 3.50: Damage ratio from 2076 to 2086 under operating scenario A4

Axial force range in kN, ΔN	Average cross-sectional Area in sqm, A	Stress range in MPa, $\Delta\sigma$	Total cycles in 10 years n_i	Number of cycles to failure, N_i	n_i/N_i
3792	0.0222	170.81	3650	243871.98	0.0149669
1992	0.0222	89.73	25550	2786691	0.0091686
1800	0.0222	81.08	3650	4089295.5	0.0008926
1752	0.0222	78.92	21900	4529670.5	0.0048348
816	0.0222	36.76	153300	81613893	0.0018784
720	0.0222	32.43	102000	131054968	0.0007783
672	0.0222	30.27	109500	170150930	0.0006435
624	0.0222	28.11	87600	225227371	0.0003889
552	0.0222	24.86	25550	358180704	7.133E-05
264	0.0222	11.89	76650	5.838E+09	1.313E-05
120	0.0222	5.41	54750	1.153E+11	4.747E-07
96	0.0222	4.32	47450	2.683E+11	1.768E-07
				Total damage ratio from 2086 to 2096 =	0.0336371

Table 3.51: Damage ratio from 2086 to 2096 under operating scenario A4

Axial force range in kN, ΔN	Average cross-sectional Area in sqm, A	Stress range in MPa, Δσ	Total cycles in 10 years n_i	Number of cycles to failure, N_i	n_i/N_i
3792	0.0221	171.58	3650	239741.16	0.0152248
1992	0.0221	90.14	25550	2739488.8	0.0093266
1800	0.0221	81.45	3650	4020029.2	0.000908
1752	0.0221	79.28	21900	4452944.9	0.0049181
816	0.0221	36.92	153300	80231480	0.0019107
720	0.0221	32.58	102000	128835099	0.0007917
672	0.0221	30.41	109500	167268836	0.0006546
624	0.0221	28.24	87600	221412368	0.0003956
552	0.0221	24.98	25550	352113676	7.256E-05
264	0.0221	11.95	76650	5.739E+09	1.336E-05
120	0.0221	5.43	54750	1.134E+11	4.829E-07
96	0.0221	4.34	47450	2.638E+11	1.799E-07
Total damage ratio from 2096 to 2106 =					0.0342166

Table 3.52: Damage ratio from 2096 to 2106 under operating scenario A4

Axial force range in kN, ΔN	Average cross-sectional Area in sqm, A	Stress range in MPa, Δσ	Total cycles in 10 years n_i	Number of cycles to failure, N_i	n_i/N_i
3792	0.022	172.36	3650	235662.06	0.0154883
1992	0.022	90.55	25550	2692877.4	0.009488
1800	0.022	81.82	3650	3951629.9	0.0009237
1752	0.022	79.64	21900	4377179.8	0.0050032
816	0.022	37.09	153300	78866372	0.0019438
720	0.022	32.73	102000	126643020	0.0008054
672	0.022	30.55	109500	164422821	0.000666
624	0.022	28.36	87600	217645121	0.0004025
552	0.022	25.09	25550	346122597	7.382E-05
264	0.022	12.00	76650	5.641E+09	1.359E-05
120	0.022	5.45	54750	1.115E+11	4.912E-07
96	0.022	4.36	47450	2.593E+11	1.83E-07
Total damage ratio from 2106 to 2116 =					0.0348089

Table 3.53: Damage ratio from 2106 to 2116 under operating scenario A4

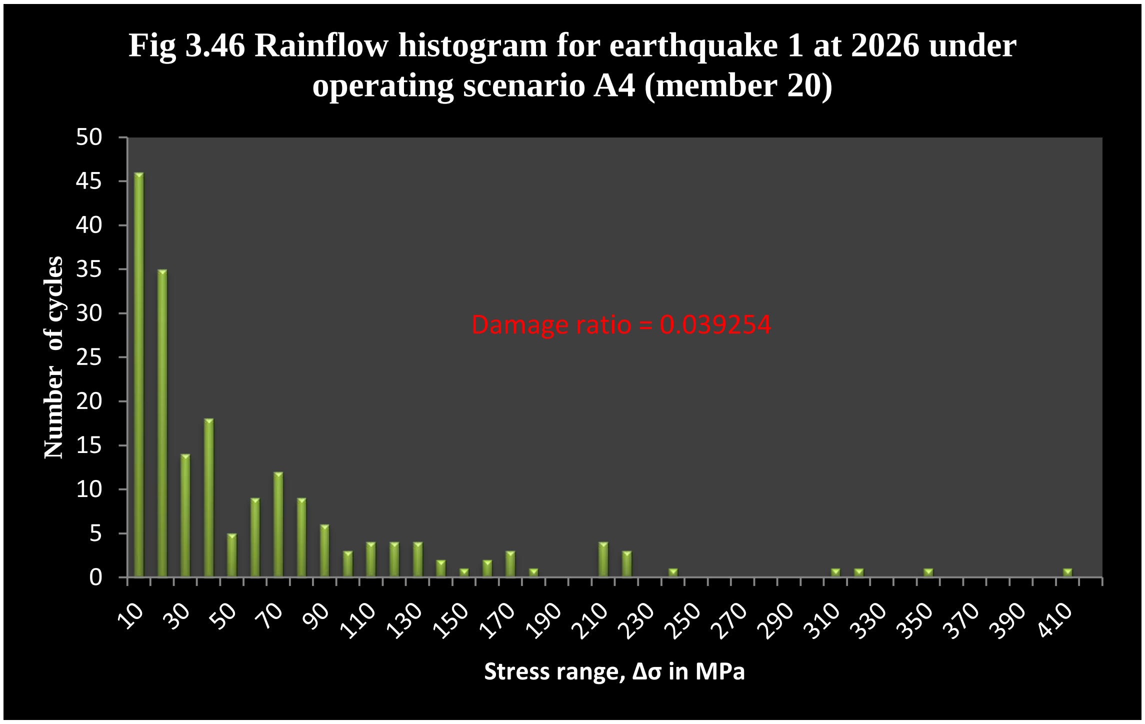

Figure 3.46 : Damage ratio for earthquake 1 in the year 2026 under operating scenario A4

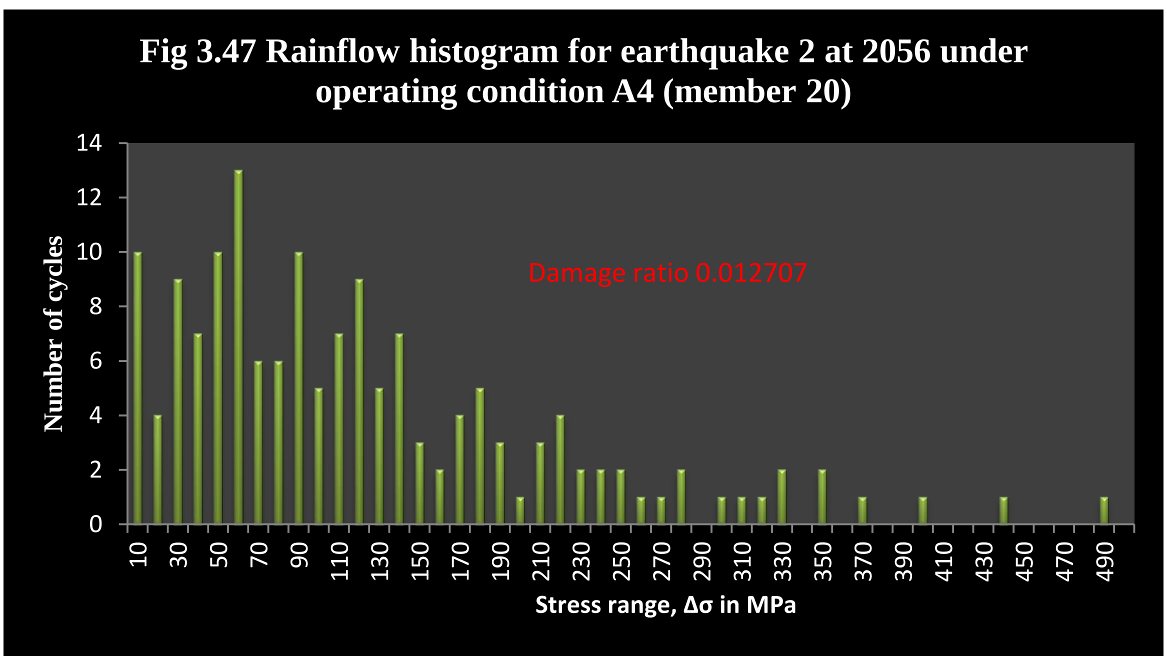

Figure 3.47 : Damage ratio for earthquake 2 in the year 2056 under operating scenario A4

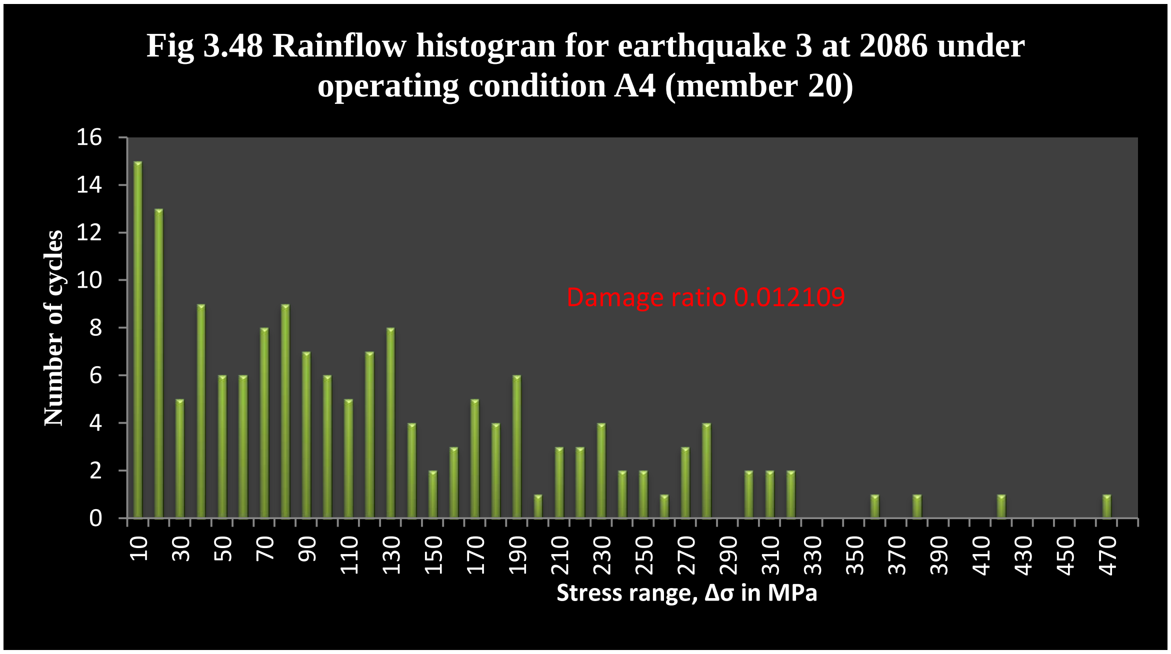

Figure 3.48 : Damage ratio for earthquake 3 in the year 2086 under operating scenario A4

In the following table and figure, the cumulative damage ratio from the year 1966 to 2116 for operating scenario A4 is shown

Year	Time period, years	Damage ratio	cumulative time, years	cumulative Damage ratio
1966-1976	10	0.0250437	10	0.0250437
1976-1986	10	0.0258494	20	0.0508931
1986-1996	10	0.0271205	30	0.0780136
1996-2006	10	0.0275616	40	0.1055752
2006-2016	10	0.0280119	50	0.1335871
2016-2026	10	0.0289408	60	0.1625279
2026 (EQ 1)		0.003925	60	0.1664529
2026-2036	10	0.0294198	70	0.1958727
2036-2046	10	0.0299089	80	0.2257816
2046-2056	10	0.0309183	90	0.2566999
2056(EQ 2)	0	0.012707	90	0.2694069
2056-2066	10	0.0314392	100	0.3008461
2066-2076	10	0.0319712	110	0.3328173
2076-2086	10	0.0330698	120	0.3658872
2086(EQ 3)		0.012109	120	0.3779962
2086-2096	10	0.0336371	130	0.4116332
2096-2106	10	0.0342166	140	0.4458499
2106-2116	10	0.0348089	150	0.4806588

Table 3.54: Cumulative Damage ratio under operating scenario A4

Fig 3.49 Cumulative damage ratio for operating condition A4

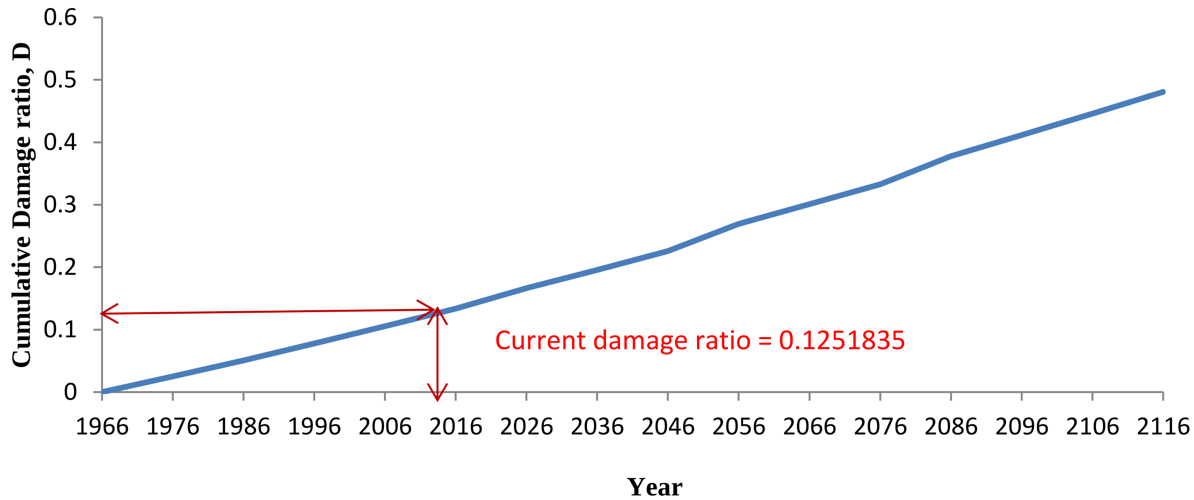

3.8.5 OPERATING SCENARIO B1:

Under this operating condition passenger, goods, through and mixed train loads are applied according to the frequency specified by Italian code. Three Earthquakes events of magnitude described before are applied at 60, 90 and 120 years from year of bridge construction (i.e. in the year 2026, 2056 and2086). It is also assumed that there is no degradation of bridge material due to corrosion and there is no maintenance program carried out. For this operating scenario, the damage ratio for the first 10 years after the bridge construction is shown in the following tabl

Axial force range, ΔN	Area of the cross-section, A	Stress range, Δσ	Total cycles in 10 years n_i	Number of cycles to failure, N_i	n_i/N_i
3792	0.024	158	18250	327553.0012	0.05571617
1992	0.024	83	54750	3742902.364	0.01462769
1800	0.024	75	18250	5492476.145	0.00332273
1752	0.024	73	109500	6083959.261	0.01799815
816	0.024	34	328500	109618480.6	0.00299676
720	0.024	30	219000	176024521.4	0.00124414
672	0.024	28	547500	228535677.8	0.00239569
624	0.024	26	438000	302510777.1	0.00144788
552	0.024	23	54750	481085058.1	0.00011381
264	0.024	11	164250	7840975184	2.0948E-05
120	0.024	5	200750	1.54916E+11	1.2959E-06
96	0.024	4	237250	3.60417E+11	6.5827E-07
Total damage ratio in Ist ten years, D=					0.09988591

Table 3.55: Damage ratio for first 10 years (1966-1976) under B1

Similarly, for every 10 years the same damage ratio will be found. The damage ratio for the earthquakes can be calculated from the rain flow histogram .Assuming no reduction in the cross-sectional area, the calculated damage ratio for the first earthquake, which will occur in the year 2026 is 0.00332. The calculated damage ratio for the second earthquake, which will occur in the year 2056, is 0.00997. The calculated damage ratio for the third earthquake, which will occur in the year 2086, is 0.009. In the following table and figure, the cumulative damage ratio from the year 1966 to 2116 for operating scenario B1 is shown

Year	Time period, years	Damage ratio	cumulative time, years	cumulative Damage ratio
1966-1976	10	0.09988591	10	0.09988591
1976-1986	10	0.09988591	20	0.19977182
1986-1996	10	0.09988591	30	0.29965773
1996-2006	10	0.09988591	40	0.39954364
2006-2016	10	0.09988591	50	0.49942955
2016-2026	10	0.09988591	60	0.59931546
2026 (EQ 1)		0.00322	60	0.60253546
2026-2036	10	0.09988591	70	0.70242137
2036-2046	10	0.09988591	80	0.80230728
2046-2056	10	0.09988591	90	0.90219319
2056(EQ 2)	0	0.00997	90	0.91216319
2056-2066	10	0.09988591	100	1.0120491
2066-2076	10	0.09988591	110	1.11193501
2076-2086	10	0.09988591	120	1.21182092
2086(EQ 3)		0.009	120	1.22082092
2086-2096	10	0.09988591	130	1.32070683
2096-2106	10	0.09988591	140	1.42059274
2106-2116	10	0.09988591	150	1.52047865

Table 3.56: Cumulative Damage ratio under operating scenario B1

Fig 3.50 Cumulative damage ratio in different years under operating scenario B1

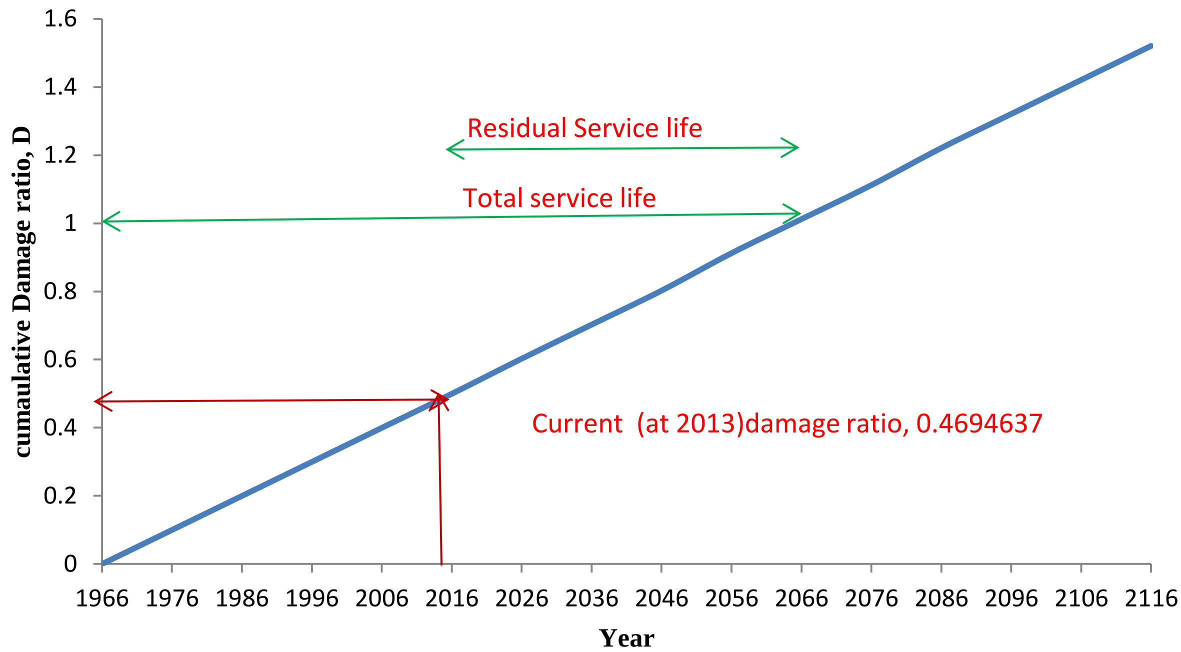

From the figure,

At current period, (2013) the cumulative damage ratio is 0.4694637

The service life of the bridge is 100 years

The residual service life is 53 years

3.8.6 OPERATING SCENARIO B2:

Under this operating condition passenger, goods, through and mixed train loads are applied according to the frequency specified by Italian code. Three Earthquakes events of magnitude described before are applied at 60, 90 and 120 years from year of bridge construction (i.e. in the year 2026, 2056 and2086). It is also assumed that there is thickness loss of bridge material due to corrosion and there is no maintenance program carried out. For this operating scenario, the damage ratio due to train load for the first 10 years, after the bridge construction is 0.09988591 as calculated before. The damage ratio in other decades are shown in the following tables

Axial force range, ΔN	Average cross-sectional Area A	Stress range, Δσ	Total cycles in 10 years n_i	Number of cycles to failure, N_i	n_i/N_i
3792	0.0238	159.33	18250	317343.38	0.0575087
1992	0.0238	83.70	54750	3626238.5	0.0150983
1800	0.0238	75.63	18250	5321279.2	0.0034296
1752	0.0238	73.61	109500	5894326.2	0.0185772
816	0.0238	34.29	328500	106201743	0.0030932
720	0.0238	30.25	219000	170537950	0.0012842
672	0.0238	28.24	547500	221412368	0.0024728
624	0.0238	26.22	438000	293081711	0.0014945
552	0.0238	23.19	54750	466089947	0.0001175
264	0.0238	11.09	164250	7.597E+09	2.162E-05
120	0.0238	5.04	200750	1.501E+11	1.338E-06
96	0.0238	4.03	237250	3.492E+11	6.794E-07
Total damage ratio from 1976 to 1986 =					0.1030995

Table 3.57: Damage ratio from 1976 to 1986 under operating scenario B2

Axial force range, ΔN	Average cross-sectional Area A	Stress range, Δσ	Total cycles in 10 years n_i	Number of cycles to failure, N_i	n_i/N_i
3792	0.0235	161.36	18250	302470.51	0.0603365
1992	0.0235	84.77	54750	3456288.2	0.0158407
1800	0.0235	76.60	18250	5071887.7	0.0035983
1752	0.0235	74.55	109500	5618077.8	0.0194907
816	0.0235	34.72	328500	101224404	0.0032453
720	0.0235	30.64	219000	162545378	0.0013473
672	0.0235	28.60	547500	211035473	0.0025944
624	0.0235	26.55	438000	279345901	0.0015679
552	0.0235	23.49	54750	444245790	0.0001232
264	0.0235	11.23	164250	7.241E+09	2.268E-05
120	0.0235	5.11	200750	1.431E+11	1.403E-06
96	0.0235	4.09	237250	3.328E+11	7.129E-07
Total damage ratio from 1986 to1996 =					0.108169

Table 3.57: Damage ratio from 1986 to 1996 under operating scenario B2

Axial force range, ΔN	Average cross-sectional Area A	Stress range, Δσ	Total cycles in 10 years n_i	Number of cycles to failure, N_i	n_i/N_i
3792	0.0233	162.75	18250	292844.48	0.0623198
1992	0.0233	85.49	54750	3346293	0.0163614
1800	0.0233	77.25	18250	4910476.6	0.0037165
1752	0.0233	75.19	109500	5439284.4	0.0201313
816	0.0233	35.02	328500	98002972	0.0033519
720	0.0233	30.90	219000	157372426	0.0013916
672	0.0233	28.84	547500	204319339	0.0026796
624	0.0233	26.78	438000	270455811	0.0016195
552	0.0233	23.69	54750	430107816	0.0001273
264	0.0233	11.33	164250	7.01E+09	2.343E-05
120	0.0233	5.15	200750	1.385E+11	1.449E-06
96	0.0233	4.12	237250	3.222E+11	7.363E-07
Total damage ratio from 1996 to2006 =					0.1117246

Table 3.58: Damage ratio from 1996 to 2006 under operating scenario B2

Axial force range, ΔN	Average cross-sectional Area A	Stress range, Δσ	Total cycles in 10 years n_i	Number of cycles to failure, N_i	n_i/N_i
3792	0.0231	164.16	18250	283445.77	0.0643862
1992	0.0231	86.23	54750	3238895.2	0.0169039
1800	0.0231	77.92	18250	4752877	0.0038398
1752	0.0231	75.84	109500	5264712.9	0.0207989
816	0.0231	35.32	328500	94857608	0.0034631
720	0.0231	31.17	219000	152321625	0.0014377
672	0.0231	29.09	547500	197761798	0.0027685
624	0.0231	27.01	438000	261775649	0.0016732
552	0.0231	23.90	54750	416303691	0.0001315
264	0.0231	11.43	164250	6.785E+09	2.421E-05
120	0.0231	5.19	200750	1.341E+11	1.498E-06
96	0.0231	4.16	237250	3.119E+11	7.607E-07
Total damage ratio from 2006 to2016 =					0.1154292

Table 3.59: Damage ratio from 2006 to 2016 under operating scenario B2

Axial force range, ΔN	Average cross-sectional Area A	Stress range, Δσ	Total cycles in 10 years n_i	Number of cycles to failure, N_i	n_i/N_i
3792	0.0229	165.59	18250	274270.89	0.0665401
1992	0.0229	86.99	54750	3134055.1	0.0174694
1800	0.0229	78.60	18250	4599030.7	0.0039682
1752	0.0229	76.51	109500	5094298.9	0.0214946
816	0.0229	35.63	328500	91787154	0.0035789
720	0.0229	31.44	219000	147391113	0.0014858
672	0.0229	29.34	547500	191360429	0.0028611
624	0.0229	27.25	438000	253302209	0.0017292
552	0.0229	24.10	54750	402828320	0.0001359
264	0.0229	11.53	164250	6.566E+09	2.502E-05
120	0.0229	5.24	200750	1.297E+11	1.548E-06
96	0.0229	4.19	237250	3.018E+11	7.861E-07
Total damage ratio from 2016 to2026 =					0.1192906

Table 3.59: Damage ratio from 2016 to 2026 under operating scenario B2

Axial force range, ΔN	Average cross-sectional Area A	Stress range, Δσ	Total cycles in 10 years n_i	Number of cycles to failure, N_i	n_i/N_i
3792	0.0227	167.05	18250	265316.4	0.0687858
1992	0.0227	87.75	54750	3031733.4	0.018059
1800	0.0227	79.30	18250	4448879.9	0.0041022
1752	0.0227	77.18	109500	4927978.5	0.0222201
816	0.0227	35.95	328500	88790455	0.0036997
720	0.0227	31.72	219000	142579037	0.001536
672	0.0227	29.60	547500	185112827	0.0029577
624	0.0227	27.49	438000	245032311	0.0017875
552	0.0227	24.32	54750	389676641	0.0001405
264	0.0227	11.63	164250	6.351E+09	2.586E-05
120	0.0227	5.29	200750	1.255E+11	1.6E-06
96	0.0227	4.23	237250	2.919E+11	8.127E-07
Total damage ratio from 2026 to2036 =					0.1233167

Table 3.60: Damage ratio from 2026 to 2036 under operating scenario B2

Axial force range, ΔN	Average cross-sectional Area A	Stress range, Δσ	Total cycles in 10 years n_i	Number of cycles to failure, N_i	n_i/N_i
3792	0.0225	168.53	18250	256578.87	0.0711282
1992	0.0225	88.53	54750	2931890.9	0.018674
1800	0.0225	80.00	18250	4302367.4	0.0042419
1752	0.0225	77.87	109500	4765688	0.0229767
816	0.0225	36.27	328500	85866367	0.0038257
720	0.0225	32.00	219000	137883558	0.0015883
672	0.0225	29.87	547500	179016606	0.0030584
624	0.0225	27.73	438000	236962794	0.0018484
552	0.0225	24.53	54750	376843630	0.0001453
264	0.0225	11.73	164250	6.142E+09	2.674E-05
120	0.0225	5.33	200750	1.213E+11	1.654E-06
96	0.0225	4.27	237250	2.823E+11	8.404E-07
Total damage ratio from 2036 to2046 =					0.1275161

Table 3.61: Damage ratio from 2036 to 2046 under operating scenario B2

Axial force range in kN, ΔN	Average cross-sectional Area in sqm, A	Stress range in MPa, Δσ	Total cycles in 10 years n_i	Number of cycles to failure, N_i	n_i/N_i
3792	0.0223	170.04	18250	248054.92	0.0735724
1992	0.0223	89.33	54750	2834488.9	0.0193157
1800	0.0223	80.72	18250	4159436	0.0043876
1752	0.0223	78.57	109500	4607364.4	0.0237663
816	0.0223	36.59	328500	83013752	0.0039572
720	0.0223	32.29	219000	133302850	0.0016429
672	0.0223	30.13	547500	173069394	0.0031635
624	0.0223	27.98	438000	229090518	0.0019119
552	0.0223	24.75	54750	364324294	0.0001503
264	0.0223	11.84	164250	5.938E+09	2.766E-05
120	0.0223	5.38	200750	1.173E+11	1.711E-06
96	0.0223	4.30	237250	2.729E+11	8.692E-07
Total damage ratio from 2046 to2056 =					0.1318979

Table 3.62: Damage ratio from 2046 to 2056 under operating scenario B2

Axial force range in kN, ΔN	Average cross-sectional Area in sqm, A	Stress range in MPa, Δσ	Total cycles in 10 years n_i	Number of cycles to failure, N_i	n_i/N_i
3792	0.0221	171.58	18250	239741.16	0.0761238
1992	0.0221	90.14	54750	2739488.8	0.0199855
1800	0.0221	81.45	18250	4020029.2	0.0045398
1752	0.0221	79.28	109500	4452944.9	0.0245905
816	0.0221	36.92	328500	80231480	0.0040944
720	0.0221	32.58	219000	128835099	0.0016998
672	0.0221	30.41	547500	167268836	0.0032732
624	0.0221	28.24	438000	221412368	0.0019782
552	0.0221	24.98	54750	352113676	0.0001555
264	0.0221	11.95	164250	5.739E+09	2.862E-05
120	0.0221	5.43	200750	1.134E+11	1.771E-06
96	0.0221	4.34	237250	2.638E+11	8.994E-07
Total damage ratio from 2056 to2066 =					0.1364719

Table 3.63: Damage ratio from 2056 to 2066 under operating scenario B2

Axial force range in kN, ΔN	Average cross-sectional Area in sqm, A	Stress range in MPa, Δσ	Total cycles in 10 years n_i	Number of cycles to failure, N_i	n_i/N_i
3792	0.0219	173.15	18250	231634.25	0.078788
1992	0.0219	90.96	54750	2646852.2	0.0206849
1800	0.0219	82.19	18250	3884090.8	0.0046987
1752	0.0219	80.00	109500	4302367.4	0.0254511
816	0.0219	37.26	328500	77518430	0.0042377
720	0.0219	32.88	219000	124478505	0.0017593
672	0.0219	30.68	547500	161612594	0.0033877
624	0.0219	28.49	438000	213925248	0.0020474
552	0.0219	25.21	54750	340206855	0.0001609
264	0.0219	12.05	164250	5.545E+09	2.962E-05
120	0.0219	5.48	200750	1.096E+11	1.832E-06
96	0.0219	4.38	237250	2.549E+11	9.309E-07
Total damage ratio from 2066 to2076 =					0.1412482

Table 3.64: Damage ratio from 2066 to 2076 under operating scenario B2

Axial force range in kN, ΔN	Average cross-sectional Area in sqm, A	Stress range in MPa, $\Delta\sigma$	Total cycles in 10 years n_i	Number of cycles to failure, N_i	n_i/N_i
3792	0.0217	174.75	18250	223730.85	0.0815712
1992	0.0217	91.80	54750	2556541.2	0.0214157
1800	0.0217	82.95	18250	3751565	0.0048646
1752	0.0217	80.74	109500	4155569.9	0.0263502
816	0.0217	37.60	328500	74873489	0.0043874
720	0.0217	33.18	219000	120231279	0.0018215
672	0.0217	30.97	547500	156098347	0.0035074
624	0.0217	28.76	438000	206626084	0.0021198
552	0.0217	25.44	54750	328598943	0.0001666
264	0.0217	12.17	164250	5.356E+09	3.067E-05
120	0.0217	5.53	200750	1.058E+11	1.897E-06
96	0.0217	4.42	237250	2.462E+11	9.637E-07
Total damage ratio from 2076 to 2086 =					0.1462379

Table 3.65: Damage ratio from 2076 to 2086 under operating scenario B2

Axial force range in kN, ΔN	Average cross-sectional Area in sqm, A	Stress range in MPa, $\Delta\sigma$	Total cycles in 10 years n_i	Number of cycles to failure, N_i	n_i/N_i
3792	0.0215	176.37	18250	216027.67	0.0844799
1992	0.0215	92.65	54750	2468518	0.0221793
1800	0.0215	83.72	18250	3622396.4	0.0050381
1752	0.0215	81.49	109500	4012491.2	0.0272898
816	0.0215	37.95	328500	72295551	0.0045438
720	0.0215	33.49	219000	116091645	0.0018864
672	0.0215	31.26	547500	150723789	0.0036325
624	0.0215	29.02	438000	199511827	0.0021954
552	0.0215	25.67	54750	317285089	0.0001726
264	0.0215	12.28	164250	5.171E+09	3.176E-05
120	0.0215	5.58	200750	1.022E+11	1.965E-06
96	0.0215	4.47	237250	2.377E+11	9.981E-07
Total damage ratio from 2086 to 2096 =					0.1514525

Table 3.66: Damage ratio from 2086 to 2096 under operating scenario B2

Axial force range in kN, ΔN	Average cross-sectional Area in sqm, A	Stress range in MPa, $\Delta\sigma$	Total cycles in 10 years n_i	Number of cycles to failure, N_i	n_i/N_i
3792	0.0213	178.03	18250	208521.42	0.087521
1992	0.0213	93.52	54750	2382745.1	0.0229777
1800	0.0213	84.51	18250	3496530	0.0052195
1752	0.0213	82.25	109500	3873070.3	0.0282721
816	0.0213	38.31	328500	69783518	0.0047074
720	0.0213	33.80	219000	112057842	0.0019543
672	0.0213	31.55	547500	145486632	0.0037632
624	0.0213	29.30	438000	192579446	0.0022744
552	0.0213	25.92	54750	306260473	0.0001788
264	0.0213	12.39	164250	4.992E+09	3.291E-05
120	0.0213	5.63	200750	9.862E+10	2.036E-06
96	0.0213	4.51	237250	2.294E+11	1.034E-06
Total damage ratio from 2096 to 2106 =					0.1569044

Table 3.67: Damage ratio from 2096 to 2106 under operating scenario B2

Axial force range in kN, ΔN	Average cross-sectional Area in sqm, A	Stress range in MPa, $\Delta\sigma$	Total cycles in 10 years n_i	Number of cycles to failure, N_i	n_i/N_i
3792	0.0211	179.72	18250	201208.84	0.0907018
1992	0.0211	94.41	54750	2299185.3	0.0238128
1800	0.0211	85.31	18250	3373911.2	0.0054092
1752	0.0211	83.03	109500	3737246.7	0.0292996
816	0.0211	38.67	328500	67336300	0.0048785
720	0.0211	34.12	219000	108128118	0.0020254
672	0.0211	31.85	547500	140384604	0.0039
624	0.0211	29.57	438000	185825934	0.002357
552	0.0211	26.16	54750	295520315	0.0001853
264	0.0211	12.51	164250	4.817E+09	3.41E-05
120	0.0211	5.69	200750	9.516E+10	2.11E-06
96	0.0211	4.55	237250	2.214E+11	1.072E-06
Total damage ratio from 2106 to 2116 =					0.1626068

Table 3.68: Damage ratio from 2106 to 2116 under operating scenario B2

In the following table and figure, the cumulative damage ratio from the year 1966 to 2116 for operating scenario B2 is shown

Year	Time period, years	Damage ratio	cumulative time, years	cumulative Damage ratio
1966-1976	10	0.09988591	10	0.0998859
1976-1986	10	0.10309946	20	0.2029854
1986-1996	10	0.108169	30	0.3111544
1996-2006	10	0.11172459	40	0.422879
2006-2016	10	0.11542924	50	0.5383082
2016-2026	10	0.11929057	60	0.6575988
2026 (EQ 1)		0.00408	60	0.6616788
2026-2036	10	0.12331666	70	0.7849954
2036-2046	10	0.12751608	80	0.9125115
2046-2056	10	0.13189793	90	1.0444094
2056(EQ 2)	0	0.01349	90	1.0578994
2056-2066	10	0.1364719	100	1.1943713
2066-2076	10	0.14124824	110	1.3356196
2076-2086	10	0.1462379	120	1.4818575
2086(EQ 3)		0.01342	120	1.4952775
2086-2096	10	0.1514525	130	1.64673
2096-2106	10	0.15690442	140	1.8036344
2106-2116	10	0.16260683	150	1.9662412

Table 3.69: Cumulative Damage ratio from 1966 to 2116 under operating scenario B2

Fig 51 Cumulative damage ratio for operating condition B2

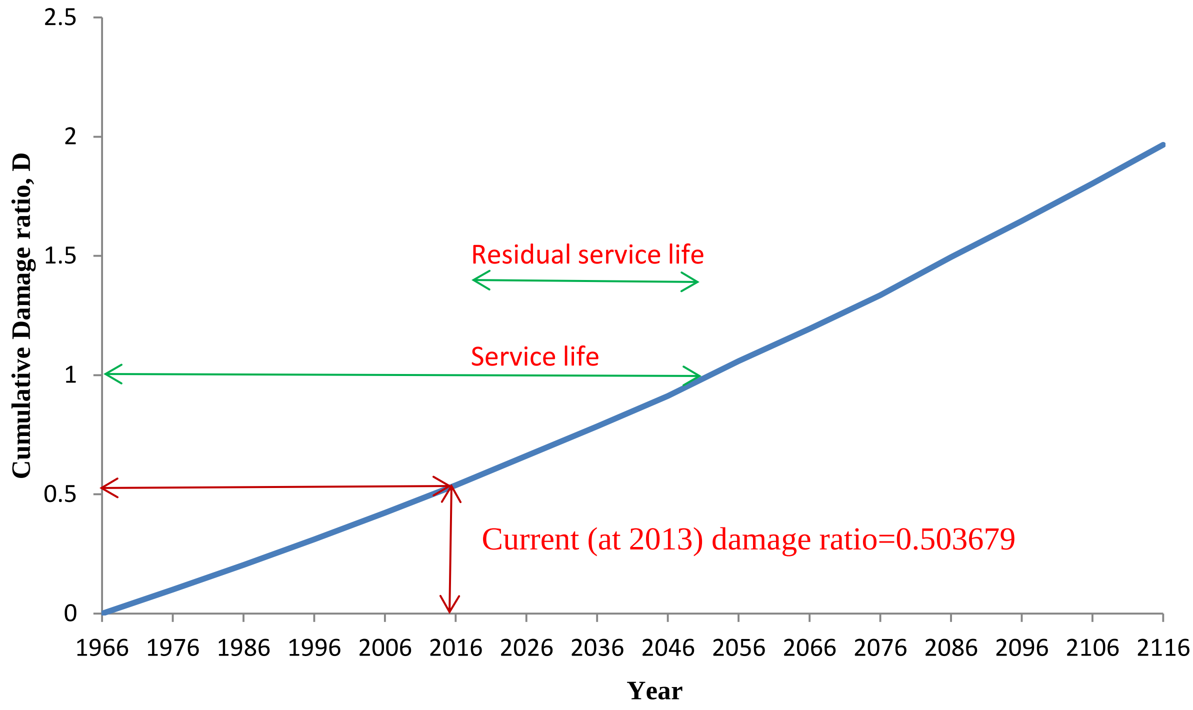

From the figure,

At current period, (2013) the cumulative damage ratio is 0.503679

The service life of the bridge is 86.6 years

The residual service life is 39.6 years

3.8.7 OPERATING SCENARIO B3:

Under this operating condition passenger, goods, through and mixed train loads are applied according to the frequency specified by Italian code. Three Earthquakes events of magnitude described before are applied at 60, 90 and 120 years from year of bridge construction (i.e. in the year 2026, 2056 and2086). It is also assumed that a total number of three corrosion protective paintings are provide at the interval of every ten years for the first thirty years from the year of bridge construction and the thickness loss of bridge material due to corrosion initiates after forty years of bridge construction, i.e. in the year 2006 .For this operating scenario, the damage ratio due to train load for the first 10 (1966-76) years, after the bridge construction is 0.09988591 as calculated before. The damage ratio due to train load for the next three decades (1976-1986, 1986-1996 and 1996-2006) are also 0.09988591 as calculated before. The damage ratio in other decades are shown in the following tables

Axial force range, ΔN	Average cross-sectional Area A	Stress range, Δσ	Total cycles in 10 years n_i	Number of cycles to failure, N_i	n_i/N_i
3792	0.0238	159.33	18250	317343.38	0.0575087
1992	0.0238	83.70	54750	3626238.5	0.0150983
1800	0.0238	75.63	18250	5321279.2	0.0034296
1752	0.0238	73.61	109500	5894326.2	0.0185772
816	0.0238	34.29	328500	106201743	0.0030932
720	0.0238	30.25	219000	170537950	0.0012842
672	0.0238	28.24	547500	221412368	0.0024728
624	0.0238	26.22	438000	293081711	0.0014945
552	0.0238	23.19	54750	466089947	0.0001175
264	0.0238	11.09	164250	7.597E+09	2.162E-05
120	0.0238	5.04	200750	1.501E+11	1.338E-06
96	0.0238	4.03	237250	3.492E+11	6.794E-07
				Total damage ratio from 2006 to2016 =	0.1030995

Table 3.70: Damage ratio from 2006 to 2016 under operating scenario B3

Axial force range, ΔN	Average cross-sectional Area A	Stress range, Δσ	Total cycles in 10 years n_i	Number of cycles to failure, N_i	n_i/N_i
3792	0.0235	161.36	18250	302470.51	0.0603365
1992	0.0235	84.77	54750	3456288.2	0.0158407
1800	0.0235	76.60	18250	5071887.7	0.0035983
1752	0.0235	74.55	109500	5618077.8	0.0194907
816	0.0235	34.72	328500	101224404	0.0032453
720	0.0235	30.64	219000	162545378	0.0013473
672	0.0235	28.60	547500	211035473	0.0025944
624	0.0235	26.55	438000	279345901	0.0015679
552	0.0235	23.49	54750	444245790	0.0001232
264	0.0235	11.23	164250	7.241E+09	2.268E-05
120	0.0235	5.11	200750	1.431E+11	1.403E-06
96	0.0235	4.09	237250	3.328E+11	7.129E-07
				Total damage ratio from 2016 to2026 =	0.108169

Table 3.71: Damage ratio from 2016 to 2026 under operating scenario B

Axial force range, ΔN	Average cross-sectional Area A	Stress range, Δσ	Total cycles in 10 years n_i	Number of cycles to failure, N_i	n_i/N_i
3792	0.0233	162.75	18250	292844.48	0.0623198
1992	0.0233	85.49	54750	3346293	0.0163614
1800	0.0233	77.25	18250	4910476.6	0.0037165
1752	0.0233	75.19	109500	5439284.4	0.0201313
816	0.0233	35.02	328500	98002972	0.0033519
720	0.0233	30.90	219000	157372426	0.0013916
672	0.0233	28.84	547500	204319339	0.0026796
624	0.0233	26.78	438000	270455811	0.0016195
552	0.0233	23.69	54750	430107816	0.0001273
264	0.0233	11.33	164250	7.01E+09	2.343E-05
120	0.0233	5.15	200750	1.385E+11	1.449E-06
96	0.0233	4.12	237250	3.222E+11	7.363E-07
				Total damage ratio from 2026 to2036 =	0.1117246

Table 3.72: Damage ratio from 2026 to 2036 under operating scenario B3

Axial force range, ΔN	Average cross-sectional Area A	Stress range, Δσ	Total cycles in 10 years n_i	Number of cycles to failure, N_i	n_i/N_i
3792	0.0231	164.16	18250	283445.77	0.0643862
1992	0.0231	86.23	54750	3238895.2	0.0169039
1800	0.0231	77.92	18250	4752877	0.0038398
1752	0.0231	75.84	109500	5264712.9	0.0207989
816	0.0231	35.32	328500	94857608	0.0034631
720	0.0231	31.17	219000	152321625	0.0014377
672	0.0231	29.09	547500	197761798	0.0027685
624	0.0231	27.01	438000	261775649	0.0016732
552	0.0231	23.90	54750	416303691	0.0001315
264	0.0231	11.43	164250	6.785E+09	2.421E-05
120	0.0231	5.19	200750	1.341E+11	1.498E-06
96	0.0231	4.16	237250	3.119E+11	7.607E-07
				Total damage ratio from 2036 to2046 =	0.1154292

Table 3.73: Damage ratio from 2036 to 2046 under operating scenario B3

Axial force range in kN, ΔN	Average cross-sectional Area in sqm, A	Stress range in MPa, Δσ	Total cycles in 10 years n_i	Number of cycles to failure, N_i	n_i/N_i
3792	0.0229	165.59	18250	274270.89	0.0665401
1992	0.0229	86.99	54750	3134055.1	0.0174694
1800	0.0229	78.60	18250	4599030.7	0.0039682
1752	0.0229	76.51	109500	5094298.9	0.0214946
816	0.0229	35.63	328500	91787154	0.0035789
720	0.0229	31.44	219000	147391113	0.0014858
672	0.0229	29.34	547500	191360429	0.0028611
624	0.0229	27.25	438000	253302209	0.0017292
552	0.0229	24.10	54750	402828320	0.0001359
264	0.0229	11.53	164250	6.566E+09	2.502E-05
120	0.0229	5.24	200750	1.297E+11	1.548E-06
96	0.0229	4.19	237250	3.018E+11	7.861E-07
				Total damage ratio from 2046 to2056 =	0.1192906

Table 3.74: Damage ratio from 2046 to 2056 under operating scenario B3

Axial force range in kN, ΔN	Average cross-sectional Area in sqm, A	Stress range in MPa, Δσ	Total cycles in 10 years n_i	Number of cycles to failure, N_i	n_i/N_i
3792	0.0227	167.05	18250	265316.4	0.0687858
1992	0.0227	87.75	54750	3031733.4	0.018059
1800	0.0227	79.30	18250	4448879.9	0.0041022
1752	0.0227	77.18	109500	4927978.5	0.0222201
816	0.0227	35.95	328500	88790455	0.0036997
720	0.0227	31.72	219000	142579037	0.001536
672	0.0227	29.60	547500	185112827	0.0029577
624	0.0227	27.49	438000	245032311	0.0017875
552	0.0227	24.32	54750	389676641	0.0001405
264	0.0227	11.63	164250	6.351E+09	2.586E-05
120	0.0227	5.29	200750	1.255E+11	1.6E-06
96	0.0227	4.23	237250	2.919E+11	8.127E-07
				Total damage ratio from 2056 to2066 =	0.1233167

Table 3.75: Damage ratio from 2056 to 2066 under operating scenario B3

Axial force range in kN, ΔN	Average cross-sectional Area in sqm, A	Stress range in MPa, Δσ	Total cycles in 10 years n_i	Number of cycles to failure, N_i	n_i/N_i
3792	0.0225	168.53	18250	256578.87	0.0711282
1992	0.0225	88.53	54750	2931890.9	0.018674
1800	0.0225	80.00	18250	4302367.4	0.0042419
1752	0.0225	77.87	109500	4765688	0.0229767
816	0.0225	36.27	328500	85866367	0.0038257
720	0.0225	32.00	219000	137883558	0.0015883
672	0.0225	29.87	547500	179016606	0.0030584
624	0.0225	27.73	438000	236962794	0.0018484
552	0.0225	24.53	54750	376843630	0.0001453
264	0.0225	11.73	164250	6.142E+09	2.674E-05
120	0.0225	5.33	200750	1.213E+11	1.654E-06
96	0.0225	4.27	237250	2.823E+11	8.404E-07
Total damage ratio from 2066 to2076 =					0.1275161

Table 3.76: Damage ratio from 2066 to 2076 under operating scenario B3

Axial force range in kN, ΔN	Average cross-sectional Area in sqm, A	Stress range in MPa, Δσ	Total cycles in 10 years n_i	Number of cycles to failure, N_i	n_i/N_i
3792	0.0223	170.04	18250	248054.92	0.0735724
1992	0.0223	89.33	54750	2834488.9	0.0193157
1800	0.0223	80.72	18250	4159436	0.0043876
1752	0.0223	78.57	109500	4607364.4	0.0237663
816	0.0223	36.59	328500	83013752	0.0039572
720	0.0223	32.29	219000	133302850	0.0016429
672	0.0223	30.13	547500	173069394	0.0031635
624	0.0223	27.98	438000	229090518	0.0019119
552	0.0223	24.75	54750	364324294	0.0001503
264	0.0223	11.84	164250	5.938E+09	2.766E-05
120	0.0223	5.38	200750	1.173E+11	1.711E-06
96	0.0223	4.30	237250	2.729E+11	8.692E-07
Total damage ratio from 2076 to 2086 =					0.1318979

Table 3.77: Damage ratio from 2076 to 2086 under operating scenario B3

Axial force range in kN, ΔN	Average cross-sectional Area in sqm, A	Stress range in MPa, Δσ	Total cycles in 10 years n_i	Number of cycles to failure, N_i	n_i/N_i
3792	0.0221	171.58	18250	239741.16	0.0761238
1992	0.0221	90.14	54750	2739488.8	0.0199855
1800	0.0221	81.45	18250	4020029.2	0.0045398
1752	0.0221	79.28	109500	4452944.9	0.0245905
816	0.0221	36.92	328500	80231480	0.0040944
720	0.0221	32.58	219000	128835099	0.0016998
672	0.0221	30.41	547500	167268836	0.0032732
624	0.0221	28.24	438000	221412368	0.0019782
552	0.0221	24.98	54750	352113676	0.0001555
264	0.0221	11.95	164250	5.739E+09	2.862E-05
120	0.0221	5.43	200750	1.134E+11	1.771E-06
96	0.0221	4.34	237250	2.638E+11	8.994E-07
				Total damage ratio from 2086 to 2096 =	0.1364719

Table 3.78: Damage ratio from 2086 to 2096 under operating scenario B3

Axial force range in kN, ΔN	Average cross-sectional Area in sqm, A	Stress range in MPa, Δσ	Total cycles in 10 years n_i	Number of cycles to failure, N_i	n_i/N_i
3792	0.0219	173.15	18250	231634.25	0.078788
1992	0.0219	90.96	54750	2646852.2	0.0206849
1800	0.0219	82.19	18250	3884090.8	0.0046987
1752	0.0219	80.00	109500	4302367.4	0.0254511
816	0.0219	37.26	328500	77518430	0.0042377
720	0.0219	32.88	219000	124478505	0.0017593
672	0.0219	30.68	547500	161612594	0.0033877
624	0.0219	28.49	438000	213925248	0.0020474
552	0.0219	25.21	54750	340206855	0.0001609
264	0.0219	12.05	164250	5.545E+09	2.962E-05
120	0.0219	5.48	200750	1.096E+11	1.832E-06
96	0.0219	4.38	237250	2.549E+11	9.309E-07
				Total damage ratio from 2096 to 2106 =	0.1412482

Table 3.79: Damage ratio from 2096 to 2106 under operating scenario B3

Axial force range in kN, ΔN	Average cross-sectional Area in sqm, A	Stress range in MPa, Δσ	Total cycles in 10 years n_i	Number of cycles to failure, N_i	n_i/N_i
3792	0.0217	174.75	18250	223730.85	0.0815712
1992	0.0217	91.80	54750	2556541.2	0.0214157
1800	0.0217	82.95	18250	3751565	0.0048646
1752	0.0217	80.74	109500	4155569.9	0.0263502
816	0.0217	37.60	328500	74873489	0.0043874
720	0.0217	33.18	219000	120231279	0.0018215
672	0.0217	30.97	547500	156098347	0.0035074
624	0.0217	28.76	438000	206626084	0.0021198
552	0.0217	25.44	54750	328598943	0.0001666
264	0.0217	12.17	164250	5.356E+09	3.067E-05
120	0.0217	5.53	200750	1.058E+11	1.897E-06
96	0.0217	4.42	237250	2.462E+11	9.637E-07
Total damage ratio from 2106 to 2116 =					0.1462379

Table 3.80: Damage ratio from 2106 to 2116 under operating scenario B3

In the following table and figure, the cumulative damage ratio from the year 1966 to 2116 for operating scenario B3 is shown

Year	Time period, years	Damage ratio	cumulative time, years	cumulative Damage ratio
1966-1976	10	0.0998859	10	0.0998859
1976-1986	10	0.0998859	20	0.1997718
1986-1996	10	0.0998859	30	0.2996577
1996-2006	10	0.0998859	40	0.3995437
2006-2016	10	0.1030995	50	0.5026431
2016-2026	10	0.108169	60	0.6108121
2026 (EQ 1)		0.0036	60	0.6144121
2026-2036	10	0.1117246	70	0.7261367
2036-2046	10	0.1154292	80	0.8415659
2046-2056	10	0.1192906	90	0.9608565
2056(EQ 2)	0	0.01223	90	0.9730865
2056-2066	10	0.1233167	100	1.0964032
2066-2076	10	0.1275161	110	1.2239192
2076-2086	10	0.1318979	120	1.3558172
2086(EQ 3)		0.012109	120	1.3679262
2086-2096	10	0.1364719	130	1.5043981
2096-2106	10	0.1412482	140	1.6456463
2106-2116	10	0.1462379	150	1.7918842

Table 3.81: Cumulative Damage ratio under operating scenario B

Fig 3.52 Cumulative damage ratio for operating condition B3

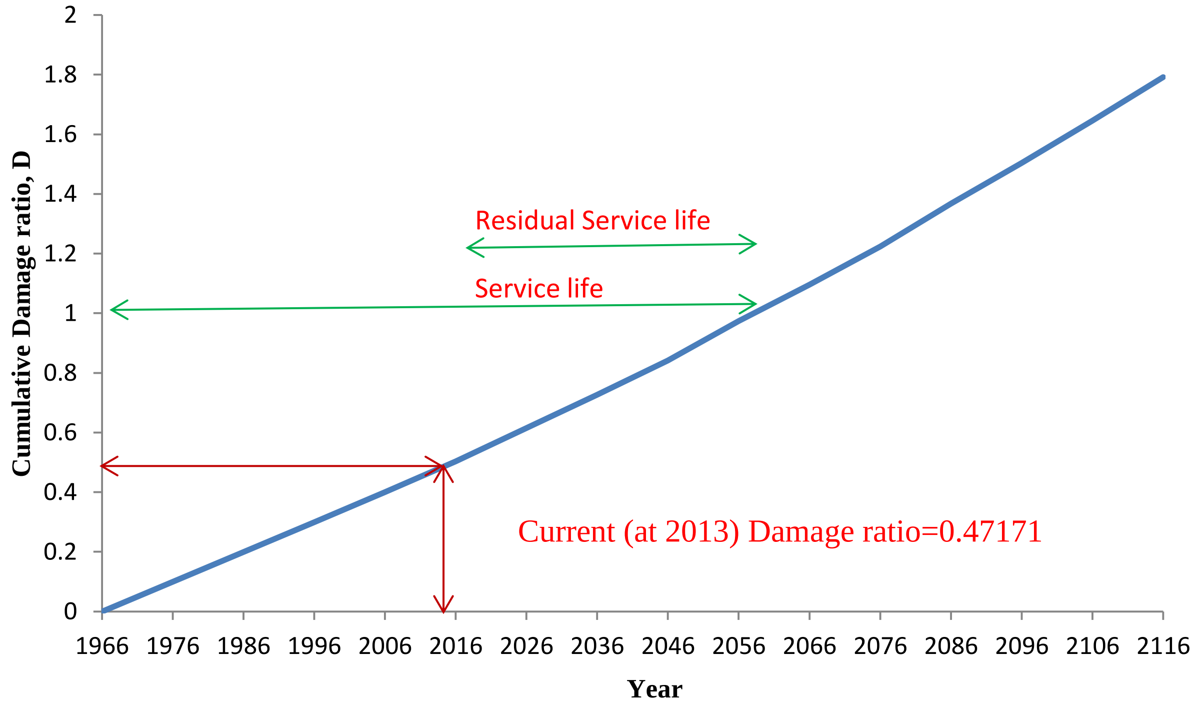

From the figure,

At current period, (2013) the cumulative damage ratio is 0.47171

The service life of the bridge is 92.2 years

The residual service life is 45.2 years

<u>3.8.8 OPERATING SCENARIO B4:</u>

Under this operating condition passenger, goods, through and mixed train loads are applied according to the frequency specified by Italian code. Three Earthquakes events of magnitude described before are applied at 60, 90 and 120 years from year of bridge construction (i.e. in the year 2026, 2056 and2086). It is also assumed that corrosion protective paintings are provide at the interval of every thirty years from the year of bridge construction and the thickness loss of bridge material due to corrosion initiated after 10 years of bridge construction, i.e. in the year1976 and continues as described before in paragraph 3.6.3 .For this operating scenario, the damage ratio due to train load for the first 10 (1966-76) years, after the bridge construction is 0.09988591 as calculated before. The damage ratio in other decades are shown in the following tables

Axial force range, ΔN	Average cross-sectional Area A	Stress range, Δσ	Total cycles in 10 years n_i	Number of cycles to failure, N_i	n_i/N_i
3792	0.0238	159.33	18250	317343.38	0.0575087
1992	0.0238	83.70	54750	3626238.5	0.0150983
1800	0.0238	75.63	18250	5321279.2	0.0034296
1752	0.0238	73.61	109500	5894326.2	0.0185772
816	0.0238	34.29	328500	106201743	0.0030932
720	0.0238	30.25	219000	170537950	0.0012842
672	0.0238	28.24	547500	221412368	0.0024728
624	0.0238	26.22	438000	293081711	0.0014945
552	0.0238	23.19	54750	466089947	0.0001175
264	0.0238	11.09	164250	7.597E+09	2.162E-05
120	0.0238	5.04	200750	1.501E+11	1.338E-06
96	0.0238	4.03	237250	3.492E+11	6.794E-07
Total damage ratio from 1976 to 1986 =					0.1030995

Table 3.82: Damage ratio from 1976 to 1986 under operating scenario B4

Axial force range, ΔN	Average cross-sectional Area A	Stress range, Δσ	Total cycles in 10 years n_i	Number of cycles to failure, N_i	n_i/N_i
3792	0.0235	161.36	18250	302470.51	0.0603365
1992	0.0235	84.77	54750	3456288.2	0.0158407
1800	0.0235	76.60	18250	5071887.7	0.0035983
1752	0.0235	74.55	109500	5618077.8	0.0194907
816	0.0235	34.72	328500	101224404	0.0032453
720	0.0235	30.64	219000	162545378	0.0013473
672	0.0235	28.60	547500	211035473	0.0025944
624	0.0235	26.55	438000	279345901	0.0015679
552	0.0235	23.49	54750	444245790	0.0001232
264	0.0235	11.23	164250	7.241E+09	2.268E-05
120	0.0235	5.11	200750	1.431E+11	1.403E-06
96	0.0235	4.09	237250	3.328E+11	7.129E-07
Total damage ratio from 1986 to1996 =					0.108169

Table 3.83: Damage ratio from 1986 to 1996 under operating scenario B4

Axial force range, ΔN	Average cross-sectional Area A	Stress range, Δσ	Total cycles in 10 years n_i	Number of cycles to failure, N_i	n_i/N_i
3792	0.0234	162.05	18250	297628.87	0.061318
1992	0.0234	85.13	54750	3400963.4	0.0160984
1800	0.0234	76.92	18250	4990702.1	0.0036568
1752	0.0234	74.87	109500	5528149.3	0.0198077
816	0.0234	34.87	328500	99604106	0.0032981
720	0.0234	30.77	219000	159943516	0.0013692
672	0.0234	28.72	547500	207657430	0.0026366
624	0.0234	26.67	438000	274874414	0.0015935
552	0.0234	23.59	54750	437134752	0.0001252
264	0.0234	11.28	164250	7.125E+09	2.305E-05
120	0.0234	5.13	200750	1.408E+11	1.426E-06
96	0.0234	4.10	237250	3.275E+11	7.244E-07
Total damage ratio from 1996 to2006 =					0.1099286

Table 3.84: Damage ratio from 1996 to 2006 under operating scenario B4

Axial force range, ΔN	Average cross-sectional Area A	Stress range, Δσ	Total cycles in 10 years n_i	Number of cycles to failure, N_i	n_i/N_i
3792	0.0233	162.75	18250	292844.48	0.0623198
1992	0.0233	85.49	54750	3346293	0.0163614
1800	0.0233	77.25	18250	4910476.6	0.0037165
1752	0.0233	75.19	109500	5439284.4	0.0201313
816	0.0233	35.02	328500	98002972	0.0033519
720	0.0233	30.90	219000	157372426	0.0013916
672	0.0233	28.84	547500	204319339	0.0026796
624	0.0233	26.78	438000	270455811	0.0016195
552	0.0233	23.69	54750	430107816	0.0001273
264	0.0233	11.33	164250	7.01E+09	2.343E-05
120	0.0233	5.15	200750	1.385E+11	1.449E-06
96	0.0233	4.12	237250	3.222E+11	7.363E-07
Total damage ratio from 2006 to2016 =					0.1117246

Table 3.85: Damage ratio from 2006 to 2016 under operating scenario B4

Axial force range, ΔN	Average cross-sectional Area A	Stress range, Δσ	Total cycles in 10 years n_i	Number of cycles to failure, N_i	n_i/N_i
3792	0.0231	164.16	18250	283445.77	0.0643862
1992	0.0231	86.23	54750	3238895.2	0.0169039
1800	0.0231	77.92	18250	4752877	0.0038398
1752	0.0231	75.84	109500	5264712.9	0.0207989
816	0.0231	35.32	328500	94857608	0.0034631
720	0.0231	31.17	219000	152321625	0.0014377
672	0.0231	29.09	547500	197761798	0.0027685
624	0.0231	27.01	438000	261775649	0.0016732
552	0.0231	23.90	54750	416303691	0.0001315
264	0.0231	11.43	164250	6.785E+09	2.421E-05
120	0.0231	5.19	200750	1.341E+11	1.498E-06
96	0.0231	4.16	237250	3.119E+11	7.607E-07
Total damage ratio from 2016 to2026 =					0.1154292

Table 3.86: Damage ratio from 2016 to 2026 under operating scenario B4

Axial force range, ΔN	Average cross-sectional Area A	Stress range, Δσ	Total cycles in 10 years n_i	Number of cycles to failure, N_i	n_i/N_i
3792	0.023	164.87	18250	278830.56	0.0654519
1992	0.023	86.61	54750	3186157.9	0.0171837
1800	0.023	78.26	18250	4675488.3	0.0039033
1752	0.023	76.17	109500	5178990.2	0.0211431
816	0.023	35.48	328500	93313090	0.0035204
720	0.023	31.30	219000	149841449	0.0014615
672	0.023	29.22	547500	194541743	0.0028143
624	0.023	27.13	438000	257513288	0.0017009
552	0.023	24.00	54750	409525229	0.0001337
264	0.023	11.48	164250	6.675E+09	2.461E-05
120	0.023	5.22	200750	1.319E+11	1.522E-06
96	0.023	4.17	237250	3.068E+11	7.733E-07
Total damage ratio from 2026 to2036 =					0.1173398

Table 3.87: Damage ratio from 2026 to 2036 under operating scenario B4

Axial force range, ΔN	Average cross-sectional Area A	Stress range, Δσ	Total cycles in 10 years n_i	Number of cycles to failure, N_i	n_i/N_i
3792	0.0229	165.59	18250	274270.89	0.0665401
1992	0.0229	86.99	54750	3134055.1	0.0174694
1800	0.0229	78.60	18250	4599030.7	0.0039682
1752	0.0229	76.51	109500	5094298.9	0.0214946
816	0.0229	35.63	328500	91787154	0.0035789
720	0.0229	31.44	219000	147391113	0.0014858
672	0.0229	29.34	547500	191360429	0.0028611
624	0.0229	27.25	438000	253302209	0.0017292
552	0.0229	24.10	54750	402828320	0.0001359
264	0.0229	11.53	164250	6.566E+09	2.502E-05
120	0.0229	5.24	200750	1.297E+11	1.548E-06
96	0.0229	4.19	237250	3.018E+11	7.861E-07
Total damage ratio from 2036 to2046 =					0.1192906

Table 3.88: Damage ratio from 2036 to 2046 under operating scenario B4

Axial force range in kN, ΔN	Average cross-sectional Area in sqm, A	Stress range in MPa, Δσ	Total cycles in 10 years n_i	Number of cycles to failure, N_i	n_i/N_i
3792	0.0227	167.05	18250	265316.4	0.0687858
1992	0.0227	87.75	54750	3031733.4	0.018059
1800	0.0227	79.30	18250	4448879.9	0.0041022
1752	0.0227	77.18	109500	4927978.5	0.0222201
816	0.0227	35.95	328500	88790455	0.0036997
720	0.0227	31.72	219000	142579037	0.001536
672	0.0227	29.60	547500	185112827	0.0029577
624	0.0227	27.49	438000	245032311	0.0017875
552	0.0227	24.32	54750	389676641	0.0001405
264	0.0227	11.63	164250	6.351E+09	2.586E-05
120	0.0227	5.29	200750	1.255E+11	1.6E-06
96	0.0227	4.23	237250	2.919E+11	8.127E-07
Total damage ratio from 2046 to2056 =					0.1233167

Table 3.89: Damage ratio from 2046 to 2056 under operating scenario B4

Axial force range in kN, ΔN	Average cross-sectional Area in sqm, A	Stress range in MPa, Δσ	Total cycles in 10 years n_i	Number of cycles to failure, N_i	n_i/N_i
3792	0.0226	167.79	18250	260920.73	0.0699446
1992	0.0226	88.14	54750	2981504.7	0.0183632
1800	0.0226	79.65	18250	4375172.4	0.0041713
1752	0.0226	77.52	109500	4846333.5	0.0225944
816	0.0226	36.11	328500	87319406	0.0037621
720	0.0226	31.86	219000	140216837	0.0015619
672	0.0226	29.73	547500	182045943	0.0030075
624	0.0226	27.61	438000	240972701	0.0018176
552	0.0226	24.42	54750	383220615	0.0001429
264	0.0226	11.68	164250	6.246E+09	2.63E-05
120	0.0226	5.31	200750	1.234E+11	1.627E-06
96	0.0226	4.25	237250	2.871E+11	8.264E-07
Total damage ratio from 2056 to2066 =					0.1253941

Table 3.90: Damage ratio from 2056 to 2066 under operating scenario B4

Axial force range in kN, ΔN	Average cross-sectional Area in sqm, A	Stress range in MPa, Δσ	Total cycles in 10 years n_i	Number of cycles to failure, N_i	n_i/N_i
3792	0.0225	168.53	18250	256578.87	0.0711282
1992	0.0225	88.53	54750	2931890.9	0.018674
1800	0.0225	80.00	18250	4302367.4	0.0042419
1752	0.0225	77.87	109500	4765688	0.0229767
816	0.0225	36.27	328500	85866367	0.0038257
720	0.0225	32.00	219000	137883558	0.0015883
672	0.0225	29.87	547500	179016606	0.0030584
624	0.0225	27.73	438000	236962794	0.0018484
552	0.0225	24.53	54750	376843630	0.0001453
264	0.0225	11.73	164250	6.142E+09	2.674E-05
120	0.0225	5.33	200750	1.213E+11	1.654E-06
96	0.0225	4.27	237250	2.823E+11	8.404E-07
Total damage ratio from 2066 to2076 =					0.1275161

Table 3.91: Damage ratio from 2066 to 2076 under operating scenario B4

Axial force range in kN, ΔN	Average cross-sectional Area in sqm, A	Stress range in MPa, Δσ	Total cycles in 10 years n_i	Number of cycles to failure, N_i	n_i/N_i
3792	0.0223	170.04	18250	248054.92	0.0735724
1992	0.0223	89.33	54750	2834488.9	0.0193157
1800	0.0223	80.72	18250	4159436	0.0043876
1752	0.0223	78.57	109500	4607364.4	0.0237663
816	0.0223	36.59	328500	83013752	0.0039572
720	0.0223	32.29	219000	133302850	0.0016429
672	0.0223	30.13	547500	173069394	0.0031635
624	0.0223	27.98	438000	229090518	0.0019119
552	0.0223	24.75	54750	364324294	0.0001503
264	0.0223	11.84	164250	5.938E+09	2.766E-05
120	0.0223	5.38	200750	1.173E+11	1.711E-06
96	0.0223	4.30	237250	2.729E+11	8.692E-07
Total damage ratio from 2076 to 2086 =					0.1318979

Table 3.92: Damage ratio from 2076 to 2086 under operating scenario B4

Axial force range in kN, ΔN	Average cross-sectional Area in sqm, A	Stress range in MPa, Δσ	Total cycles in 10 years n_i	Number of cycles to failure, N_i	n_i/N_i
3792	0.0222	170.81	18250	243871.98	0.0748343
1992	0.0222	89.73	54750	2786691	0.019647
1800	0.0222	81.08	18250	4089295.5	0.0044629
1752	0.0222	78.92	109500	4529670.5	0.0241739
816	0.0222	36.76	328500	81613893	0.004025
720	0.0222	32.43	219000	131054968	0.0016711
672	0.0222	30.27	547500	170150930	0.0032177
624	0.0222	28.11	438000	225227371	0.0019447
552	0.0222	24.86	54750	358180704	0.0001529
264	0.0222	11.89	164250	5.838E+09	2.814E-05
120	0.0222	5.41	200750	1.153E+11	1.741E-06
96	0.0222	4.32	237250	2.683E+11	8.841E-07
Total damage ratio from 2086 to 2096 =					0.1341603

Table 3.93: Damage ratio from 2086 to 2096 under operating scenario B4

Axial force range in kN, ΔN	Average cross-sectional Area in sqm, A	Stress range in MPa, Δσ	Total cycles in 10 years n_i	Number of cycles to failure, N_i	n_i/N_i
3792	0.0221	171.58	18250	239741.16	0.0761238
1992	0.0221	90.14	54750	2739488.8	0.0199855
1800	0.0221	81.45	18250	4020029.2	0.0045398
1752	0.0221	79.28	109500	4452944.9	0.0245905
816	0.0221	36.92	328500	80231480	0.0040944
720	0.0221	32.58	219000	128835099	0.0016998
672	0.0221	30.41	547500	167268836	0.0032732
624	0.0221	28.24	438000	221412368	0.0019782
552	0.0221	24.98	54750	352113676	0.0001555
264	0.0221	11.95	164250	5.739E+09	2.862E-05
120	0.0221	5.43	200750	1.134E+11	1.771E-06
96	0.0221	4.34	237250	2.638E+11	8.994E-07
Total damage ratio from 2096 to 2106 =					0.1364719

Table 3.94: Damage ratio from 2096 to 2106 under operating scenario B4

Axial force range in kN, ΔN	Average cross-sectional Area in sqm, A	Stress range in MPa, Δσ	Total cycles in 10 years n_i	Number of cycles to failure, N_i	n_i/N_i
3792	0.022	172.36	18250	235662.06	0.0774414
1992	0.022	90.55	54750	2692877.4	0.0203314
1800	0.022	81.82	18250	3951629.9	0.0046183
1752	0.022	79.64	109500	4377179.8	0.0250161
816	0.022	37.09	328500	78866372	0.0041653
720	0.022	32.73	219000	126643020	0.0017293
672	0.022	30.55	547500	164422821	0.0033298
624	0.022	28.36	438000	217645121	0.0020125
552	0.022	25.09	54750	346122597	0.0001582
264	0.022	12.00	164250	5.641E+09	2.912E-05
120	0.022	5.45	200750	1.115E+11	1.801E-06
96	0.022	4.36	237250	2.593E+11	9.149E-07
Total damage ratio from 2106 to 2116 =					0.1388341

Table 3.95: Damage ratio from 2106 to 2116 under operating scenario B4

In the following table and figure, the cumulative damage ratio from the year 1966 to 2116 for operating scenario B4 is shown

Year	Time period, years	Damage ratio	cumulative time, years	cumulative Damage ratio
1966-1976	10	0.0998859	10	0.0998859
1976-1986	10	0.1030995	20	0.2029854
1986-1996	10	0.108169	30	0.3111544
1996-2006	10	0.1099286	40	0.421083
2006-2016	10	0.1117246	50	0.5328076
2016-2026	10	0.1154292	60	0.6482368
2026 (EQ 1)		0.003925	60	0.6521618
2026-2036	10	0.1173398	70	0.7695017
2036-2046	10	0.1192906	80	0.8887922
2046-2056	10	0.1233167	90	1.0121089
2056(EQ 2)	0	0.012707	90	1.0248159
2056-2066	10	0.1253941	100	1.15021
2066-2076	10	0.1275161	110	1.2777261
2076-2086	10	0.1318979	120	1.409624
2086(EQ 3)		0.012109	120	1.421733
2086-2096	10	0.1341603	130	1.5558933
2096-2106	10	0.1364719	140	1.6923652
2106-2116	10	0.1388341	150	1.8311993

Table 3.96: Cumulative Damage ratio under operating scenario B4

Fig 3.53 Cumulative damage ratio for operating condition B4

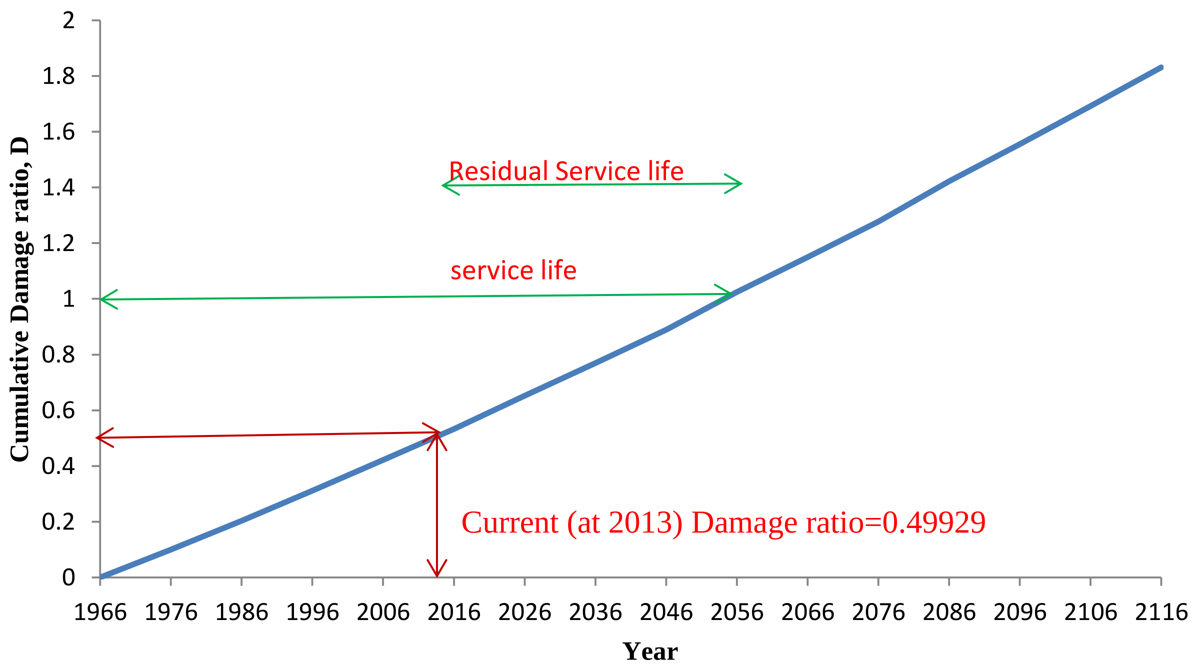

From the figure,

At current period, (2013) the cumulative damage ratio is 0.49929

The service life of the bridge is 89 years

The residual service life is 42 years

3.8.9 OPERATING SCENARIO C1:

Under this operating condition only passenger or Express train loads are applied according to the frequency specified by RFI for all four types of train (15 per day). Three Earthquakes events of magnitude described before are applied at 60, 90 and 120 years from year of bridge construction (i.e. in the year 2026, 2056 and2086). It is also assumed that there is no degradation of bridge material due to corrosion and there is no maintenance program carried out. For this operating scenario, the damage ratio for the first 10 years after the bridge construction is shown in the following table

Axial force range, ΔN	Area of the cross-section, A	Stress range, $\Delta\sigma$	Total cycles in 10 years n_i	Number of cycles to failure, N_i	n_i/N_i
1992	0.024	83	54750	3742902.364	0.01462769
816	0.024	34	328500	109618480.6	0.00299676
720	0.024	30	219000	176024521.4	0.00124414
552	0.024	23	54750	481085058.1	0.00011381
264	0.024	11	164250	7840975184	2.0948E-05
120	0.024	5	54750	1.54916E+11	3.5342E-07
Total damage ratio in Ist ten years (19966-1976), D=					0.01900369

Table 3.97: Damage ratio for the 1st ten years(1966 to 1976) under operating scenario C1

Similarly, for every 10 years the same damage ratio will be found. The damage ratio for the earthquakes can be calculated from the rainflow histogram .Assuming no reduction in the cross-sectional area, the calculated damage ratio for the first earthquake, which will occur in the year 2026 is 0.00332. The calculated damage ratio for the second earthquake, which will occur in the year 2056 is 0.00997. The calculated damage ratio for the third earthquake, which will occur in the year 2086 is 0.009. In the following table and figure, the cumulative damage ratio from the year 1966 to 2116 for operating scenario C1 is shown

Year	Time period, years	Damage ratio	cumulative time, years	cumulative Damage ratio
1966-1976	10	0.019003694	10	0.019003694
1976-1986	10	0.019003694	20	0.038007389
1986-1996	10	0.019003694	30	0.057011083
1996-2006	10	0.019003694	40	0.076014778
2006-2016	10	0.019003694	50	0.095018472
2016-2026	10	0.019003694	60	0.114022167
2026 (EQ 1)		0.00322	60	0.117242167
2026-2036	10	0.019003694	70	0.136245861
2036-2046	10	0.019003694	80	0.155249556
2046-2056	10	0.019003694	90	0.17425325
2056(EQ 2)	0	0.00997	90	0.18422325
2056-2066	10	0.019003694	100	0.203226945
2066-2076	10	0.019003694	110	0.222230639
2076-2086	10	0.019003694	120	0.241234334
2086(EQ 3)		0.009	120	0.250234334
2086-2096	10	0.019003694	130	0.269238028
2096-2106	10	0.019003694	140	0.288241723
2106-2116	10	0.019003694	150	0.307245417

Table 3.98: Cumulative Damage ratio under operating scenario C1

Fig 3.54 Cumulative damage ratio in different years under operating scenario C1

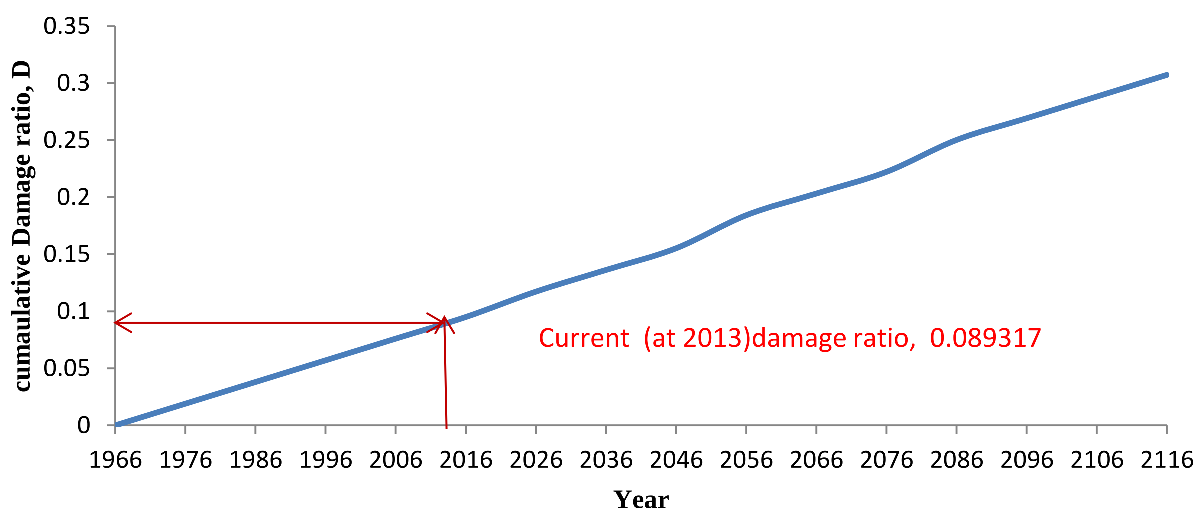

3.8.10 OPERATING SCENARIO C2:

Under this operating condition only passenger or Express train loads are applied according to the frequency specified by RFI for all four types of train (15 per day). Three Earthquakes events of magnitude described before are applied at 60, 90 and 120 years from year of bridge construction (i.e. in the year 2026, 2056 and2086). It is also assumed that there is thickness loss of bridge material due to corrosion and there is no maintenance program carried out. For this operating scenario, the damage ratio due to train load for the first 10 years, after the bridge construction 0.019003694 as calculated before. The damage ratio in other decades are shown in the following tables

Axial force range, ΔN	Average cross-sectional Area A	Stress range, Δσ	Total cycles in 10 years n_i	Number of cycles to failure, N_i	n_i/N_i
1992	0.0238	83.70	54750	3626238.5	0.0150983
816	0.0238	34.29	328500	106201743	0.0030932
720	0.0238	30.25	219000	170537950	0.0012842
552	0.0238	23.19	54750	466089947	0.0001175
264	0.0238	11.09	164250	7.597E+09	2.162E-05
120	0.0238	5.04	54750	1.501E+11	3.648E-07
Total damage ratio from 1976 to 1986 =					0.0196151

Table 3.99 Damage ratio from 1976 to 1986 under operating scenario C2

Axial force range, ΔN	Average cross-sectional Area A	Stress range, Δσ	Total cycles in 10 years n_i	Number of cycles to failure, N_i	n_i/N_i
1992	0.0235	84.77	54750	3456288.2	0.0158407
816	0.0235	34.72	328500	101224404	0.0032453
720	0.0235	30.64	219000	162545378	0.0013473
552	0.0235	23.49	54750	444245790	0.0001232
264	0.0235	11.23	164250	7.241E+09	2.268E-05
120	0.0235	5.11	54750	1.431E+11	3.827E-07
Total damage ratio from 1986 to1996 =					0.0205796

Table 3.100: Damage ratio from 1986 to 1996 under operating scenario C2

Axial force range, ΔN	Average cross-sectional Area A	Stress range, Δσ	Total cycles in 10 years n_i	Number of cycles to failure, N_i	n_i/N_i
1992	0.0233	85.49	54750	3346293	0.0163614
816	0.0233	35.02	328500	98002972	0.0033519
720	0.0233	30.90	219000	157372426	0.0013916
552	0.0233	23.69	54750	430107816	0.0001273
264	0.0233	11.33	164250	7.01E+09	2.343E-05
120	0.0233	5.15	54750	1.385E+11	3.953E-07
Total damage ratio from 1996 to2006 =					0.0212561

Table 3.101: Damage ratio from 1996 to 2006 under operating scenario C2

Axial force range, ΔN	Average cross-sectional Area A	Stress range, Δσ	Total cycles in 10 years n_i	Number of cycles to failure, N_i	n_i/N_i
1992	0.0231	86.23	54750	3238895.2	0.0169039
816	0.0231	35.32	328500	94857608	0.0034631
720	0.0231	31.17	219000	152321625	0.0014377
552	0.0231	23.90	54750	416303691	0.0001315
264	0.0231	11.43	164250	6.785E+09	2.421E-05
120	0.0231	5.19	54750	1.341E+11	4.084E-07
Total damage ratio from 2006 to2016 =					0.0219609

Table 3.102: Damage ratio from 2006 to 2016 under operating scenario C2

Axial force range, ΔN	Average cross-sectional Area A	Stress range, Δσ	Total cycles in 10 years n_i	Number of cycles to failure, N_i	n_i/N_i
1992	0.0229	86.99	54750	3134055.1	0.0174694
816	0.0229	35.63	328500	91787154	0.0035789
720	0.0229	31.44	219000	147391113	0.0014858
552	0.0229	24.10	54750	402828320	0.0001359
264	0.0229	11.53	164250	6.566E+09	2.502E-05
120	0.0229	5.24	54750	1.297E+11	4.221E-07
Total damage ratio from 2016 to2026 =					0.0226955

Table 3.103: Damage ratio from 2016 to 2026 under operating scenario C2

Axial force range, ΔN	Average cross-sectional Area A	Stress range, Δσ	Total cycles in 10 years n_i	Number of cycles to failure, N_i	n_i/N_i
1992	0.0227	87.75	54750	3031733.4	0.018059
816	0.0227	35.95	328500	88790455	0.0036997
720	0.0227	31.72	219000	142579037	0.001536
552	0.0227	24.32	54750	389676641	0.0001405
264	0.0227	11.63	164250	6.351E+09	2.586E-05
120	0.0227	5.29	54750	1.255E+11	4.363E-07
Total damage ratio from 2026 to2036 =					0.0234615

Table 3.104: Damage ratio from 2026 to 2036 under operating scenario C2

Axial force range, ΔN	Average cross-sectional Area A	Stress range, Δσ	Total cycles in 10 years n_i	Number of cycles to failure, N_i	n_i/N_i
1992	0.0225	88.53	54750	2931890.9	0.018674
816	0.0225	36.27	328500	85866367	0.0038257
720	0.0225	32.00	219000	137883558	0.0015883
552	0.0225	24.53	54750	376843630	0.0001453
264	0.0225	11.73	164250	6.142E+09	2.674E-05
120	0.0225	5.33	54750	1.213E+11	4.512E-07
Total damage ratio from 2036 to2046 =					0.0242604

Table 3.105: Damage ratio from 2036 to 2046 under operating scenario C2

Axial force range in kN, ΔN	Average cross-sectional Area in sqm, A	Stress range in MPa, Δσ	Total cycles in 10 years n_i	Number of cycles to failure, N_i	n_i/N_i
1992	0.0223	89.33	54750	2834488.9	0.0193157
816	0.0223	36.59	328500	83013752	0.0039572
720	0.0223	32.29	219000	133302850	0.0016429
552	0.0223	24.75	54750	364324294	0.0001503
264	0.0223	11.84	164250	5.938E+09	2.766E-05
120	0.0223	5.38	54750	1.173E+11	4.667E-07
Total damage ratio from 2046 to2056 =					0.0250941

Table 3.106: Damage ratio from 2046 to 2056 under operating scenario C2

Axial force range in kN, ΔN	Average cross-sectional Area in sqm, A	Stress range in MPa, $\Delta\sigma$	Total cycles in 10 years n_i	Number of cycles to failure, N_i	n_i/N_i
1992	0.0221	90.14	54750	2739488.8	0.0199855
816	0.0221	36.92	328500	80231480	0.0040944
720	0.0221	32.58	219000	128835099	0.0016998
552	0.0221	24.98	54750	352113676	0.0001555
264	0.0221	11.95	164250	5.739E+09	2.862E-05
120	0.0221	5.43	54750	1.134E+11	4.829E-07
Total damage ratio from 2056 to2066 =					0.0259643

Table 3.107: Damage ratio from 2056 to 2066 under operating scenario C2

Axial force range in kN, ΔN	Average cross-sectional Area in sqm, A	Stress range in MPa, $\Delta\sigma$	Total cycles in 10 years n_i	Number of cycles to failure, N_i	n_i/N_i
1992	0.0219	90.96	54750	2646852.2	0.0206849
816	0.0219	37.26	328500	77518430	0.0042377
720	0.0219	32.88	219000	124478505	0.0017593
552	0.0219	25.21	54750	340206855	0.0001609
264	0.0219	12.05	164250	5.545E+09	2.962E-05
120	0.0219	5.48	54750	1.096E+11	4.998E-07
Total damage ratio from 2066 to2076 =					0.026873

Table 3.108: Damage ratio from 2066 to 2076 under operating scenario C2

Axial force range in kN, ΔN	Average cross-sectional Area in sqm, A	Stress range in MPa, $\Delta\sigma$	Total cycles in 10 years n_i	Number of cycles to failure, N_i	n_i/N_i
1992	0.0217	91.80	54750	2556541.2	0.0214157
816	0.0217	37.60	328500	74873489	0.0043874
720	0.0217	33.18	219000	120231279	0.0018215
552	0.0217	25.44	54750	328598943	0.0001666
264	0.0217	12.17	164250	5.356E+09	3.067E-05
120	0.0217	5.53	54750	1.058E+11	5.174E-07
Total damage ratio from 2076 to 2086 =					0.0278223

Table 3.109: Damage ratio from 2076 to 2086 under operating scenario C2

Axial force range in kN, ΔN	Average cross-sectional Area in sqm, A	Stress range in MPa, Δσ	Total cycles in 10 years n_i	Number of cycles to failure, N_i	n_i/N_i
1992	0.0215	92.65	54750	2468518	0.0221793
816	0.0215	37.95	328500	72295551	0.0045438
720	0.0215	33.49	219000	116091645	0.0018864
552	0.0215	25.67	54750	317285089	0.0001726
264	0.0215	12.28	164250	5.171E+09	3.176E-05
120	0.0215	5.58	54750	1.022E+11	5.359E-07
Total damage ratio from 2086 to 2096 =					0.0288144

Table 3.110: Damage ratio from 2086 to 2096 under operating scenario C2

Axial force range in kN, ΔN	Average cross-sectional Area in sqm, A	Stress range in MPa, Δσ	Total cycles in 10 years n_i	Number of cycles to failure, N_i	n_i/N_i
1992	0.0213	93.52	54750	2382745.1	0.0229777
816	0.0213	38.31	328500	69783518	0.0047074
720	0.0213	33.80	219000	112057842	0.0019543
552	0.0213	25.92	54750	306260473	0.0001788
264	0.0213	12.39	164250	4.992E+09	3.291E-05
120	0.0213	5.63	54750	9.862E+10	5.552E-07
Total damage ratio from 2096 to 2106 =					0.0298517

Table 3.111: Damage ratio from 2096 to 2106 under operating scenario C2

Axial force range in kN, ΔN	Average cross-sectional Area in sqm, A	Stress range in MPa, Δσ	Total cycles in 10 years n_i	Number of cycles to failure, N_i	n_i/N_i
1992	0.0211	94.41	54750	2299185.3	0.0238128
816	0.0211	38.67	328500	67336300	0.0048785
720	0.0211	34.12	219000	108128118	0.0020254
552	0.0211	26.16	54750	295520315	0.0001853
264	0.0211	12.51	164250	4.817E+09	3.41E-05
120	0.0211	5.69	54750	9.516E+10	5.753E-07
Total damage ratio from 2106 to 2116 =					0.0309366

Table 3.112: Damage ratio from 2106 to 2116 under operating scenario C2

In the following table and figure, the cumulative damage ratio from the year 1966 to 2116 for operating scenario C2 is shown

Year	Time period, years	Damage ratio	cumulative time, years	cumulative Damage ratio
1966-1976	10	0.01900369	10	0.0190037
1976-1986	10	0.01961508	20	0.0386188
1986-1996	10	0.02057958	30	0.0591984
1996-2006	10	0.02125605	40	0.0804544
2006-2016	10	0.02196088	50	0.1024153
2016-2026	10	0.02269551	60	0.1251108
2026 (EQ 1)		0.00408	60	0.1291908
2026-2036	10	0.02346149	70	0.1526523
2036-2046	10	0.02426044	80	0.1769127
2046-2056	10	0.02509411	90	0.2020068
2056(EQ 2)	0	0.01349	90	0.2154968
2056-2066	10	0.02596432	100	0.2414612
2066-2076	10	0.02687304	110	0.2683342
2076-2086	10	0.02782235	120	0.2961565
2086(EQ 3)		0.01342	120	0.3095765
2086-2096	10	0.02881444	130	0.338391
2096-2106	10	0.02985169	140	0.3682427
2106-2116	10	0.0309366	150	0.3991793

Table 3.113: Cumulative Damage ratio under operating scenario C2

Fig 3.55 Cumulative damage ratio for operating condition C2

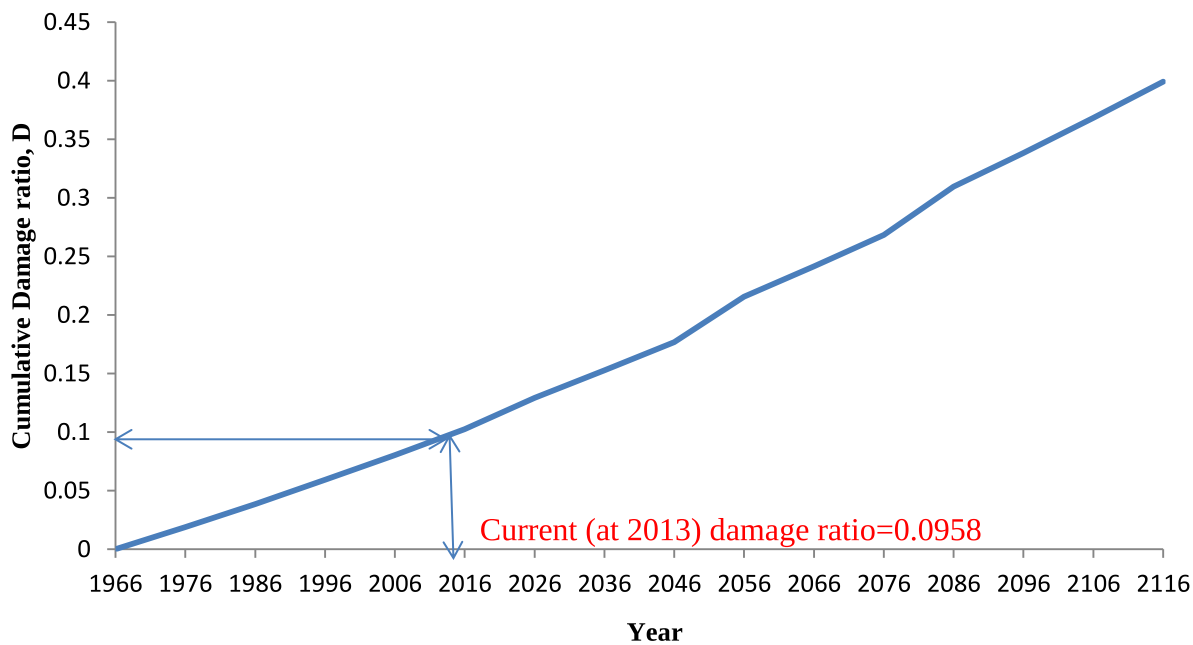

3.8.11 OPERATING SCENARIO C3:

Under this operating condition only passenger or Express train loads are applied according to the frequency specified by RFI for all four types of train (15 per day). Three Earthquakes events of magnitude described before are applied at 60, 90 and 120 years from year of bridge construction (i.e. in the year 2026, 2056 and2086). It is also assumed that a total number of three corrosion protective paintings are provide at the interval of every ten years for the first thirty years from the year of bridge construction and the thickness loss of bridge material due to corrosion initiates after forty years of bridge construction, i.e. in the year 2006 .For this operating scenario, the damage ratio due to train load for the first 10 (1966-76) years, after the bridge construction is 0.01900369 as calculated before. The damage ratio due to train load for the next three decades (1976-1986, 1986-1996 and 1996-2006) are also 0.01900369 as calculated before. The damage ratio in other decades are shown in the following tables

Axial force range, ΔN	Average cross-sectional Area A	Stress range, Δσ	Total cycles in 10 years n_i	Number of cycles to failure, N_i	n_i/N_i
1992	0.0238	83.70	54750	3626238.5	0.0150983
816	0.0238	34.29	328500	106201743	0.0030932
720	0.0238	30.25	219000	170537950	0.0012842
552	0.0238	23.19	54750	466089947	0.0001175
264	0.0238	11.09	164250	7.597E+09	2.162E-05
120	0.0238	5.04	200750	1.501E+11	1.338E-06
Total damage ratio from 2006 to2016 =					0.0196161

Table 3.114: Damage ratio from 2006 to 2016 under operating scenario C3

Axial force range, ΔN	Average cross-sectional Area A	Stress range, Δσ	Total cycles in 10 years n_i	Number of cycles to failure, N_i	n_i/N_i
1992	0.0235	84.77	54750	3456288.2	0.0158407
816	0.0235	34.72	328500	101224404	0.0032453
720	0.0235	30.64	219000	162545378	0.0013473
552	0.0235	23.49	54750	444245790	0.0001232
264	0.0235	11.23	164250	7.241E+09	2.268E-05
120	0.0235	5.11	54750	1.431E+11	3.827E-07
Total damage ratio from 2016 to2026 =					0.0205796

Table 3.115: Damage ratio from 2016 to 2026 under operating scenario C3

Axial force range, ΔN	Average cross-sectional Area A	Stress range, Δσ	Total cycles in 10 years n_i	Number of cycles to failure, N_i	n_i/N_i
1992	0.0233	85.49	54750	3346293	0.0163614
816	0.0233	35.02	328500	98002972	0.0033519
720	0.0233	30.90	219000	157372426	0.0013916
552	0.0233	23.69	54750	430107816	0.0001273
264	0.0233	11.33	164250	7.01E+09	2.343E-05
120	0.0233	5.15	54750	1.385E+11	3.953E-07
				Total damage ratio from 2026 to2036 =	0.0212561

Table 3.116: Damage ratio from 2026 to 2036 under operating scenario C3

Axial force range, ΔN	Average cross-sectional Area A	Stress range, Δσ	Total cycles in 10 years n_i	Number of cycles to failure, N_i	n_i/N_i
1992	0.0231	86.23	54750	3238895.2	0.0169039
816	0.0231	35.32	328500	94857608	0.0034631
720	0.0231	31.17	219000	152321625	0.0014377
552	0.0231	23.90	54750	416303691	0.0001315
264	0.0231	11.43	164250	6.785E+09	2.421E-05
120	0.0231	5.19	54750	1.341E+11	4.084E-07
				Total damage ratio from 2036 to2046 =	0.0219609

Table 3.117: Damage ratio from 2036 to 2046 under operating scenario C3

Axial force range in kN, ΔN	Average cross-sectional Area in sqm, A	Stress range in MPa, Δσ	Total cycles in 10 years n_i	Number of cycles to failure, N_i	n_i/N_i
1992	0.0229	86.99	54750	3134055.1	0.0174694
816	0.0229	35.63	328500	91787154	0.0035789
720	0.0229	31.44	219000	147391113	0.0014858
552	0.0229	24.10	54750	402828320	0.0001359
264	0.0229	11.53	164250	6.566E+09	2.502E-05
120	0.0229	5.24	200750	1.297E+11	1.548E-06
				Total damage ratio from 2046 to2056 =	0.0226966

Table 3.118: Damage ratio from 2046 to 2056 under operating scenario C3

Axial force range in kN, ΔN	Average cross-sectional Area in sqm, A	Stress range in MPa, Δσ	Total cycles in 10 years n_i	Number of cycles to failure, N_i	n_i/N_i
1992	0.0227	87.75	54750	3031733.4	0.018059
816	0.0227	35.95	328500	88790455	0.0036997
720	0.0227	31.72	219000	142579037	0.001536
552	0.0227	24.32	54750	389676641	0.0001405
264	0.0227	11.63	164250	6.351E+09	2.586E-05
120	0.0227	5.29	54750	1.255E+11	4.363E-07
Total damage ratio from 2056 to2066 =					0.0234615

Table 3.119: Damage ratio from 2056 to 2066 under operating scenario C3

Axial force range in kN, ΔN	Average cross-sectional Area in sqm, A	Stress range in MPa, Δσ	Total cycles in 10 years n_i	Number of cycles to failure, N_i	n_i/N_i
1992	0.0225	88.53	54750	2931890.9	0.018674
816	0.0225	36.27	328500	85866367	0.0038257
720	0.0225	32.00	219000	137883558	0.0015883
552	0.0225	24.53	54750	376843630	0.0001453
264	0.0225	11.73	164250	6.142E+09	2.674E-05
120	0.0225	5.33	54750	1.213E+11	4.512E-07
Total damage ratio from 2066 to2076 =					0.0242604

Table 3.120: Damage ratio from 2066 to 2076 under operating scenario C3

Axial force range in kN, ΔN	Average cross-sectional Area in sqm, A	Stress range in MPa, Δσ	Total cycles in 10 years n_i	Number of cycles to failure, N_i	n_i/N_i
1992	0.0223	89.33	54750	2834488.9	0.0193157
816	0.0223	36.59	328500	83013752	0.0039572
720	0.0223	32.29	219000	133302850	0.0016429
552	0.0223	24.75	54750	364324294	0.0001503
264	0.0223	11.84	164250	5.938E+09	2.766E-05
120	0.0223	5.38	54750	1.173E+11	4.667E-07
Total damage ratio from 2076 to 2086 =					0.0250941

Table 3.121: Damage ratio from 2076 to 2086 under operating scenario C3

Axial force range in kN, ΔN	Average cross-sectional Area in sqm, A	Stress range in MPa, Δσ	Total cycles in 10 years n_i	Number of cycles to failure, N_i	n_i/N_i
1992	0.0221	90.14	54750	2739488.8	0.0199855
816	0.0221	36.92	328500	80231480	0.0040944
720	0.0221	32.58	219000	128835099	0.0016998
552	0.0221	24.98	54750	352113676	0.0001555
264	0.0221	11.95	164250	5.739E+09	2.862E-05
120	0.0221	5.43	54750	1.134E+11	4.829E-07
Total damage ratio from 2086 to 2096 =					0.0259643

Table 3.122: Damage ratio from 2086 to 2096 under operating scenario C3

Axial force range in kN, ΔN	Average cross-sectional Area in sqm, A	Stress range in MPa, Δσ	Total cycles in 10 years n_i	Number of cycles to failure, N_i	n_i/N_i
1992	0.0219	90.96	54750	2646852.2	0.0206849
816	0.0219	37.26	328500	77518430	0.0042377
720	0.0219	32.88	219000	124478505	0.0017593
552	0.0219	25.21	54750	340206855	0.0001609
264	0.0219	12.05	164250	5.545E+09	2.962E-05
120	0.0219	5.48	54750	1.096E+11	4.998E-07
Total damage ratio from 2096 to 2106 =					0.026873

Table 3.123: Damage ratio from 2096 to 2106 under operating scenario C3

Axial force range in kN, ΔN	Average cross-sectional Area in sqm, A	Stress range in MPa, Δσ	Total cycles in 10 years n_i	Number of cycles to failure, N_i	n_i/N_i
1992	0.0217	91.80	54750	2556541.2	0.0214157
816	0.0217	37.60	328500	74873489	0.0043874
720	0.0217	33.18	219000	120231279	0.0018215
552	0.0217	25.44	54750	328598943	0.0001666
264	0.0217	12.17	164250	5.356E+09	3.067E-05
120	0.0217	5.53	54750	1.058E+11	5.174E-07
Total damage ratio from 2106 to 2116 =					0.0278223

Table 3.124: Damage ratio from 2106 to 2116 under operating scenario C3

In the following table and figure, the cumulative damage ratio from the year 1966 to 2116 for operating scenario C3 is shown

Year	Time period, years	Damage ratio	cumulative time, years	cumulative Damage ratio
1966-1976	10	0.0190037	10	0.0190037
1976-1986	10	0.0190037	20	0.0380074
1986-1996	10	0.0190037	30	0.0570111
1996-2006	10	0.0190037	40	0.0760148
2006-2016	10	0.0196161	50	0.0956308
2016-2026	10	0.0205796	60	0.1162104
2026 (EQ 1)		0.0036	60	0.1198104
2026-2036	10	0.0212561	70	0.1410665
2036-2046	10	0.0219609	80	0.1630273
2046-2056	10	0.0226966	90	0.185724
2056(EQ 2)	0	0.01223	90	0.197954
2056-2066	10	0.0234615	100	0.2214155
2066-2076	10	0.0242604	110	0.2456759
2076-2086	10	0.0250941	120	0.27077
2086(EQ 3)		0.012109	120	0.282879
2086-2096	10	0.0259643	130	0.3088433
2096-2106	10	0.026873	140	0.3357164
2106-2116	10	0.0278223	150	0.3635387

Table 3.125: Cumulative Damage ratio under operating scenario C3

Fig 3.56 Cumulative damage ratio for operating condition C3

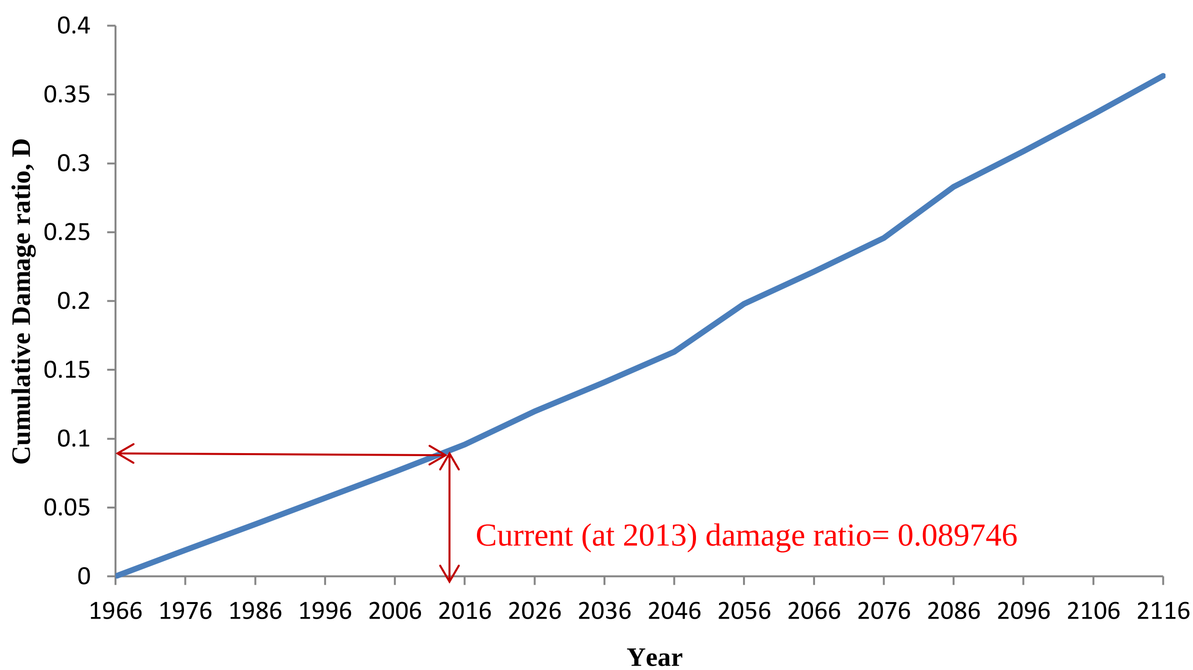

3.8.12 OPERATING SCENARIO C4:

Under this operating condition only passenger or Express train loads are applied according to the frequency specified by RFI for all four types of train (15 per day). Three Earthquakes events of magnitude described before are applied at 60, 90 and 120 years from year of bridge construction (i.e. in the year 2026, 2056 and2086). It is also assumed that corrosion protective paintings are provide at the interval of every thirty years from the year of bridge construction and the thickness loss of bridge material due to corrosion initiated after 10 years of bridge construction, i.e. in the year1976 and continues as described before in paragraph 3.6.3. For this operating scenario, the damage ratio due to train load for the first 10 (1966-76) years, after the bridge construction is 0.01900369 as calculated before. The damage ratio in other decades are shown in the following tables

Axial force range, ΔN	Average cross-sectional Area A	Stress range, Δσ	Total cycles in 10 years n_i	Number of cycles to failure, N_i	n_i/N_i
1992	0.0238	83.70	54750	3626238.5	0.0150983
816	0.0238	34.29	328500	106201743	0.0030932
720	0.0238	30.25	219000	170537950	0.0012842
552	0.0238	23.19	54750	466089947	0.0001175
264	0.0238	11.09	164250	7.597E+09	2.162E-05
120	0.0238	5.04	200750	1.501E+11	1.338E-06
Total damage ratio from 1976 to 1986 =					0.0196161

Table 3.126: Damage ratio from 1976 to 1986 under operating scenario C4

Axial force range, ΔN	Average cross-sectional Area A	Stress range, Δσ	Total cycles in 10 years n_i	Number of cycles to failure, N_i	n_i/N_i
1992	0.0235	84.77	54750	3456288.2	0.0158407
816	0.0235	34.72	328500	101224404	0.0032453
720	0.0235	30.64	219000	162545378	0.0013473
552	0.0235	23.49	54750	444245790	0.0001232
264	0.0235	11.23	164250	7.241E+09	2.268E-05
120	0.0235	5.11	54750	1.431E+11	3.827E-07
Total damage ratio from 1986 to1996 =					0.0205796

Table 3.127: Damage ratio from 1986 to 1996 under operating scenario C4

Axial force range, ΔN	Average cross-sectional Area A	Stress range, Δσ	Total cycles in 10 years n_i	Number of cycles to failure, N_i	n_i/N_i
1992	0.0234	85.13	54750	3400963.4	0.0160984
816	0.0234	34.87	328500	99604106	0.0032981
720	0.0234	30.77	219000	159943516	0.0013692
552	0.0234	23.59	54750	437134752	0.0001252
264	0.0234	11.28	164250	7.125E+09	2.305E-05
120	0.0234	5.13	54750	1.408E+11	3.889E-07
Total damage ratio from 1996 to2006 =					0.0209144

Table 3.128: Damage ratio from 1996 to 2006 under operating scenario C4

Axial force range, ΔN	Average cross-sectional Area A	Stress range, Δσ	Total cycles in 10 years n_i	Number of cycles to failure, N_i	n_i/N_i
1992	0.0233	85.49	54750	3346293	0.0163614
816	0.0233	35.02	328500	98002972	0.0033519
720	0.0233	30.90	219000	157372426	0.0013916
552	0.0233	23.69	54750	430107816	0.0001273
264	0.0233	11.33	164250	7.01E+09	2.343E-05
120	0.0233	5.15	54750	1.385E+11	3.953E-07
Total damage ratio from 2006 to2016 =					0.0212561

Table 3.129: Damage ratio from 2006 to 2016 under operating scenario C4

Axial force range, ΔN	Average cross-sectional Area A	Stress range, Δσ	Total cycles in 10 years n_i	Number of cycles to failure, N_i	n_i/N_i
1992	0.0231	86.23	54750	3238895.2	0.0169039
816	0.0231	35.32	328500	94857608	0.0034631
720	0.0231	31.17	219000	152321625	0.0014377
552	0.0231	23.90	54750	416303691	0.0001315
264	0.0231	11.43	164250	6.785E+09	2.421E-05
120	0.0231	5.19	54750	1.341E+11	4.084E-07
Total damage ratio from 2016 to2026 =					0.0219609

Table 3.130: Damage ratio from 2016 to 2026 under operating scenario C4

Axial force range, ΔN	Average cross-sectional Area A	Stress range, Δσ	Total cycles in 10 years n_i	Number of cycles to failure, N_i	n_i/N_i
1992	0.023	86.61	54750	3186157.9	0.0171837
816	0.023	35.48	328500	93313090	0.0035204
720	0.023	31.30	219000	149841449	0.0014615
552	0.023	24.00	54750	409525229	0.0001337
264	0.023	11.48	164250	6.675E+09	2.461E-05
120	0.023	5.22	54750	1.319E+11	4.152E-07
				Total damage ratio from 2026 to2036 =	0.0223244

Table 3.131: Damage ratio from 2026 to 2036 under operating scenario C4

Axial force range, ΔN	Average cross-sectional Area A	Stress range, Δσ	Total cycles in 10 years n_i	Number of cycles to failure, N_i	n_i/N_i
1992	0.0229	86.99	54750	3134055.1	0.0174694
816	0.0229	35.63	328500	91787154	0.0035789
720	0.0229	31.44	219000	147391113	0.0014858
552	0.0229	24.10	54750	402828320	0.0001359
264	0.0229	11.53	164250	6.566E+09	2.502E-05
120	0.0229	5.24	54750	1.297E+11	4.221E-07
				Total damage ratio from 2036 to2046 =	0.0226955

Table 3.132: Damage ratio from 2036 to 2046 under operating scenario C4

Axial force range in kN, ΔN	Average cross-sectional Area in sqm, A	Stress range in MPa, Δσ	Total cycles in 10 years n_i	Number of cycles to failure, N_i	n_i/N_i
1992	0.0227	87.75	54750	3031733.4	0.018059
816	0.0227	35.95	328500	88790455	0.0036997
720	0.0227	31.72	219000	142579037	0.001536
552	0.0227	24.32	54750	389676641	0.0001405
264	0.0227	11.63	164250	6.351E+09	2.586E-05
120	0.0227	5.29	54750	1.255E+11	4.363E-07
				Total damage ratio from 2046 to2056 =	0.0234615

Table 3.133: Damage ratio from 2046 to 2056 under operating scenario C4

Axial force range in kN, ΔN	Average cross-sectional Area in sqm, A	Stress range in MPa, Δσ	Total cycles in 10 years n_i	Number of cycles to failure, N_i	n_i/N_i
1992	0.0226	88.14	54750	2981504.7	0.0183632
816	0.0226	36.11	328500	87319406	0.0037621
720	0.0226	31.86	219000	140216837	0.0015619
552	0.0226	24.42	54750	383220615	0.0001429
264	0.0226	11.68	164250	6.246E+09	2.63E-05
120	0.0226	5.31	54750	1.234E+11	4.437E-07
Total damage ratio from 2056 to2066 =					0.0238567

Table 3.134: Damage ratio from 2056 to 2066 under operating scenario C4

Axial force range in kN, ΔN	Average cross-sectional Area in sqm, A	Stress range in MPa, Δσ	Total cycles in 10 years n_i	Number of cycles to failure, N_i	n_i/N_i
1992	0.0225	88.53	54750	2931890.9	0.018674
816	0.0225	36.27	328500	85866367	0.0038257
720	0.0225	32.00	219000	137883558	0.0015883
552	0.0225	24.53	54750	376843630	0.0001453
264	0.0225	11.73	164250	6.142E+09	2.674E-05
120	0.0225	5.33	54750	1.213E+11	4.512E-07
Total damage ratio from 2066 to2076 =					0.0242604

Table 3.135: Damage ratio from 2066 to 2076 under operating scenario C4

Axial force range in kN, ΔN	Average cross-sectional Area in sqm, A	Stress range in MPa, Δσ	Total cycles in 10 years n_i	Number of cycles to failure, N_i	n_i/N_i
1992	0.0223	89.33	54750	2834488.9	0.0193157
816	0.0223	36.59	328500	83013752	0.0039572
720	0.0223	32.29	219000	133302850	0.0016429
552	0.0223	24.75	54750	364324294	0.0001503
264	0.0223	11.84	164250	5.938E+09	2.766E-05
120	0.0223	5.38	54750	1.173E+11	4.667E-07
Total damage ratio from 2076 to 2086 =					0.0250941

Table 3.136: Damage ratio from 2076 to 2086 under operating scenario C4

Axial force range in kN, ΔN	Average cross-sectional Area in sqm, A	Stress range in MPa, Δσ	Total cycles in 10 years n_i	Number of cycles to failure, N_i	n_i/N_i
1992	0.0222	89.73	54750	2786691	0.019647
816	0.0222	36.76	328500	81613893	0.004025
720	0.0222	32.43	219000	131054968	0.0016711
552	0.0222	24.86	54750	358180704	0.0001529
264	0.0222	11.89	164250	5.838E+09	2.814E-05
120	0.0222	5.41	54750	1.153E+11	4.747E-07
				Total damage ratio from 2086 to 2096 =	0.0255245

Table 3.137: Damage ratio from 2086 to 2096 under operating scenario C4

Axial force range in kN, ΔN	Average cross-sectional Area in sqm, A	Stress range in MPa, Δσ	Total cycles in 10 years n_i	Number of cycles to failure, N_i	n_i/N_i
1992	0.0221	90.14	54750	2739488.8	0.0199855
816	0.0221	36.92	328500	80231480	0.0040944
720	0.0221	32.58	219000	128835099	0.0016998
552	0.0221	24.98	54750	352113676	0.0001555
264	0.0221	11.95	164250	5.739E+09	2.862E-05
120	0.0221	5.43	54750	1.134E+11	4.829E-07
				Total damage ratio from 2096 to 2106 =	0.0259643

Table 3.138: Damage ratio from 2096 to 2106 under operating scenario C4

Axial force range in kN, ΔN	Average cross-sectional Area in sqm, A	Stress range in MPa, Δσ	Total cycles in 10 years n_i	Number of cycles to failure, N_i	n_i/N_i
1992	0.022	90.55	54750	2692877.4	0.0203314
816	0.022	37.09	328500	78866372	0.0041653
720	0.022	32.73	219000	126643020	0.0017293
552	0.022	25.09	54750	346122597	0.0001582
264	0.022	12.00	164250	5.641E+09	2.912E-05
120	0.022	5.45	54750	1.115E+11	4.912E-07
				Total damage ratio from 2106 to 2116 =	0.0264137

Table 3.139: Damage ratio from 2096 to 2106 under operating scenario C4

In the following table and figure, the cumulative damage ratio from the year 1966 to 2116 for operating scenario C4 is shown

Year	Time period, years	Damage ratio	cumulative time, years	cumulative Damage ratio
1966-1976	10	0.0190037	10	0.0190037
1976-1986	10	0.0196151	20	0.0386188
1986-1996	10	0.0205796	30	0.0591984
1996-2006	10	0.0209144	40	0.0801127
2006-2016	10	0.0212561	50	0.1013688
2016-2026	10	0.0219609	60	0.1233296
2026 (EQ 1)		0.003925	60	0.1272546
2026-2036	10	0.0223244	70	0.149579
2036-2046	10	0.0226955	80	0.1722745
2046-2056	10	0.0234615	90	0.195736
2056(EQ 2)	0	0.012707	90	0.208443
2056-2066	10	0.0238567	100	0.2322998
2066-2076	10	0.0242604	110	0.2565602
2076-2086	10	0.0250941	120	0.2816543
2086(EQ 3)		0.012109	120	0.2937633
2086-2096	10	0.0255245	130	0.3192878
2096-2106	10	0.0259643	140	0.3452522
2106-2116	10	0.0264137	150	0.3716659

Table 3.140: Cumulative Damage ratio under operating scenario C4

Fig 3.57 Cumulative damage ratio for operating condition C4

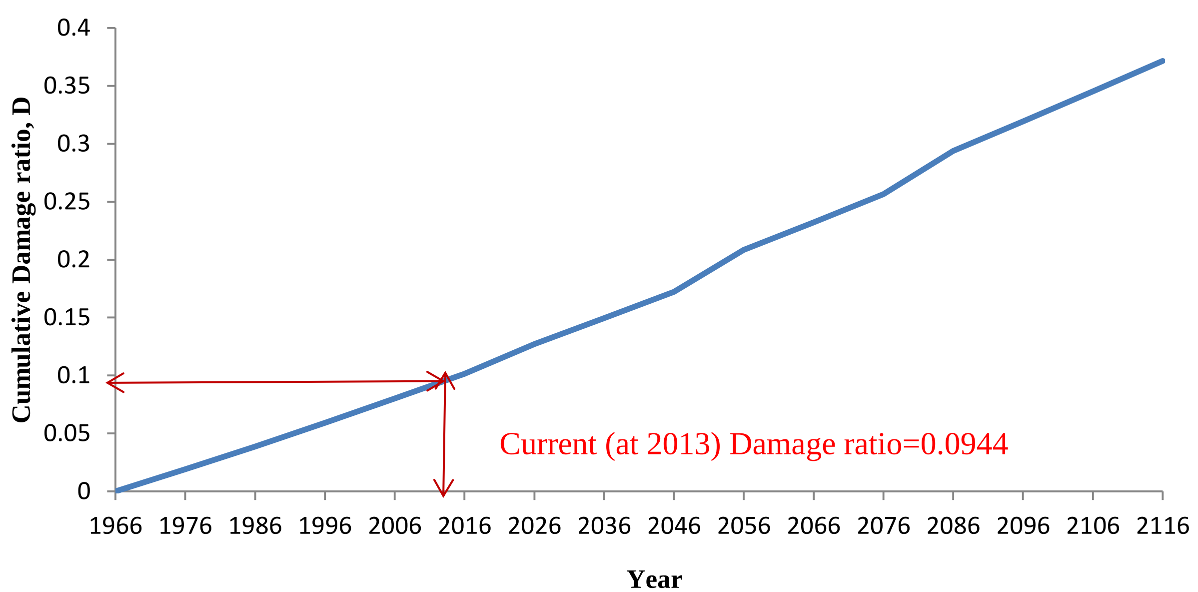

3.8.13 OPERATING SCENARIO D1:

Under this operating condition only passenger or Express train loads are applied according to the frequency specified by Italian code for all four types of train (55 per day). Three Earthquakes events of magnitude described before are applied at 60, 90 and 120 years from year of bridge construction (i.e. in the year 2026, 2056 and2086). It is also assumed that there is no degradation of bridge material due to corrosion and there is no maintenance program carried out. For this operating scenario, the damage ratio for the first 10 years after the bridge construction is shown in the following table

Axial force range, ΔN	Area of the cross-section, A	Stress range, $\Delta\sigma$	Total cycles in 10 years n_i	Number of cycles to failure, N_i	n_i/N_i
1992	0.024	83	200750	3742902.364	0.05363485
816	0.024	34	1204500	109618480.6	0.01098811
720	0.024	30	803000	176024521.4	0.00456186
552	0.024	23	200750	481085058.1	0.00041729
264	0.024	11	602250	7840975184	7.6808E-05
120	0.024	5	200750	1.54916E+11	1.2959E-06
Total damage ratio in Ist ten years, D=					0.06968021

Table 3.141: Damage ratio for 1st ten years (from 1966to 1976) under operating scenario D1

Similarly, for every 10 years the same damage ratio will be found. The damage ratio for the earthquakes can be calculated from the rain flow histogram .Assuming no reduction in the cross-sectional area, the calculated damage ratio for the first earthquake, which will occur in the year 2026 is 0.00332. The calculated damage ratio for the second earthquake, which will occur in the year 2056, is 0.00997. The calculated damage ratio for the third earthquake, which will occur in the year 2086, is 0.009. In the following table and figure, the cumulative damage ratio from the year 1966 to 2116 for operating scenario D1 is shown

Year	Time period, years	Damage ratio	cumulative time, years	cumulative Damage ratio
1966-1976	10	0.069680213	10	0.069680213
1976-1986	10	0.069680213	20	0.139360426
1986-1996	10	0.069680213	30	0.209040639
1996-2006	10	0.069680213	40	0.278720852
2006-2016	10	0.069680213	50	0.348401065
2016-2026	10	0.069680213	60	0.418081278
2026 (EQ 1)		0.00322	60	0.421301278
2026-2036	10	0.069680213	70	0.490981491
2036-2046	10	0.069680213	80	0.560661705
2046-2056	10	0.069680213	90	0.630341918
2056(EQ 2)	0	0.00997	90	0.640311918
2056-2066	10	0.069680213	100	0.709992131
2066-2076	10	0.069680213	110	0.779672344
2076-2086	10	0.069680213	120	0.849352557
2086(EQ 3)		0.009	120	0.858352557
2086-2096	10	0.069680213	130	0.92803277
2096-2106	10	0.069680213	140	0.997712983
2106-2116	10	0.069680213	150	1.067393196

Table 3.142: Cumulative Damage ratio under operating scenario D1

Fig 3.58 Cumulative damage ratio in different years under operating scenario D1

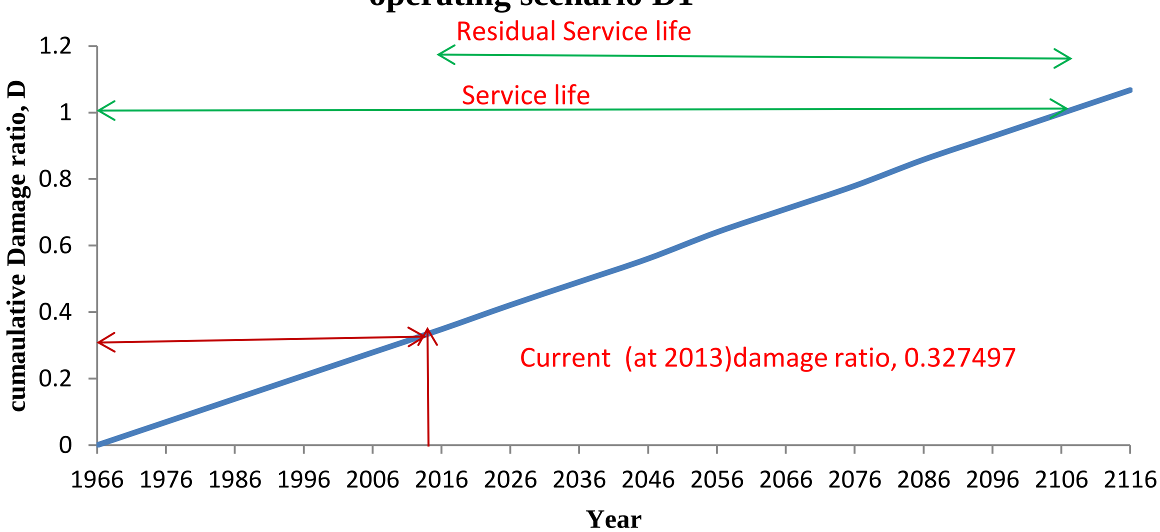

From the figure,

At current period, (2013) the cumulative damage ratio is 0.327497

The service life of the bridge is 140.3 years

The residual service life is 93.3 years

3.8.14 OPERATING SCENARIO D2:

Under this operating condition only passenger or Express train loads are applied according to the frequency specified by Italian code for all four types of train (55 per day). Three Earthquakes events of magnitude described before are applied at 60, 90 and 120 years from year of bridge construction (i.e. in the year 2026, 2056 and2086). It is also assumed that there is thickness loss of bridge material due to corrosion and there is no maintenance program carried out. For this operating scenario, the damage ratio due to train load for the first 10 years, after the bridge construction is 0.069680213 as calculated before. The damage ratio in other decades are shown in the following tables

Axial force range, ΔN	Average cross-sectional Area A	Stress range, Δσ	Total cycles in 10 years n_i	Number of cycles to failure, N_i	n_i/N_i
1992	0.0238	83.70	200750	3626238.5	0.0553604
816	0.0238	34.29	1204500	106201743	0.0113416
720	0.0238	30.25	803000	170537950	0.0047086
552	0.0238	23.19	200750	466089947	0.0004307
264	0.0238	11.09	602250	7.597E+09	7.928E-05
120	0.0238	5.04	200750	1.501E+11	1.338E-06
Total damage ratio from 1976 to 1986 =					0.071922

Table 3.143: Damage ratio from 1976 to 1986 under operating scenario D2

Axial force range, ΔN	Average cross-sectional Area A	Stress range, Δσ	Total cycles in 10 years n_i	Number of cycles to failure, N_i	n_i/N_i
1992	0.0235	84.77	200750	3456288.2	0.0580825
816	0.0235	34.72	1204500	101224404	0.0118993
720	0.0235	30.64	803000	162545378	0.0049402
552	0.0235	23.49	200750	444245790	0.0004519
264	0.0235	11.23	602250	7.241E+09	8.318E-05
120	0.0235	5.11	200750	1.431E+11	1.403E-06
Total damage ratio from 1986 to1996 =					0.0754585

Table 3.144: Damage ratio from 1986 to 1996 under operating scenario D2

Axial force range, ΔN	Average cross-sectional Area A	Stress range, Δσ	Total cycles in 10 years n_i	Number of cycles to failure, N_i	n_i/N_i
1992	0.0233	85.49	200750	3346293	0.0599918
816	0.0233	35.02	1204500	98002972	0.0122904
720	0.0233	30.90	803000	157372426	0.0051025
552	0.0233	23.69	200750	430107816	0.0004667
264	0.0233	11.33	602250	7.01E+09	8.591E-05
120	0.0233	5.15	200750	1.385E+11	1.449E-06
				Total damage ratio from 1996 to2006 =	0.0779389

Table 3.145: Damage ratio from 1996 to 2006 under operating scenario D2

Axial force range, ΔN	Average cross-sectional Area A	Stress range, Δσ	Total cycles in 10 years n_i	Number of cycles to failure, N_i	n_i/N_i
1992	0.0231	86.23	200750	3238895.2	0.061981
816	0.0231	35.32	1204500	94857608	0.012698
720	0.0231	31.17	803000	152321625	0.0052717
552	0.0231	23.90	200750	416303691	0.0004822
264	0.0231	11.43	602250	6.785E+09	8.876E-05
120	0.0231	5.19	200750	1.341E+11	1.498E-06
				Total damage ratio from 2006 to2016 =	0.0805232

Table 3.146: Damage ratio from 2006 to 2016 under operating scenario D2

Axial force range, ΔN	Average cross-sectional Area A	Stress range, Δσ	Total cycles in 10 years n_i	Number of cycles to failure, N_i	n_i/N_i
1992	0.0229	86.99	200750	3134055.1	0.0640544
816	0.0229	35.63	1204500	91787154	0.0131228
720	0.0229	31.44	803000	147391113	0.0054481
552	0.0229	24.10	200750	402828320	0.0004984
264	0.0229	11.53	602250	6.566E+09	9.173E-05
120	0.0229	5.24	200750	1.297E+11	1.548E-06
				Total damage ratio from 2016 to2026 =	0.0832169

Table 3.147: Damage ratio from 2016 to 2026 under operating scenario D2

Axial force range, ΔN	Average cross-sectional Area A	Stress range, Δσ	Total cycles in 10 years n_i	Number of cycles to failure, N_i	n_i/N_i
1992	0.0227	87.75	200750	3031733.4	0.0662162
816	0.0227	35.95	1204500	88790455	0.0135656
720	0.0227	31.72	803000	142579037	0.005632
552	0.0227	24.32	200750	389676641	0.0005152
264	0.0227	11.63	602250	6.351E+09	9.483E-05
120	0.0227	5.29	200750	1.255E+11	1.6E-06
Total damage ratio from 2026 to2036 =					0.0860255

Table 3.148: Damage ratio from 2026 to 2036 under operating scenario D2

Axial force range, ΔN	Average cross-sectional Area A	Stress range, Δσ	Total cycles in 10 years n_i	Number of cycles to failure, N_i	n_i/N_i
1992	0.0225	88.53	200750	2931890.9	0.0684712
816	0.0225	36.27	1204500	85866367	0.0140276
720	0.0225	32.00	803000	137883558	0.0058238
552	0.0225	24.53	200750	376843630	0.0005327
264	0.0225	11.73	602250	6.142E+09	9.805E-05
120	0.0225	5.33	200750	1.213E+11	1.654E-06
Total damage ratio from 2036 to2046 =					0.088955

Table 3.149: Damage ratio from 2036 to 2046 under operating scenario D2

Axial force range in kN, ΔN	Average cross-sectional Area in sqm, A	Stress range in MPa, Δσ	Total cycles in 10 years n_i	Number of cycles to failure, N_i	n_i/N_i
1992	0.0223	89.33	200750	2834488.9	0.0708241
816	0.0223	36.59	1204500	83013752	0.0145096
720	0.0223	32.29	803000	133302850	0.0060239
552	0.0223	24.75	200750	364324294	0.000551
264	0.0223	11.84	602250	5.938E+09	0.0001014
120	0.0223	5.38	200750	1.173E+11	1.711E-06
Total damage ratio from 2046 to2056 =					0.0920117

Table 3.150: Damage ratio from 2046 to 2056 under operating scenario D2

Axial force range in kN, ΔN	Average cross-sectional Area in sqm, A	Stress range in MPa, $\Delta\sigma$	Total cycles in 10 years n_i	Number of cycles to failure, N_i	n_i/N_i
1992	0.0221	90.14	200750	2739488.8	0.0732801
816	0.0221	36.92	1204500	80231480	0.0150128
720	0.0221	32.58	803000	128835099	0.0062328
552	0.0221	24.98	200750	352113676	0.0005701
264	0.0221	11.95	602250	5.739E+09	0.0001049
120	0.0221	5.43	200750	1.134E+11	1.771E-06
Total damage ratio from 2056 to2066 =					0.0952025

Table 3.151: Damage ratio from 2056 to 2066 under operating scenario D2

Axial force range in kN, ΔN	Average cross-sectional Area in sqm, A	Stress range in MPa, $\Delta\sigma$	Total cycles in 10 years n_i	Number of cycles to failure, N_i	n_i/N_i
1992	0.0219	90.96	200750	2646852.2	0.0758448
816	0.0219	37.26	1204500	77518430	0.0155382
720	0.0219	32.88	803000	124478505	0.0064509
552	0.0219	25.21	200750	340206855	0.0005901
264	0.0219	12.05	602250	5.545E+09	0.0001086
120	0.0219	5.48	200750	1.096E+11	1.832E-06
Total damage ratio from 2066 to2076 =					0.0985345

Table 3.152: Damage ratio from 2066 to 2076 under operating scenario D2

Axial force range in kN, ΔN	Average cross-sectional Area in sqm, A	Stress range in MPa, $\Delta\sigma$	Total cycles in 10 years n_i	Number of cycles to failure, N_i	n_i/N_i
1992	0.0217	91.80	200750	2556541.2	0.0785241
816	0.0217	37.60	1204500	74873489	0.0160871
720	0.0217	33.18	803000	120231279	0.0066788
552	0.0217	25.44	200750	328598943	0.0006109
264	0.0217	12.17	602250	5.356E+09	0.0001125
120	0.0217	5.53	200750	1.058E+11	1.897E-06
Total damage ratio from 2076 to 2086 =					0.1020153

Table 3.153: Damage ratio from 2076 to 2086 under operating scenario D2

Axial force range in kN, ΔN	Average cross-sectional Area in sqm, A	Stress range in MPa, $\Delta\sigma$	Total cycles in 10 years n_i	Number of cycles to failure, N_i	n_i/N_i
1992	0.0215	92.65	200750	2468518	0.0813241
816	0.0215	37.95	1204500	72295551	0.0166608
720	0.0215	33.49	803000	116091645	0.0069169
552	0.0215	25.67	200750	317285089	0.0006327
264	0.0215	12.28	602250	5.171E+09	0.0001165
120	0.0215	5.58	200750	1.022E+11	1.965E-06
				Total damage ratio from 2086 to 2096 =	0.105653

Table 3.154: Damage ratio from 2086 to 2096 under operating scenario D2

Axial force range in kN, ΔN	Average cross-sectional Area in sqm, A	Stress range in MPa, $\Delta\sigma$	Total cycles in 10 years n_i	Number of cycles to failure, N_i	n_i/N_i
1992	0.0213	93.52	200750	2382745.1	0.0842516
816	0.0213	38.31	1204500	69783518	0.0172605
720	0.0213	33.80	803000	112057842	0.0071659
552	0.0213	25.92	200750	306260473	0.0006555
264	0.0213	12.39	602250	4.992E+09	0.0001207
120	0.0213	5.63	200750	9.862E+10	2.036E-06
				Total damage ratio from 2096 to 2106 =	0.1094562

Table 3.155: Damage ratio from 2096 to 2106 under operating scenario D2

Axial force range in kN, ΔN	Average cross-sectional Area in sqm, A	Stress range in MPa, $\Delta\sigma$	Total cycles in 10 years n_i	Number of cycles to failure, N_i	n_i/N_i
1992	0.0211	94.41	200750	2299185.3	0.0873135
816	0.0211	38.67	1204500	67336300	0.0178878
720	0.0211	34.12	803000	108128118	0.0074264
552	0.0211	26.16	200750	295520315	0.0006793
264	0.0211	12.51	602250	4.817E+09	0.000125
120	0.0211	5.69	200750	9.516E+10	2.11E-06
				Total damage ratio from 2106 to 2116 =	0.1134342

Table 3.156: Damage ratio from 2106 to 2116 under operating scenario D2

In the following table and figure, the cumulative damage ratio from the year 1966 to 2116 for operating scenario D2 is shown

Year	Time period, years	Damage ratio	cumulative time, years	cumulative Damage ratio
1966-1976	10	0.06968021	10	0.0696802
1976-1986	10	0.07192197	20	0.1416022
1986-1996	10	0.07545847	30	0.2170607
1996-2006	10	0.07793885	40	0.2949995
2006-2016	10	0.08052321	50	0.3755227
2016-2026	10	0.08321686	60	0.4587396
2026 (EQ 1)		0.00408	60	0.4628196
2026-2036	10	0.08602545	70	0.548845
2036-2046	10	0.08895496	80	0.6378
2046-2056	10	0.09201173	90	0.7298117
2056(EQ 2)	0	0.01349	90	0.7433017
2056-2066	10	0.09520252	100	0.8385042
2066-2076	10	0.09853449	110	0.9370387
2076-2086	10	0.10201527	120	1.039054
2086(EQ 3)		0.01342	120	1.052474
2086-2096	10	0.10565296	130	1.158127
2096-2106	10	0.10945621	140	1.2675832
2106-2116	10	0.1134342	150	1.3810174

Table 3.157: Cumulative Damage ratio under operating scenario D2

Fig 3.59 Cumulative damage ratio for operating condition D2

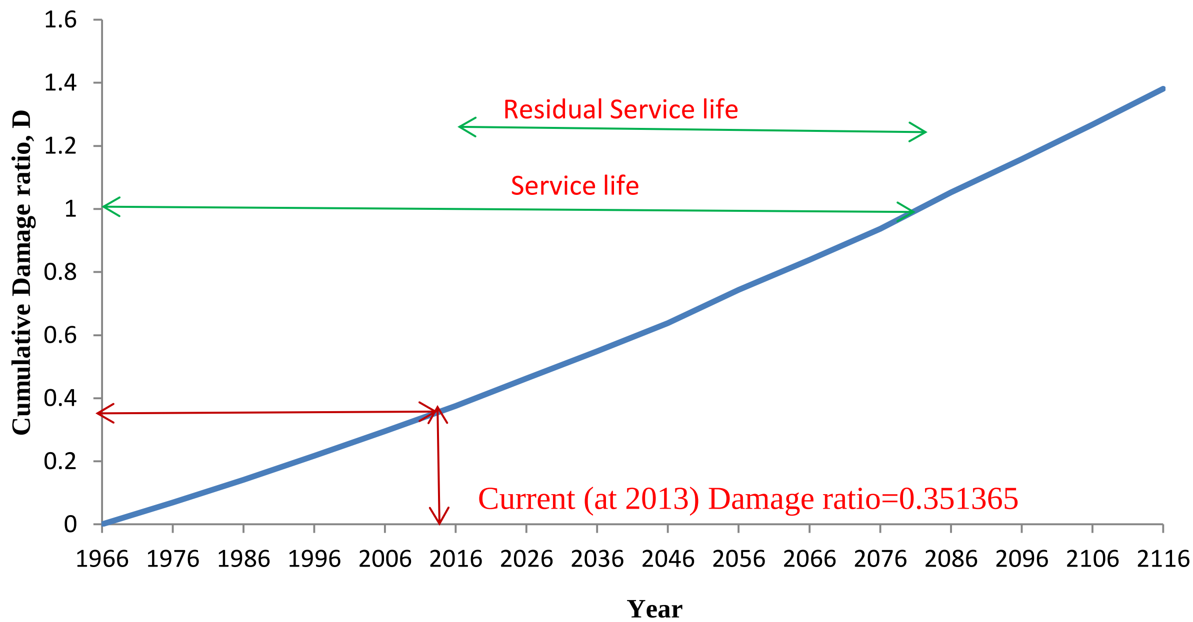

From the figure,

At current period, (2013) the cumulative damage ratio is 0.351365

The service life of the bridge is 116.2 years

The residual service life is 69.2 years

3.8.15 OPERATING SCENARIO D3:

Under this operating condition only passenger or Express train loads are applied according to the frequency specified by Italian code for all four types of train (55 per day). Three Earthquakes events of magnitude described before are applied at 60, 90 and 120 years from year of bridge construction (i.e. in the year 2026, 2056 and2086). It is also assumed that a total number of three corrosion protective paintings are provide at the interval of every ten years for the first thirty years from the year of bridge construction and the thickness loss of bridge material due to corrosion initiates after forty years of bridge construction, i.e. in the year 2006 .For this operating scenario, the damage ratio due to train load for the first 10 (1966-76) years, after the bridge construction is 0.06968621 as calculated before. The damage ratio due to train load for the next three decades (1976-1986, 1986-1996 and 1996-2006) are also 0.06968621 as calculated before. The damage ratio in other decades are shown in the following tables

Axial force range, ΔN	Average cross-sectional Area A	Stress range, Δσ	Total cycles in 10 years n_i	Number of cycles to failure, N_i	n_i/N_i
1992	0.0238	83.70	200750	3626238.5	0.0553604
816	0.0238	34.29	1204500	106201743	0.0113416
720	0.0238	30.25	803000	170537950	0.0047086
552	0.0238	23.19	200750	466089947	0.0004307
264	0.0238	11.09	602250	7.597E+09	7.928E-05
120	0.0238	5.04	200750	1.501E+11	1.338E-06
				Total damage ratio from 2006 to2016 =	0.071922

Table 3.158: Damage ratio from 2006 to 2016 under operating scenario D3

Axial force range, ΔN	Average cross-sectional Area A	Stress range, Δσ	Total cycles in 10 years n_i	Number of cycles to failure, N_i	n_i/N_i
1992	0.0235	84.77	200750	3456288.2	0.0580825
816	0.0235	34.72	1204500	101224404	0.0118993
720	0.0235	30.64	803000	162545378	0.0049402
552	0.0235	23.49	200750	444245790	0.0004519
264	0.0235	11.23	602250	7.241E+09	8.318E-05
120	0.0235	5.11	200750	1.431E+11	1.403E-06
				Total damage ratio from 2016 to2026 =	0.0754585

Table 3.159: Damage ratio from 2016 to 2026 under operating scenario D3

Axial force range, ΔN	Average cross-sectional Area A	Stress range, Δσ	Total cycles in 10 years n_i	Number of cycles to failure, N_i	n_i/N_i
1992	0.0233	85.49	200750	3346293	0.0599918
816	0.0233	35.02	1204500	98002972	0.0122904
720	0.0233	30.90	803000	157372426	0.0051025
552	0.0233	23.69	200750	430107816	0.0004667
264	0.0233	11.33	602250	7.01E+09	8.591E-05
120	0.0233	5.15	200750	1.385E+11	1.449E-06
Total damage ratio from 2026 to2036 =					0.0779389

Table 3.160: Damage ratio from 2026 to 2036 under operating scenario D3

Axial force range, ΔN	Average cross-sectional Area A	Stress range, Δσ	Total cycles in 10 years n_i	Number of cycles to failure, N_i	n_i/N_i
1992	0.0231	86.23	200750	3238895.2	0.061981
816	0.0231	35.32	1204500	94857608	0.012698
720	0.0231	31.17	803000	152321625	0.0052717
552	0.0231	23.90	200750	416303691	0.0004822
264	0.0231	11.43	602250	6.785E+09	8.876E-05
120	0.0231	5.19	200750	1.341E+11	1.498E-06
Total damage ratio from 2036 to2046 =					0.0805232

Table 3.161: Damage ratio from 2036 to 2046 under operating scenario D3

Axial force range in kN, ΔN	Average cross-sectional Area in sqm, A	Stress range in MPa, Δσ	Total cycles in 10 years n_i	Number of cycles to failure, N_i	n_i/N_i
1992	0.0229	86.99	200750	3134055.1	0.0640544
816	0.0229	35.63	1204500	91787154	0.0131228
720	0.0229	31.44	803000	147391113	0.0054481
552	0.0229	24.10	200750	402828320	0.0004984
264	0.0229	11.53	602250	6.566E+09	9.173E-05
120	0.0229	5.24	200750	1.297E+11	1.548E-06
Total damage ratio from 2046 to2056 =					0.0832169

Table 3.162: Damage ratio from 2046 to 2056 under operating scenario D3

Axial force range in kN, ΔN	Average cross-sectional Area in sqm, A	Stress range in MPa, Δσ	Total cycles in 10 years n_i	Number of cycles to failure, N_i	n_i/N_i
1992	0.0227	87.75	200750	3031733.4	0.0662162
816	0.0227	35.95	1204500	88790455	0.0135656
720	0.0227	31.72	803000	142579037	0.005632
552	0.0227	24.32	200750	389676641	0.0005152
264	0.0227	11.63	602250	6.351E+09	9.483E-05
120	0.0227	5.29	200750	1.255E+11	1.6E-06
Total damage ratio from 2056 to2066 =					0.0860255

Table 3.163: Damage ratio from 2056 to 2066 under operating scenario D3

Axial force range in kN, ΔN	Average cross-sectional Area in sqm, A	Stress range in MPa, Δσ	Total cycles in 10 years n_i	Number of cycles to failure, N_i	n_i/N_i
1992	0.0225	88.53	200750	2931890.9	0.0684712
816	0.0225	36.27	1204500	85866367	0.0140276
720	0.0225	32.00	803000	137883558	0.0058238
552	0.0225	24.53	200750	376843630	0.0005327
264	0.0225	11.73	602250	6.142E+09	9.805E-05
120	0.0225	5.33	200750	1.213E+11	1.654E-06
Total damage ratio from 2066 to2076 =					0.088955

Table 3.164: Damage ratio from 2066 to 2076 under operating scenario D3

Axial force range in kN, ΔN	Average cross-sectional Area in sqm, A	Stress range in MPa, Δσ	Total cycles in 10 years n_i	Number of cycles to failure, N_i	n_i/N_i
1992	0.0223	89.33	200750	2834488.9	0.0708241
816	0.0223	36.59	1204500	83013752	0.0145096
720	0.0223	32.29	803000	133302850	0.0060239
552	0.0223	24.75	200750	364324294	0.000551
264	0.0223	11.84	602250	5.938E+09	0.0001014
120	0.0223	5.38	200750	1.173E+11	1.711E-06
Total damage ratio from 2076 to 2086 =					0.0920117

Table 3.165: Damage ratio from 2076 to 2086 under operating scenario D3

Axial force range in kN, ΔN	Average cross-sectional Area in sqm, A	Stress range in MPa, Δσ	Total cycles in 10 years n_i	Number of cycles to failure, N_i	n_i/N_i
1992	0.0221	90.14	200750	2739488.8	0.0732801
816	0.0221	36.92	1204500	80231480	0.0150128
720	0.0221	32.58	803000	128835099	0.0062328
552	0.0221	24.98	200750	352113676	0.0005701
264	0.0221	11.95	602250	5.739E+09	0.0001049
120	0.0221	5.43	200750	1.134E+11	1.771E-06
Total damage ratio from 2086 to 2096 =					0.0952025

Table 3.166: Damage ratio from 2086 to 2096 under operating scenario D3

Axial force range in kN, ΔN	Average cross-sectional Area in sqm, A	Stress range in MPa, Δσ	Total cycles in 10 years n_i	Number of cycles to failure, N_i	n_i/N_i
1992	0.0219	90.96	200750	2646852.2	0.0758448
816	0.0219	37.26	1204500	77518430	0.0155382
720	0.0219	32.88	803000	124478505	0.0064509
552	0.0219	25.21	200750	340206855	0.0005901
264	0.0219	12.05	602250	5.545E+09	0.0001086
120	0.0219	5.48	200750	1.096E+11	1.832E-06
Total damage ratio from 2096 to 2106 =					0.0985345

Table 3.167: Damage ratio from 2096 to 2106 under operating scenario D3

Axial force range in kN, ΔN	Average cross-sectional Area in sqm, A	Stress range in MPa, Δσ	Total cycles in 10 years n_i	Number of cycles to failure, N_i	n_i/N_i
1992	0.0217	91.80	200750	2556541.2	0.0785241
816	0.0217	37.60	1204500	74873489	0.0160871
720	0.0217	33.18	803000	120231279	0.0066788
552	0.0217	25.44	200750	328598943	0.0006109
264	0.0217	12.17	602250	5.356E+09	0.0001125
120	0.0217	5.53	200750	1.058E+11	1.897E-06
Total damage ratio from 2106 to 2116 =					0.1020153

Table 3.168: Damage ratio from 2106 to 2116 under operating scenario D3

In the following table and figure, the cumulative damage ratio from the year 1966 to 2116 for operating scenario D3 is shown

Year	Time period, years	Damage ratio	cumulative time, years	cumulative Damage ratio
1966-1976	10	0.0696802	10	0.0696802
1976-1986	10	0.0696802	20	0.1393604
1986-1996	10	0.0696802	30	0.2090406
1996-2006	10	0.0696802	40	0.2787209
2006-2016	10	0.071922	50	0.3506428
2016-2026	10	0.0754585	60	0.4261013
2026 (EQ 1)		0.0036	60	0.4297013
2026-2036	10	0.0779389	70	0.5076402
2036-2046	10	0.0805232	80	0.5881634
2046-2056	10	0.0832169	90	0.6713802
2056(EQ 2)	0	0.01223	90	0.6836102
2056-2066	10	0.0860255	100	0.7696357
2066-2076	10	0.088955	110	0.8585906
2076-2086	10	0.0920117	120	0.9506024
2086(EQ 3)		0.012109	120	0.9627114
2086-2096	10	0.0952025	130	1.0579139
2096-2106	10	0.0985345	140	1.1564484
2106-2116	10	0.1020153	150	1.2584636

Table 3.169: Cumulative Damage ratio under operating scenario D3

Fig 3.60 Cumulative damage ratio for operating condition D3

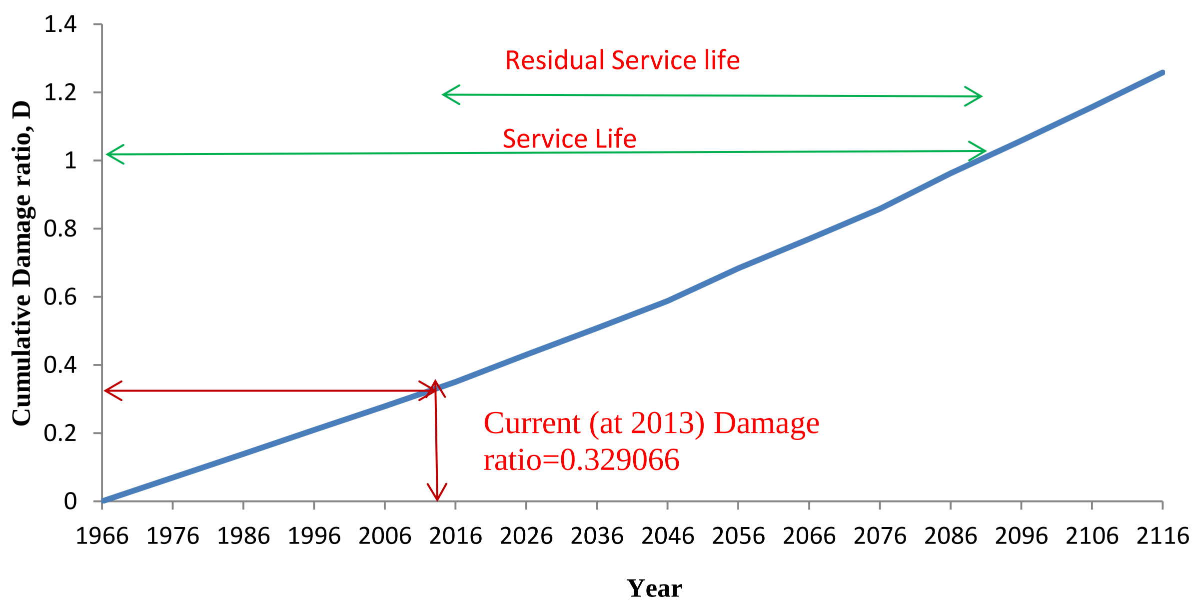

From the figure,

At current period, (2013) the cumulative damage ratio is 0.329066

The service life of the bridge is 123.9 years

The residual service life is 76.9 years

3.8.16 OPERATING SCENARIO D4:

Under this operating condition only passenger or Express train loads are applied according to the frequency specified by Italian code for all four types of train (55 per day). Three Earthquakes events of magnitude described before are applied at 60, 90 and 120 years from year of bridge construction (i.e. in the year 2026, 2056 and2086). It is also assumed that corrosion protective paintings are provide at the interval of every thirty years from the year of bridge construction and the thickness loss of bridge material due to corrosion initiated after 10 years of bridge construction, i.e. in the year1976 and continues as described before in paragraph 3.6.3. For this operating scenario, the damage ratio due to train load for the first 10 (1966-76) years, after the bridge construction is 0.0696802 as calculated before. The damage ratio in other decades are shown in the following tables

Axial force range, ΔN	Average cross-sectional Area A	Stress range, Δσ	Total cycles in 10 years n_i	Number of cycles to failure, N_i	n_i/N_i
1992	0.0238	83.70	200750	3626238.5	0.0553604
816	0.0238	34.29	1204500	106201743	0.0113416
720	0.0238	30.25	803000	170537950	0.0047086
552	0.0238	23.19	200750	466089947	0.0004307
264	0.0238	11.09	602250	7.597E+09	7.928E-05
120	0.0238	5.04	200750	1.501E+11	1.338E-06
Total damage ratio from 1976 to 1986 =					0.071922

Table 3.170: Damage ratio from 1976 to 1986 under operating scenario D4

Axial force range, ΔN	Average cross-sectional Area A	Stress range, Δσ	Total cycles in 10 years n_i	Number of cycles to failure, N_i	n_i/N_i
1992	0.0235	84.77	200750	3456288.2	0.0580825
816	0.0235	34.72	1204500	101224404	0.0118993
720	0.0235	30.64	803000	162545378	0.0049402
552	0.0235	23.49	200750	444245790	0.0004519
264	0.0235	11.23	602250	7.241E+09	8.318E-05
120	0.0235	5.11	200750	1.431E+11	1.403E-06
Total damage ratio from 1986 to1996 =					0.0754585

Table 3.171: Damage ratio from 1986 to 1996 under operating scenario D4

Axial force range, ΔN	Average cross-sectional Area A	Stress range, Δσ	Total cycles in 10 years n_i	Number of cycles to failure, N_i	n_i/N_i
1992	0.0234	85.13	200750	3400963.4	0.0590274
816	0.0234	34.87	1204500	99604106	0.0120929
720	0.0234	30.77	803000	159943516	0.0050205
552	0.0234	23.59	200750	437134752	0.0004592
264	0.0234	11.28	602250	7.125E+09	8.453E-05
120	0.0234	5.13	200750	1.408E+11	1.426E-06
Total damage ratio from 1996 to2006 =					0.076686

Table 3.172: Damage ratio from 1996 to 2006 under operating scenario D4

Axial force range, ΔN	Average cross-sectional Area A	Stress range, Δσ	Total cycles in 10 years n_i	Number of cycles to failure, N_i	n_i/N_i
1992	0.0233	85.49	200750	3346293	0.0599918
816	0.0233	35.02	1204500	98002972	0.0122904
720	0.0233	30.90	803000	157372426	0.0051025
552	0.0233	23.69	200750	430107816	0.0004667
264	0.0233	11.33	602250	7.01E+09	8.591E-05
120	0.0233	5.15	200750	1.385E+11	1.449E-06
Total damage ratio from 2006 to2016 =					0.0779389

Table 3.173: Damage ratio from 2006 to 2016 under operating scenario D4

Axial force range, ΔN	Average cross-sectional Area A	Stress range, Δσ	Total cycles in 10 years n_i	Number of cycles to failure, N_i	n_i/N_i
1992	0.0231	86.23	200750	3238895.2	0.061981
816	0.0231	35.32	1204500	94857608	0.012698
720	0.0231	31.17	803000	152321625	0.0052717
552	0.0231	23.90	200750	416303691	0.0004822
264	0.0231	11.43	602250	6.785E+09	8.876E-05
120	0.0231	5.19	200750	1.341E+11	1.498E-06
Total damage ratio from 2016 to2026 =					0.0805232

Table 3.174: Damage ratio from 2016 to 2026 under operating scenario D4

Axial force range, ΔN	Average cross-sectional Area A	Stress range, Δσ	Total cycles in 10 years n_i	Number of cycles to failure, N_i	n_i/N_i
1992	0.023	86.61	200750	3186157.9	0.0630069
816	0.023	35.48	1204500	93313090	0.0129082
720	0.023	31.30	803000	149841449	0.005359
552	0.023	24.00	200750	409525229	0.0004902
264	0.023	11.48	602250	6.675E+09	9.023E-05
120	0.023	5.22	200750	1.319E+11	1.522E-06
				Total damage ratio from 2026 to2036 =	0.081856

Table 3.175: Damage ratio from 2026 to 2036 under operating scenario D4

Axial force range, ΔN	Average cross-sectional Area A	Stress range, Δσ	Total cycles in 10 years n_i	Number of cycles to failure, N_i	n_i/N_i
1992	0.0229	86.99	200750	3134055.1	0.0640544
816	0.0229	35.63	1204500	91787154	0.0131228
720	0.0229	31.44	803000	147391113	0.0054481
552	0.0229	24.10	200750	402828320	0.0004984
264	0.0229	11.53	602250	6.566E+09	9.173E-05
120	0.0229	5.24	200750	1.297E+11	1.548E-06
				Total damage ratio from 2036 to2046 =	0.0832169

Table 3.176: Damage ratio from 2036 to 2046 under operating scenario D4

Axial force range in kN, ΔN	Average cross-sectional Area in sqm, A	Stress range in MPa, Δσ	Total cycles in 10 years n_i	Number of cycles to failure, N_i	n_i/N_i
1992	0.0227	87.75	200750	3031733.4	0.0662162
816	0.0227	35.95	1204500	88790455	0.0135656
720	0.0227	31.72	803000	142579037	0.005632
552	0.0227	24.32	200750	389676641	0.0005152
264	0.0227	11.63	602250	6.351E+09	9.483E-05
120	0.0227	5.29	200750	1.255E+11	1.6E-06
				Total damage ratio from 2046 to2056 =	0.0860255

Table 3.177: Damage ratio from 2046 to 2056 under operating scenario D4

Axial force range in kN, ΔN	Average cross-sectional Area in sqm, A	Stress range in MPa, Δσ	Total cycles in 10 years n_i	Number of cycles to failure, N_i	n_i/N_i
1992	0.0226	88.14	200750	2981504.7	0.0673318
816	0.0226	36.11	1204500	87319406	0.0137942
720	0.0226	31.86	803000	140216837	0.0057268
552	0.0226	24.42	200750	383220615	0.0005238
264	0.0226	11.68	602250	6.246E+09	9.642E-05
120	0.0226	5.31	200750	1.234E+11	1.627E-06
				Total damage ratio from 2056 to2066 =	0.0874747

Table 3.178: Damage ratio from 2056 to 2066 under operating scenario D4

Axial force range in kN, ΔN	Average cross-sectional Area in sqm, A	Stress range in MPa, Δσ	Total cycles in 10 years n_i	Number of cycles to failure, N_i	n_i/N_i
1992	0.0225	88.53	200750	2931890.9	0.0684712
816	0.0225	36.27	1204500	85866367	0.0140276
720	0.0225	32.00	803000	137883558	0.0058238
552	0.0225	24.53	200750	376843630	0.0005327
264	0.0225	11.73	602250	6.142E+09	9.805E-05
120	0.0225	5.33	200750	1.213E+11	1.654E-06
				Total damage ratio from 2066 to2076 =	0.088955

Table 3.179: Damage ratio from 2066 to 2076 under operating scenario D4

Axial force range in kN, ΔN	Average cross-sectional Area in sqm, A	Stress range in MPa, Δσ	Total cycles in 10 years n_i	Number of cycles to failure, N_i	n_i/N_i
1992	0.0223	89.33	200750	2834488.9	0.0708241
816	0.0223	36.59	1204500	83013752	0.0145096
720	0.0223	32.29	803000	133302850	0.0060239
552	0.0223	24.75	200750	364324294	0.000551
264	0.0223	11.84	602250	5.938E+09	0.0001014
120	0.0223	5.38	200750	1.173E+11	1.711E-06
				Total damage ratio from 2076 to 2086 =	0.0920117

Table 3.180: Damage ratio from 2076 to 2086 under operating scenario D4

Axial force range in kN, ΔN	Average cross-sectional Area in sqm, A	Stress range in MPa, Δσ	Total cycles in 10 years n_i	Number of cycles to failure, N_i	n_i/N_i
1992	0.0222	89.73	200750	2786691	0.0720388
816	0.0222	36.76	1204500	81613893	0.0147585
720	0.0222	32.43	803000	131054968	0.0061272
552	0.0222	24.86	200750	358180704	0.0005605
264	0.0222	11.89	602250	5.838E+09	0.0001032
120	0.0222	5.41	200750	1.153E+11	1.741E-06
Total damage ratio from 2086 to 2096 =					0.0935899

Table 3.181: Damage ratio from 2086 to 2096 under operating scenario D4

Axial force range in kN, ΔN	Average cross-sectional Area in sqm, A	Stress range in MPa, Δσ	Total cycles in 10 years n_i	Number of cycles to failure, N_i	n_i/N_i
1992	0.0221	90.14	200750	2739488.8	0.0732801
816	0.0221	36.92	1204500	80231480	0.0150128
720	0.0221	32.58	803000	128835099	0.0062328
552	0.0221	24.98	200750	352113676	0.0005701
264	0.0221	11.95	602250	5.739E+09	0.0001049
120	0.0221	5.43	200750	1.134E+11	1.771E-06
Total damage ratio from 2096 to 2106 =					0.0952025

Table 3.182: Damage ratio from 2096 to 2106 under operating scenario D4

Axial force range in kN, ΔN	Average cross-sectional Area in sqm, A	Stress range in MPa, Δσ	Total cycles in 10 years n_i	Number of cycles to failure, N_i	n_i/N_i
1992	0.022	90.55	200750	2692877.4	0.0745485
816	0.022	37.09	1204500	78866372	0.0152727
720	0.022	32.73	803000	126643020	0.0063407
552	0.022	25.09	200750	346122597	0.00058
264	0.022	12.00	602250	5.641E+09	0.0001068
120	0.022	5.45	200750	1.115E+11	1.801E-06
Total damage ratio from 2106 to 2116 =					0.0968504

Table 3.183: Damage ratio from 2106 to 2116 under operating scenario D4

In the following table and figure, the cumulative damage ratio from the year 1966 to 2116 for operating scenario D4 is shown

Year	Time period, years	Damage ratio	cumulative time, years	cumulative Damage ratio
1966-1976	10	0.0696802	10	0.0696802
1976-1986	10	0.071922	20	0.1416022
1986-1996	10	0.0754585	30	0.2170607
1996-2006	10	0.076686	40	0.2937466
2006-2016	10	0.0779389	50	0.3716855
2016-2026	10	0.0805232	60	0.4522087
2026 (EQ 1)		0.003925	60	0.4561337
2026-2036	10	0.081856	70	0.5379897
2036-2046	10	0.0832169	80	0.6212066
2046-2056	10	0.0860255	90	0.7072321
2056(EQ 2)	0	0.012707	90	0.7199391
2056-2066	10	0.0874747	100	0.8074138
2066-2076	10	0.088955	110	0.8963687
2076-2086	10	0.0920117	120	0.9883804
2086(EQ 3)		0.012109	120	1.0004894
2086-2096	10	0.0935899	130	1.0940794
2096-2106	10	0.0952025	140	1.1892819
2106-2116	10	0.0968504	150	1.2861323

Table 3.184: Cumulative Damage ratio under operating scenario D4

Fig 3.61 Cumulative damage ratio for operating condition D4

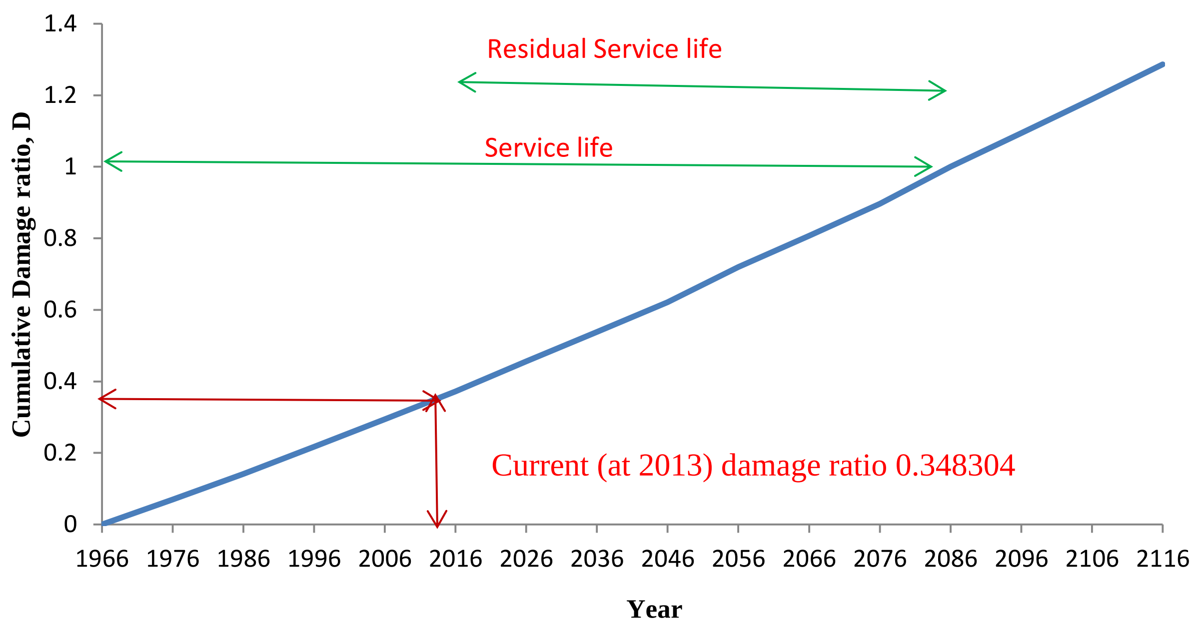

From the figure,

At current period, (2013) the cumulative damage ratio is 0.348304

The service life of the bridge is 120 years

The residual service life is 73 years

3.9 ANALYSIS AND COMPARISON OF RESULTS:

From the preceding analysis the following observations have been made

3.9.1 CUMULATIVE DAMAGE RATIO AFTER 100 YEARS FOR LOAD CATEGORY A:

Under train load category A (mixed track, RFI), the damage ratio at t=100 years for the four sub-categories are shown in the following figure

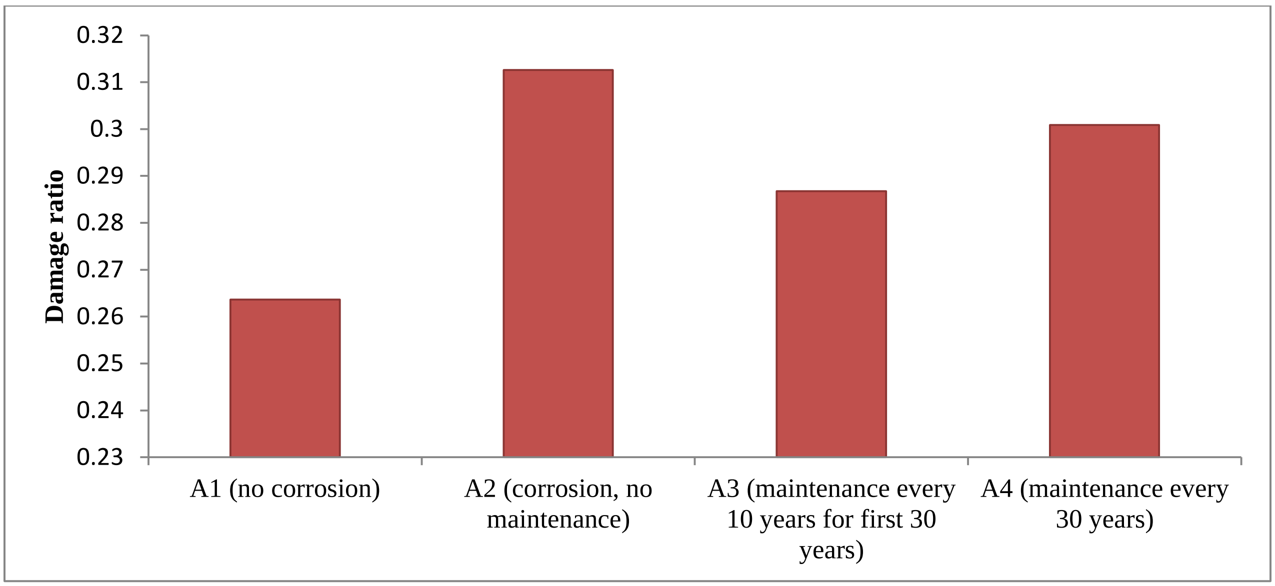

Figure 3.62: Cumulative damage ratio at t=100 years for operating scenarios A1, A2, A3,A4

From the figure, at t=100 years, corrosion increases the damage ratio to 19%, when no maintenance is done. However, when painting is provided every 10 years for the first 30 years, the increase in damage ratio from no corrosion state can be limited to 8.8%. And, for one maintenance intervention in every thirty year the increase is damage ratio from no corrosion condition is higher (14%) than the other maintenance option. So, obviously, the maintenance in every 10 years for the first thirty year is a better maintenance strategy. In the following figure the cumulative damage ratio for these subcategories in different years are shown

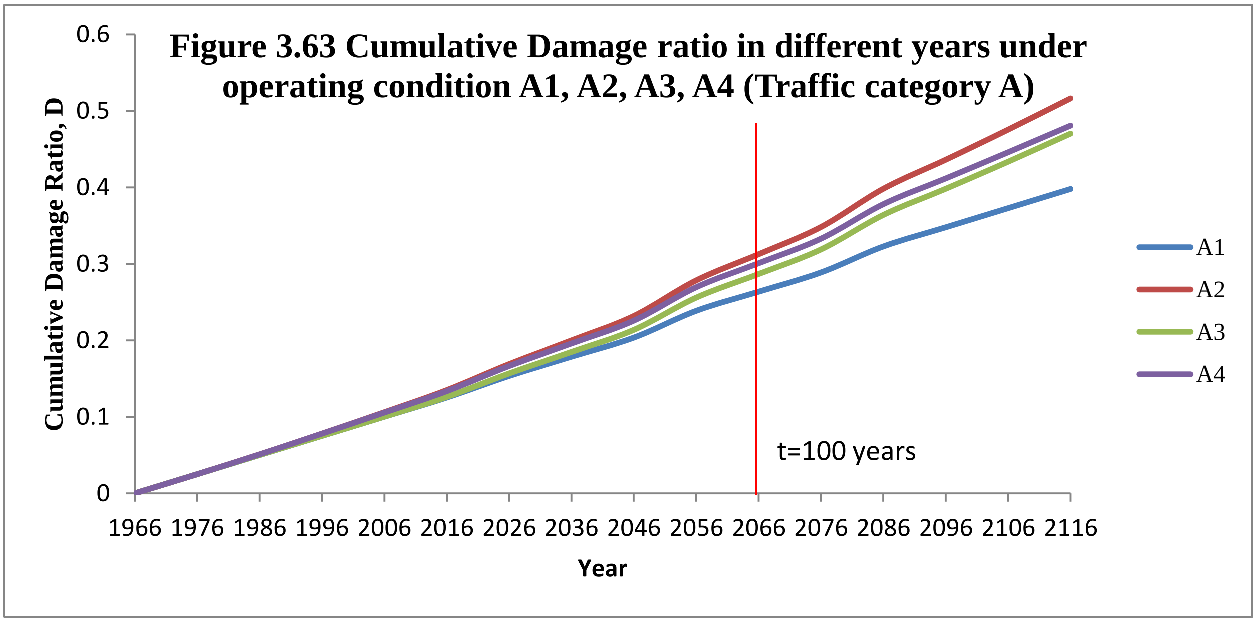

<u>**3.9.2 CUMULATIVE DAMAGE RATIO AFTER 100 YEARS FOR LOAD CATEGORY B:**</u>

Under train load category B (mixed track, Italian code), the damage ratio at t=100 years for the four sub-categories are shown in the following figure

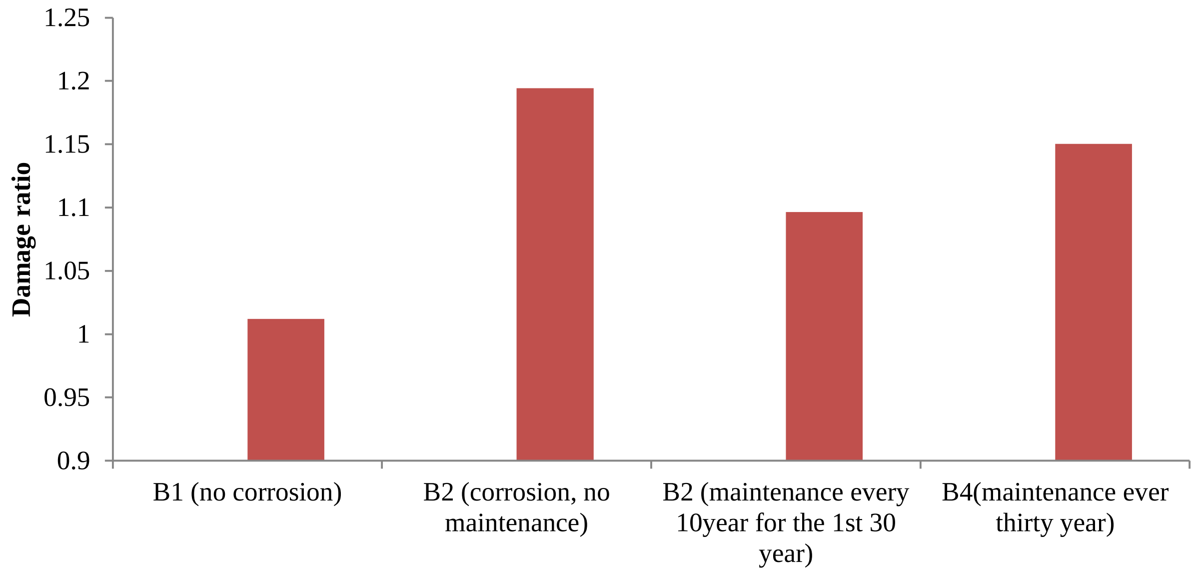

Figure 3.64: Cumulative damage ratio at t=100 years for operating scenarios B1, B2, B3,B4

From the figure, at t=100 years, corrosion increases the damage ratio to 18.5%, when no maintenance is done. However, when painting is provided every 10 years for the first 30 years, the increase in damage ratio from no corrosion state can be limited to 8.5%. And, for one maintenance intervention in every thirty year the increase is damage ratio from no corrosion condition is higher (14%) than the other maintenance option. In the following figure the cumulative damage ratio for these subcategories in different years are shown

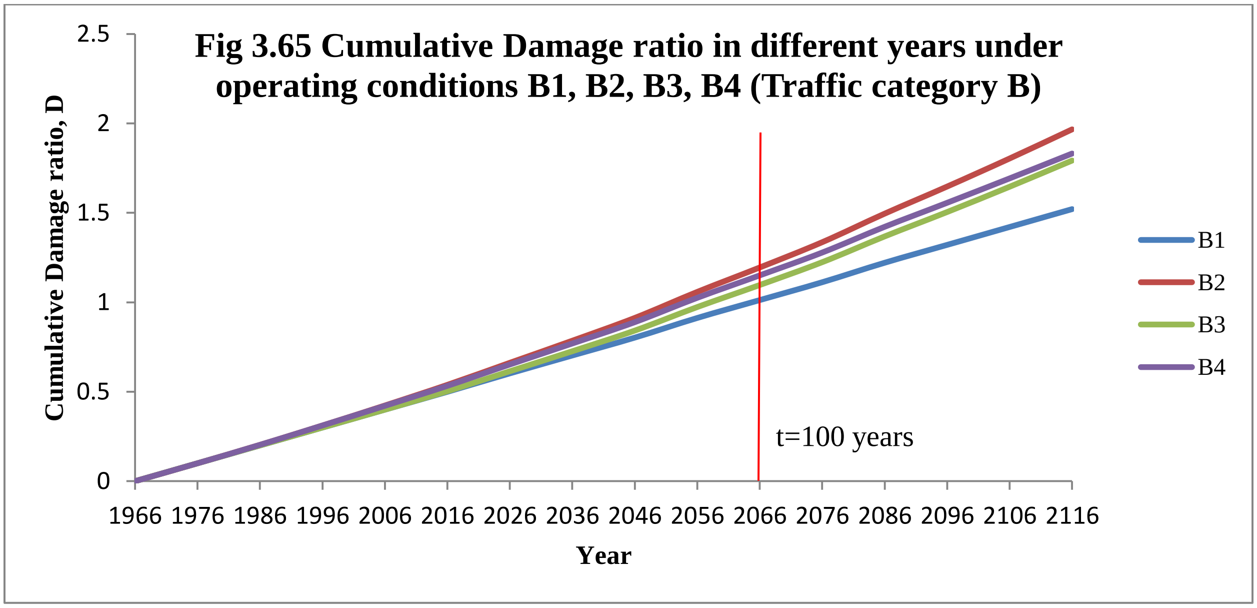

3.9.3 CUMULATIVE DAMAGE RATIO AFTER 100 YEARS FOR LOAD CATEGORY C:

Under train load category C (passenger train, RFI), the damage ratio at t=100 years for the four sub-categories are shown in the following figure

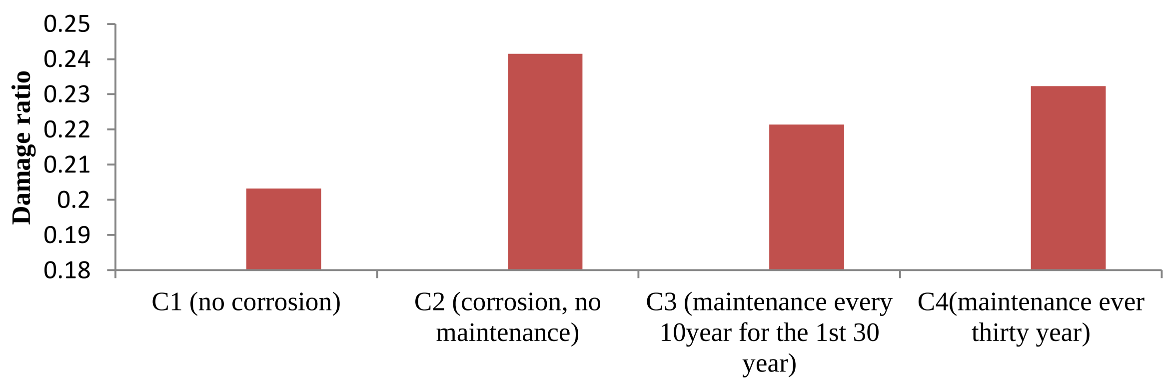

Figure 3.65: Cumulative damage ratio at t=100 years for operating scenarios C1, C2, C3,C4

From the figure, at t=100 years, corrosion increases the damage ratio to 18.8%, when no maintenance is done. However, when painting is provided every 10 years for the first 30 years, the increase in damage ratio from no corrosion state can be limited to 9%. And, for one maintenance intervention in every thirty year the increase is damage ratio from no corrosion condition is higher (14.3%) than the other maintenance option. In the following figure the cumulative damage ratio for these subcategories in different years are shown

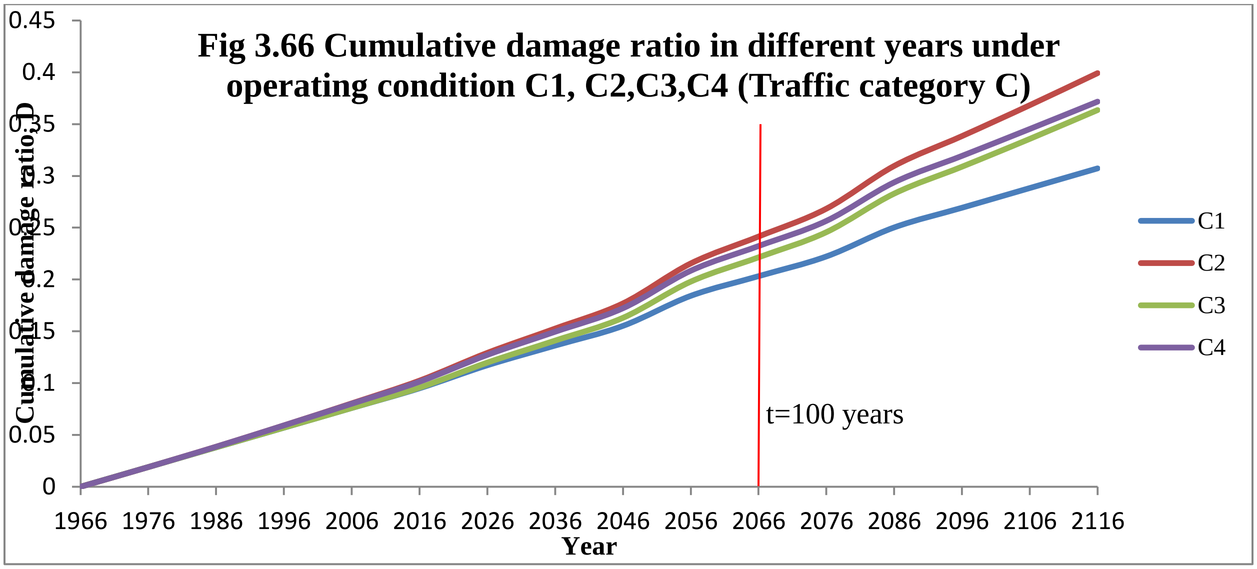

<u>**3.9.4 CUMULATIVE DAMAGE RATIO AFTER 100 YEARS FOR LOAD CATEGORY D:**</u>

Under train load category D (passenger train, Italian code), the damage ratio at t=100 years for the four sub-categories are shown in the following figure

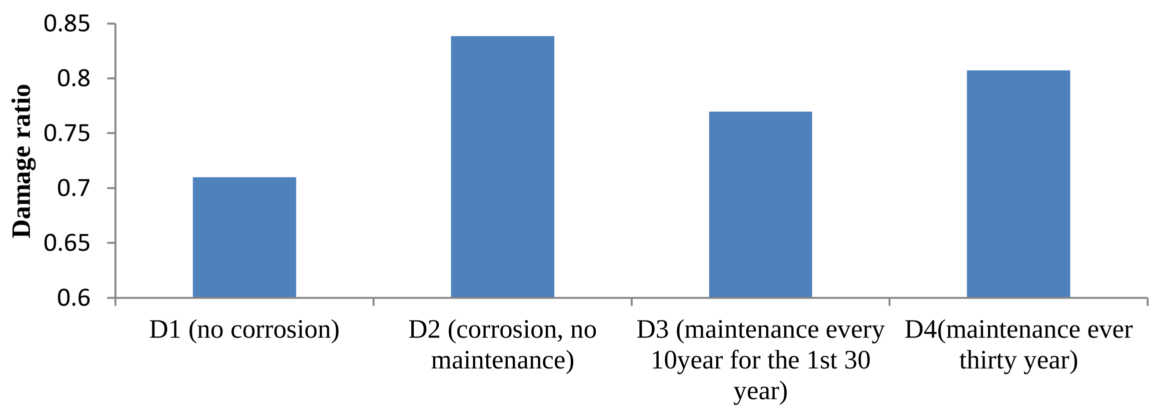

Figure 3.67: Cumulative damage ratio at t=100 years for operating scenarios D1, D2, D3, D4

From the above figure, at t=100 years, corrosion increases the damage ratio to 18.1%, when no maintenance is done. However, when painting is provided every 10 years for the first 30 years, the increase in damage ratio from no corrosion state can be limited to 8.4%. And, for one maintenance intervention in every thirty year the increase is damage ratio from no corrosion condition is higher (13.7%) than the other maintenance option. In the following figure the cumulative damage ratio for these subcategories in different years are shown

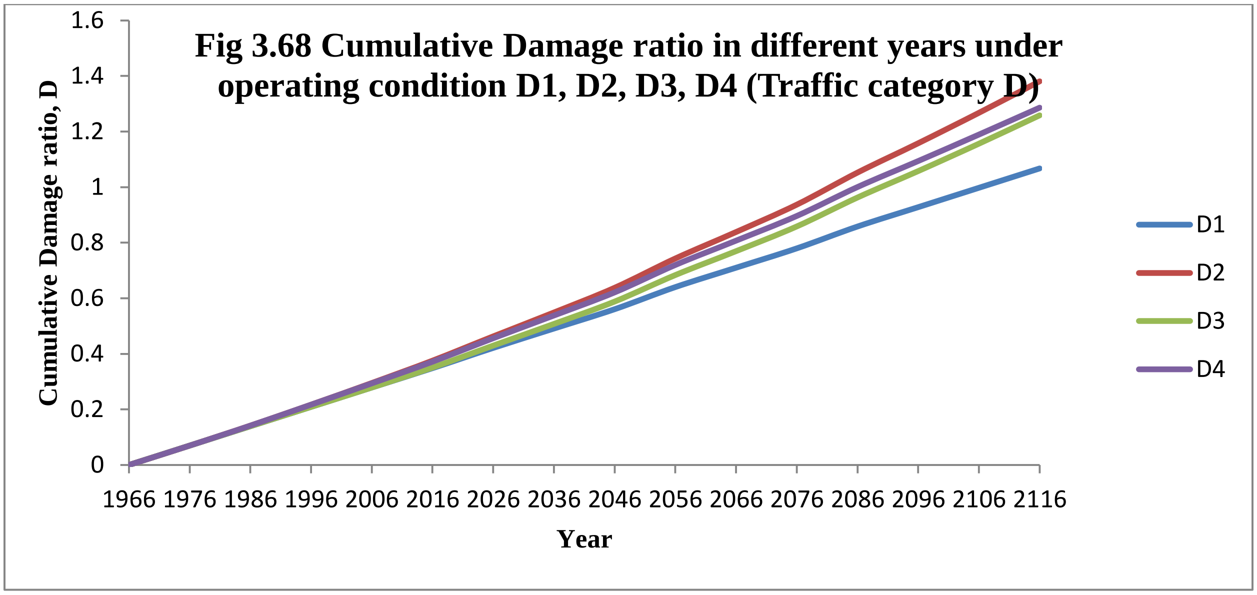

Fig 3.68 Cumulative Damage ratio in different years under operating condition D1, D2, D3, D4 (Traffic category D)

3.9.5 CUMULATIVE DAMAGE RATIO FOR ALL OPERATING SCENARIOS

After 100 years the cumulative damage ratio for all operating scenarios are shown in the following figure

Figure 3.69 Cumulative Damage ratio after 100 years

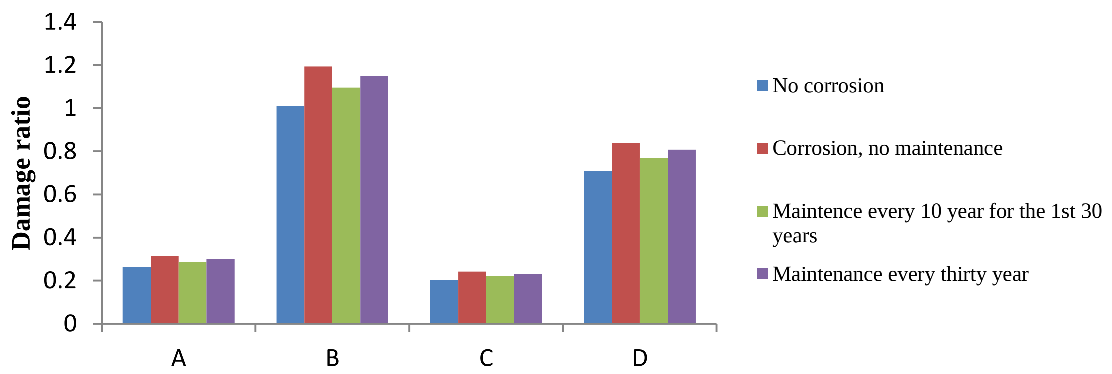

From the above figure it can be seen that the damage ratios for train load case B are higher and for train load case C it is the lowest. The maximum damage ratio occurs under operating scenario B2, where the train load is applied as per Italian code and the bridge material is allowed to corrode without maintenance. The minimum damage ratio occurs under operating scenario C1, where the only passenger trains with the frequency specified by RFI pass over the bridge and there is no corrosion. It is also noticeable that maintenance every 10 year for the first 30 years produces less damage ratios than the other maintenance program. For cumulative damage ratio after t=150 years for all operating scenarios, shown in the following figure similar observations are made

Figure 3.70 Cumulative damage ratio after 150 years

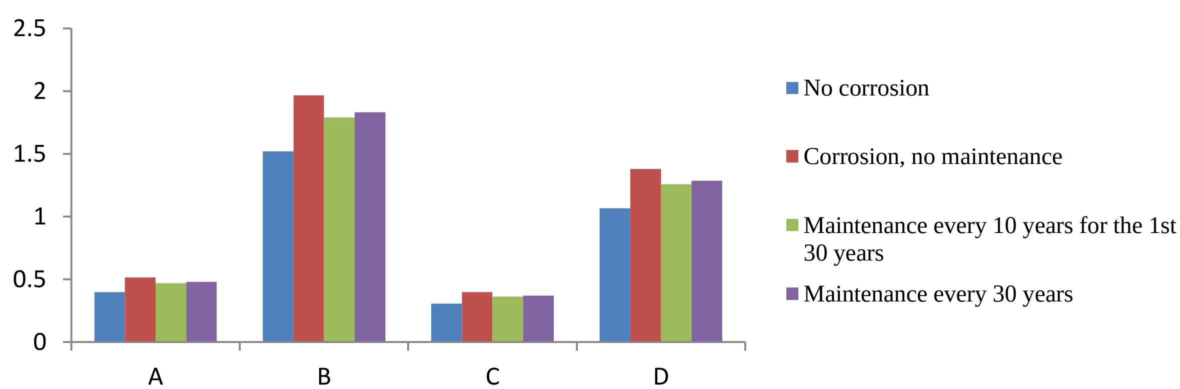

The cumulative damage ratios in different years under all operating scenarios are shown in the following figure

Fig 3.71 Cumulative damage ration in different years under different operating scenarios

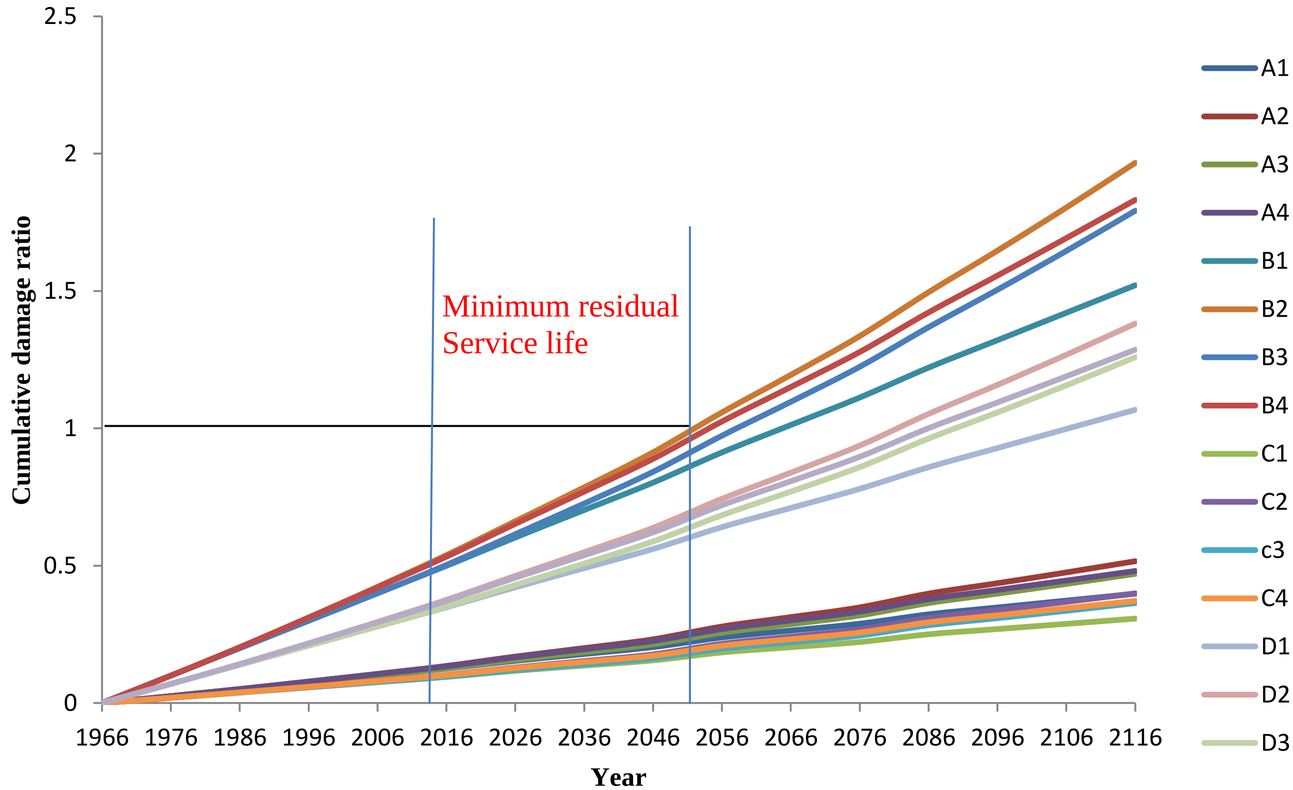

It can be seen that the minimum residual service life is 39.6 years which corresponds to operating scenario B2.

3.9.6 COMPARISON OF THE TWO MAINTENANCE PROGRAM:

So, for all load cases, maintenance in every 10 years for the first thirty years produces less damage ratio than maintenance in every 30 years option. This is because due to quicker maintenance intervention in the first maintenance strategy, the loss in thickness of the bridge material and therefore loss of resistance capacity of the member is lesser. So, the former maintenance strategy provides a greater service life and hence is the better maintenance option. For example the residual service life for B3 operating scenario where the first maintenance strategy is adopted is 45.2 years whereas the residual service life for B4 operating scenario where the second maintenance strategy is adopted is 42 years.

3.9.7 CONTRIBUTION OF THE EARTHQUAKES TO THE FATIGUE DAMAGE:

From the above analysis, it is observed that the contribution of the three earthquakes in the total cumulative damage ratio is very insignificant for all the operating scenarios compared to the damage contribution by the train load. This is because, even though the earthquakes produce stress cycle of high magnitude the number of cycles compared are very small compared to the load cycles produced by the train load. The maximum contribution of the earthquake load is observed in the operating scenario C1 which is 7.22% of the total damage ratio after 150 years

CHAPTER 4
CONCLUSION

4.1 CONCLUSION:

In conclusion, it can be said that the service life of the bridge depends on the number and magnitude of the stress cycles it is subjected to. From the results, it is observed that, the contribution of the three earthquakes in the total cumulative damage ratio is very insignificant for all the operating scenarios compared to the damage contribution by the train load. This is because, even though the earthquakes produce stress cycle of high magnitude the number of cycles compared are very small compared to the load cycles produced by the train load. Another important observation of this study is that corrosion considerably reduces the fatigue life of the bridge as it reduces the cross sectional area of the bridge member and hence increases the magnitude of the stress cycles acting upon it. From the analysis, It can be seen that the minimum residual service life of the bridge is 39.6 years under operating scenario B2, where greater number of trains permitted by the Italian code pass over the bridge increasing the number of stress cycle and absence of maintenance intervention corrodes the bridge member and increases the magnitude of the stress cycles over time. This study highlights the importance of a correct maintenance planning to avoid fatigue damage also. For all load cases, maintenance in every 10 years for the first thirty years produces less damage ratio than maintenance in every 30 years option. This is because due to quicker maintenance intervention in the first maintenance strategy, the loss in thickness of the bridge material and therefore loss of resistance capacity of the member is lesser. So, the former maintenance strategy provides a greater service life and hence is the better maintenance option.

REFERENCES

1. ASTM. (1985). Standard Practices for Cycle Counting in Fatigue Analysis. American Society for Testing and Materials Standard.

2. Cascini, L.; Landolfo, R. & Portioli, F. (2008). An integrated approach to durability design of steel structures against atmospheric corrosion. Key Engineering Materials Vols. 385-
3. 387 (2008) pp 657-660. Trans Tech Publications, Switzerland.

4. Cascini, L; D'Aniello, M.; Portioli, F. & Landolfo, R. (2012). Service life assessment of steel riveted railway bridges: A case study

5. EN ISO 9224. (1992). Corrosion of metals and alloys. Corrosivity of atmospheres. Guiding values for the corrosivity categories.

6. EN 12500 (2000). Protection of metallic materials against corrosion. Corrosion likelihood in atmospheric environment.Classification, determination and estimation of corrosivity of atmospheric environments.

7. Landolfo, R.; Cascini, L. & Portioli, F. (2010). Modeling of Metal Structure Corrosion Damage: A State of the Art Report

8. Maymon, G. (1998). Some Engineering Applications in Random Vibrations and Random Structures (Vol. 178) American Institute of Aeronautics and Astronautics.

9. Pipinato, A; Molinari, M.; Pellegrino, C;. Bursi, O.S. & Modena, C. (2009). Fatigue tests on riveted steel elements taken from a railway bridge

10. Rete Ferroviaria Italiana (RFI). Istruzioni 44F- Verifiche a fatica dei ponti ferroviari metallici. Roma 30.1.1992.

11. SAP 2000 v.11. Computers and Structures, Inc. 1995 University Avenue Berkeley, California 94704 USA.

12. Siemes, A. J. (1982). Miner's Rule with Respect to Plain Concrete Variable Amplitude Tests. ACI , 75, 343-372.

13. Socie, S. D.; & Downing, F. D. (1982). Simple Rainflow Counting Algorithms. International Journal of Fatigue, 4(1), 31-40.

14. Suguira, Y. O.; & Kunitomo. (2008). Fatigue life Estimation of a Concrete Slab Using. BWIM and Traffic census. International Conference on Heavy Vehicles. Paris.

15. Thun, H. (2006). Assessment of Fatigue Resistance and Strength in Existing Concrete Structures. Div. of Structural Engineering,. Ph D Thesis 2006:65: Luleå University of Technology.
16. http://www.public.iastate.edu/~gkstarns/ME417